12-2013

Conventional and Catalytic Pyrolysis of Pinyon Juniper Biomass

Bhuvanesh Kumar Yathavan
Utah State University

CONVENTIONAL AND CATALYTIC PYROLYSIS OF PINYON JUNIPER BIOMASS

by

Bhuvanesh Kumar Yathavan

A thesis submitted in partial fulfillment
of the requirement for the degree

of

MASTER OF SCIENCE

in

Biological Engineering

Approved:

_____	_____
Foster A. Agblevor, PhD Major Professor	Ronald Sims, PhD Committee Member
_____	_____
Issa Hamud, MS, PE Committee Member	Mark Mclellan, PhD Vice President for Research and Dean of the School of Graduate Studies

UTAH STATE UNIVERSITY
Logan, Utah

2013

ABSTRACT

Conventional and Catalytic Pyrolysis of Pinyon Juniper Biomass

by

Bhuvanesh Kumar Yathavan, Master of Science

Utah State University, 2013

Major Professor: Dr. Foster A. Agblevor
Department: Biological Engineering

Pinyon and juniper are invasive woody species in Western United States that occupy over 47 million acres of land. The US Bureau of Land Management (BLM) has embarked on harvesting these woody species to make room for range grasses for grazing. The major application of harvested pinyon-juniper (PJ) is low value firewood. Thus, there is a need to develop new high value products from this woody biomass to reduce the cost of harvesting. In this research PJ biomass was processed through pyrolysis technology to produce value added products. The first part of the thesis demonstrates the effect of PJ wood, bark and mixture biomass and temperature on the product yield and on the quality of the bio-oil produced. The second part focuses on the optimization of process parameters for maximum yield and the third part focuses on upgrading the bio-oil with an industrial catalyst (HZSM5) and an industrial waste product (red mud). The results obtained from the first part showed that PJ wood produced maximum bio-oil yield, followed by PJ mixture and bark. The bio-oil yield from PJ wood had low viscosity when compared to PJ mixture and PJ bark. The second part focused on studying the effect of process parameters (temperature, feed rate and the gas flow rate) on the total liquid, organic, water, char and gas yield. The results show that each response is affected by different factor level combinations, and maximum yield for each response was obtained at different factors level. The third part focused on catalytic pyrolysis of PJ biomass using both

HZSM-5 catalyst and red mud. The mechanisms of catalysis by the two catalysts were quite different. Whereas the HZSM-5 rejected oxygen mostly as carbon monoxide and water and produced lower amounts of carbon dioxide, on the contrary the red mud produced more carbon dioxide and water and less carbon monoxide. The higher heating value of the red mud catalyzed oil (29.46 MJ/kg) was slightly higher than that catalyzed by HZSM-5 (28.55 MJ/kg). Thus, red mud can be used to achieve similar catalytic pyrolysis results as HZSM-5 catalysts.

(109 pages)

PUBLIC ABSTRACT

Conventional and Catalytic Pyrolysis of Pinyon Juniper Biomass

Pinyon and juniper are invasive woody species which has occupied more than 47 million acres of land in Western United States. Pinyon juniper woodlands domination decreases the herbaceous vegetation, increase bare lands which in turn increases soil erosion and nutrition loss. Thus, The US Bureau of Land Management (BLM) has focused on harvesting these woody species to make room for herbaceous vegetation. The major application of harvested pinyon-juniper (PJ) is low value firewood. Thus, there is a need to develop new high value products from this woody biomass to reduce the cost of harvesting. In this study pyrolysis was carried out to investigate the feasibility of converting pinyon juniper biomass to value added products. The first part of the study was focused on biomass characterization, and effect of biomass type on product yields. The second part focuses on optimization of process parameters on product yields. The third part focuses on catalytic pyrolysis for improving the quality of bio-oil. In this study it has been shown that pinyon juniper biomass could be effectively used as biomass in fast pyrolysis and red mud, an industrial waste could be used as catalyst in catalytic pyrolysis to improve the quality of the bio-oil.

Bhuvanesh Kumar Yathavan

ACKNOWLEDGMENTS

I would like to start by thanking my major advisor Dr. Foster Agblevor. I envy his commitment and in depth knowledge in the field of research. I appreciate his time spent on my progress, his diligent guidance and advice for the problems faced in the research and finally for the opportunity to learn from him. I would also thank my committee members Dr. Ronald Sims and Mr. Issa Hamud.

A heart filled thanks to all belonging to Pandari Nilayam for their trust, love and freedom given to me. I also want to thank my colleagues for their company during my work and a special thanks to my roommates (all belonging to 944) for helping me in all aspects.

I would like to thank the Department of Biological Engineering for giving the opportunity to do my Master's degree at Utah State University and finally the Utah Science Technology and Research (USTAR) initiative for funding this project.

I would like to dedicate this work to my father, Mr. Yathavan Venogopal, my mother, Mrs. Mohanambal Yathavan, my brother, Mr. Dinesh Kumar Yathavan, and my sister, Mrs. Mahalakshmi Niranjan.

Bhuvanesh Kumar Yathavan

CONTENTS

Page

LIST OF TABLES

LIST OF FIGURES

CHAPTER 1

LITERATURE REVIEW

1. Pinyon juniper woodlands

Woodlands have intruded into many grassland ecosystems worldwide and continue to expand (Hodgkinson and Harrington, 1985). The increased in density and area of cover of woodland affects wildlife habitat, herbaceous vegetation, and ecological process which includes precipitation, nutrient cycle, and soil erosion (Scholes and Archer, 1997; Miller et al., 2005). One of the classic example of woodland expansion is the invasion of pinyon and juniper trees in Western United States (Miller and Wigand, 1994).

1.1. Classification and Distribution

Pinyon juniper woodlands occupy about 47 million acres in the Western United States which includes states of Arizona, California, Colorado, Idaho, Nevada, New Mexico, Oregon, Utah, and Wyoming (Evans, 1988; Chambers et al., 1999). The tree species associated with pinyon juniper woodlands are extremely variable, with complex distribution and patterns (West et al., 1998). The juniper trees found in the pinyon juniper woodlands consists of following species, alligator juniper (*Juniperus deppeana* Steud.), one-seed juniper *(Juniperus monosperma* (Engelm.) Sarg.), western juniper *(Juniperus occidentalis* Hook.), Utah juniper (*Juniperus osteosperma* (Torr.) Little), and Rocky Mountain juniper *(Juniperus scopulorum* Sarg.). The pinyon trees consists of following species, Mexican pinyon (Pinus cembroides Zucc.), pinyon (Pinus edulis Engelm.), and singleleaf pinyon (Pinus monophylla Torr. and Frem.) (Chambers et al., 1999).

Juniper trees are present in the Western United States for more than 30,000 years whereas pinyon trees were introduced recently, less than 2000 to 8000 years (West et al., 1998). Pinyon juniper woodlands have a wide range of climatic conditions and occur as single or mixed species. Pinyon juniper woodlands have an altitude range from 5,000 to 7,000 feet and moisture range from 10 to 14 inches (Aro, 1971). One-seed juniper along with pinyon expands from central Arizona to

New Mexico, including parts of southern Colorado and Texas (Aro, 1971). Western juniper are not usually associated with pinyon species and found in north eastern California, southwestern Idaho, northwestern Nevada, central and eastern Oregon (Miller et al., 2005). Nevada, Utah, western Colorado and northwestern Arizona woodlands consists of Utah juniper and pinyon (Aro, 1971; Baughman et al., 2010). Rocky Mountain juniper usually present in higher altitude, as a dominant species among the mixed pinyon juniper species (Aro, 1971).

1.2. Factors for expansion

Woodland expansion during pre-settlement period was mainly due to changes in temperature, precipitation and fire frequency (Miller et al., 2005). The annual temperature and precipitation was increasing slowly but, steadily after the ice age. These climatic conditions facilitated the growth of grasslands, and sage bushes. The woodlands were confined to areas where fine fuels were low (Miller and Wigand, 1994). The historic use of pinyon juniper woodland has a major impact on the current stand. The woodlands in the southwest and intermountain region were used similarly by the homesteaders. During the past 130 years the areas occupied by pinyon juniper woodlands have increased by 10 folds (Miller and Wigand 1994). Although pinyon juniper woodlands live for long periods, only 10% of trees are aged over 140 years. The tree ring chronologies shows that major establishment took place after 1870's (Miller and Tausch, 2001). The factors which contribute to the expansion of pinyon juniper woodlands are a) climate, b) livestock grazing, c) atmospheric CO_2, and d) fire (Miller et al., 2005; Ansley et al., 2006; Weisberg et al., 2007; Baughman et al., 2010).

During the period of mid 1800's and early 1900's, temperature and precipitation increased and was greater than the average of the intermountain west region (Miller et al., 2005). These condition contributed to dynamic growth of pinyon juniper woodlands (Miller and Wigand, 1994). Overgrazing by livestock starting from 1870's to the early 1900's reduced the competition offered

by the grasslands and the frequency of fire by reducing the fine fuels (Miller et al., 2005). Fire frequency in sage brush communities varied between 15 to 25 years, which usually maintains the shrubs and trees at low concentration (Miller and Wigand, 1994). After settlement, overgrazing by livestock reduced fine fuel, which ultimately reduced the frequency of fires (Ansley et al., 2006). Finally the increase in the concentration of atmospheric CO_2 also contributes to the expansion of woodlands (Knapp and Soule, 1999), by increasing the water use efficiency (Polley et al., 1993; Miller et al., 2005).

1.3. Problems

Pinyon juniper woodlands domination decreases the herbaceous vegetation, increase bare lands which in turn increases soil erosion and nutrition loss (Miller and Wigand, 1994; Brockway et al., 2002). Studies have shown that expansion of pinyon juniper woodlands have reduced the magnitude of precipitation (Miller et al., 2005), and increased soil erosion by four times (Carrara and Carroll, 2007). Pinyon juniper woodlands increases the possibility of crown fires, which promotes the infiltration of exotic species (Tausch et al., 1993). Thus due to these problems land managing agencies are focusing on reducing the population of pinyon and junipers by bulldozing, chaining (Ansley et al., 2006), hand cutting, mechanical removal (Baughman et al., 2010), and prescribed fire (Ansley et al., 2006; Baughman et al., 2010).

1.4. Current uses

The homesteaders used western juniper for food, medicine, and shelter. In Early 1900's, Western junipers were used as firewood and fencepost (Miller et al., 2005). Western juniper pitch was used on baskets to make watertight containers. Western junipers were used as firewood, chips for particle-flake board. Interior paneling, frame molds, and for flavoring gin. Annually 500,000 pinyon trees are cut to be used as Christmas tree. Honey lake power located in Wendell, California

is one of the largest users of western junipers as energy fuel. They account for using more than 100,000 tons of biomass within three years (Miller et al., 2005). The production of naval stores from pinyon and juniper trees are of great interest since it contains four times more resin compared to douglas-fir.

2. Composition of Lignocelluloses biomass

Lignocellulosic biomass is most widely available biomass (Perego and Bosetti, 2011) , which are formed from CO_2 and H_2O using sunlight as energy source (Petrus and Noordermeer, 2006). The chemical composition of lignocellulosic biomass is affected by parts of the tree (stem, branches), geographic location, climate, soil, kind of wood (Pettersen, 1984). Lignocellulosic biomass is mainly composed of cellulose (23-53%), hemicelluloses (20-35%), lignin (10-25%) and extraneous compounds (Petrus and Noordermeer, 2006). The components of the biomass are different from each other and undergo degradation at different temperature (Bridgwater, 2012a).

2.1. Cellulose

Cellulose $(C_6H_{10}O_5)_n$ is a linear, homopolymer of glucose molecule linked by $\beta(1\rightarrow4)$ glycosidic bond (Perego and Bosetti, 2011). Cellulose chain consists of about 5000-10000 glucose units. Cellulose constitutes about 40-50 wt% of dry weight of wood (Mohan et al., 2006), degrades at temperature range of 310 – 430^{o}C (Bulushev and Ross, 2011). The hydroxyl group of cellulose forms hydrogen bond with oxygen of the same chain or neighboring chain, which strengthens the chain and stimulate cellulose aggregations (Pu et al., 2011). Aggregate is a term used to represent highly ordered cellulose and reduced aggregate increases enzymatic breakdown (Pu et al., 2011). Recovery of cellulose in pure form is difficult due to its cross link with lignin and hemicelluloses. Cellulose is resistant to most of the solvent, including strong alkali (Pettersen, 1984).

2.2. Hemicellulose

Hemicellulose $(C_5H_8O_4)_n$ is the second largest polysaccharide in wood. Hemicellulose is a branched heteropolymer, which consist of xylose, mannose, galactose, rhamnose, arbinose along with glucose (Perego and Bosetti, 2011). The number of monomer sugars is between 50 – 200 units (Venderbosch and Prins, 2010). Hemicellulose accounts for about 25-35 wt% of dry wood (Mohan et al., 2006), decomposes at temperature range of 250 – 400^o C (Bulushev and Ross, 2011). Galactoglucomannans and arabinoglucuronoxylan constitutes most of hemicelluloses in softwood, while glucuronoxylan constitutes most of hemicelluloses in hardwood. Glucuronoxylan and arabinoglucuronoxylan contain (1-4)-linked β-D-xylopyranosyl units, but differs in branching and acetylating groups. Glucuronoxylan are acetylated at C2- and C3-positions and branched. Arabinoglucuronoxylan are not acetylated but branched. Galactoglucomannans contains (1→4) linked β-D-glucopyranosyl and D-mannopyranosyl units that are partially acetylated at the C2- and C3-positions. In softwood, Galactoglucomannans are important which constitutes for about 15-20 wt% of dry wood (Pu et al., 2011). Hemicelluloses are closely linked with cellulose, but unlike cellulose, hemicelluloses are hydrolyzed by acids and soluble in alkali (Pettersen, 1984).

2.3. Lignin

Lignin $[C_9H_{10}O_3(OCH_3)_{0.9\text{-}1.7}]$ is a complex polymer which are chemically different from carbohydrates (Perego and Bosetti, 2011). Lignin accounts for 23%-33% of softwoods and 16%-25% of hardwoods (Mohan et al., 2006). Lignin degrades in a wide range of temperature 300 – 500^{o}C (Bulushev and Ross, 2011) and produces oil with low oxygen content, at 500^{o}C (Butler et al., 2011). Lignin is a copolymer formed from three different phenylpropane monomers namely coniferyl alcohol, sinapyl alcohol and p-coumaryl alcohol (Pu et al., 2011). The chemical composition and percent of lignin varies in different species, trees and also in different component of the same tree. Softwood contains higher lignin content compared to hardwood (Pandey and Kim,

2011). Softwood is mainly made up of coniferyl alcohol units, while hardwood consists of approximately equal amounts of coniferal and sinapyl alcohols (Pu et al., 2011).

2.4. Extractives

Extractives are those which are soluble in organic solvents and they do not contribute to the cell wall structure. The extractives accounts for about 4 – 10 wt% of dry wood and could vary according to the climatic conditions. Extractives include wide range of organic compounds such as fats, proteins, pectins, phenolics, waxes, gums, resins, terpenes, glucosides, saponins and essential oils. These compounds act as energy reserve, protects against microbial attack, and take part in tree metabolism. Extractives composition affects the wood properties such as odor, color and defense mechanism (Pettersen, 1984).

3. Thermo-chemical conversion (Pyrolysis) of biomass

The study of pyrolysis is gaining increasing importance, as it is the first step in gasification and combustion process (Babu, 2008). Pyrolysis is thermochemical breakdown of biomass in the absence of oxidizing agent. During pyrolysis, heat is transferred into the biomass, which initially causes the evaporation of moisture. Further increase in temperature, breaks down the major constituents (cellulose, hemicelluloses, lignin) of the biomass into pyrolytic vapors and carbon rich solid called "biochar." The pyrolytic vapors consists of permanent gases (H_2, CO, CO_2, light hydrocarbons) and condensable vapors which are condensed to form mixture of organic compounds in liquid form called "bio-oil" (Neves et al., 2011). Thus, pyrolysis breaks down the organic portion of the biomass into three products namely solid (biochar), liquid (bio-oil) and gas products (Sensoz et al., 2000; Babu, 2008; Briens et al., 2008; Vamvuka, 2011). A number of reactions such as cracking, dehydration, dehydrogenation, isomerization, aromatization and condensation take place during pyrolysis (Vamvuka, 2011).

A wide variety of biomass could be used in the pyrolysis process to produce valuable products. Some of the biomass used are pine wood (Aho et al., 2008, 2011; Westerhof et al., 2010); beechwood (Schröder, 2004); mallee wood (Garcia-Perez et al., 2008; Wang et al., 2012); hybrid poplar (Mante et al., 2011; Agblevor et al., 2010b); yellow poplar wood (Kim et al., 2011); pine wood, pine bark, oak wood, and oak bark (Ingram et al., 2008); poultry litter (Agblevor et al., 2010b); salix wood (Biswas et al., 2011); beech, Miscanthus, spruce, forest residue (Blin et al., 2007); sawdust mixture (Salehi et al., 2011); olive cake (Gerçel and Gerçel, 2007); rapeseed (Sensoz et al., 2000); cassava stalk, cassava rhizome (Pattiya, 2011a); waste particle board (Cho et al., 2011); switchgrass and corn stover (Brewer et al., 2009); wheat straw (Liu et al., 2012); switchgrass, alfalfa stems, corn stover, guayule and chicken litter (Mullen et al., 2009); hazelnut shell (Gokdai et al., 2010); sugarcane bagasse (Sanderson et al., 1996); sweet sorghum and sweet sorghum bagasse (Piskorz et al., 1998); corn stover *(Zea mays L),* switchgrass *(Panicum virgatum* L), and hybrid poplar (Agblevor et al., 1995); switchgrass (*Panicum virgatum L.*) (Agblevor and Besler, 1996; Boateng et al., 2006); coal and corn cobs mixture (Rodjeen et al., 2006); red oak (Brown and Brown, 2012); hempseed (Karimi et al., 2010); softwood bark and hardwood (Garcìa-Pérez et al., 2007). The composition of biomass used along with different pyrolysis condition, affects the quality and the quantity of pyrolysis products (Mohan et al., 2006; Babu, 2008).

Pyrolysis is classified into different types based on the operating conditions. Pyrolysis product yield would be mainly biochar when operated at low temperature (< 400^{o}C) and long residence time. Bio-oil is the main product when operated at intermediate temperature (around 500^{o}C) and short residence time (Bridgwater, 2006).

Table 1. 1. Different forms of pyrolysis process [adapted from (Bridgwater, 2006)]

	Conditions	Liquid (%)	Char (%)	Gas (%)
Slow	Low temperature, around 400^{o} C, very long residence time	30	35	35
Fast	Moderate temperature, around 500^{o} C, Short hot vapour residence time, ~1 s	75	12	13

4. Fast pyrolysis

Fast pyrolysis is currently of particular interest because liquids have relatively high energy density, compared to solid, and gas. Moreover liquids can be stored, transported more easily at a lower cost. Liquids can also be upgraded to transportation fuels, which could be used in the current engines with slight modifications (Bridgwater, 2006; Vamvuka, 2011). Fast pyrolysis is illustrated as pyrolysis carried out at moderate temperature (about 500^{o}C), shot vapor residence time (1-5 s), with high heating rate, and rapid cooling of pyrolysis vapours. Fast pyrolysis product distribution are affected by number of factors which includes reactor configuration, heat transfer, heating rate, temperature, vapor residence time, secondary cracking of vapors, char separation, liquid collection (Bridgwater et al., 1999).

4.1. Reactors

Reactor plays a significant role in pyrolysis process (Bridgwater, 2006), thus much research has been focused on reactor design in order to obtain the required temperature, vapor residence time, and heating rate. Many reactor designs have been used in the past years which include bubbling fluidized bed reactors, circulating fluidized bed reactors, ablative pyrolysis reactors, fixed bed reactors, vacuum pyrolysis reactors, auger reactors, rotating cone reactors, vortex reactors, etc. Thus the configurations which have been commercialized or near commercialization are discussed below.

4.1.1. Bubbling fluidized bed reactors

In bubbling fluidized bed reactors, inert gas (usually nitrogen) is passed through sand or catalyst with minimum fluidizing velocity in order to suspend the solid. Thus the solid medium now acts as a fluid. Heat from an external source is transferred to the biomass through conduction and convection (Mohan et al., 2006). Laboratory investigation reports that maximum liquid yield is obtain in a temperature range of 400-500^{o} C, with vapor residence time of <2s (Butler et al., 2011). Another work reported that satisfactory liquid yield was obtained at 360^{o}C, with long residence time (Westerhof et al., 2010). Thus in fluidized bed reactor, the liquid yield is mainly affected by temperature, feed rate, heating rate, residence time (Butler et al., 2011). In order to obtain high heating rate the particle size of the biomass should be very small (2-3mm) (Bridgwater, 2012b), which increases the operational cost due to grinding. Short residence time is attained by using high gas flow rate. Fluidized bed reactors have good temperature control, produces a good quality bio-oil with a high concentration of desirable chemicals (Scott et al., 1999). Fluidized bed reactors were first used by research group in University of Waterloo, and they reported total liquid yield between 70 – 85 wt% on moisture free basis, which was never reproduced in further investigations (Kersten et al., 2005).

4.1.2. Circulating fluidized bed reactors

Circulating fluidized bed reactors are similar to fluidized bed reactors, but the only difference is that it contains a second reactor in which combustion of char takes place. It is similar to twin fluid-bed gasifier except that the reactor (pyrolyser) temperature is much lower (Bridgwater, 2012b). Thus the biochar is separated from the pyrolysis vapour with the help of cyclone, and combusted in the second reactor. Heat is transferred by the recirculation of heated sand from the combustion reactor. The use of char combustor to reheat would increase the ash content in the

pyrolysis reactor, which is known to act as catalyst (Scott et al., 1999). Due to high gas velocity, the residence time of char is similar to the gases and pyrolysis vapours. Hence, very fine biomass should be used. The high gas velocity causes more char attrition, which could be avoided by extensive char removal or post-treatment of bio-oil would be required (Scott et al., 1999). The quantity and quality of liquid yield are comparable to bubbling fluidized bed reactor, thus circulating fluidized bed reactors are preferred for scaling up due to energy efficiency (Vamvuka, 2011).

4.1.3. Vacuum pyrolysis reactors

In vacuum pyrolysis reactors, biomass is introduced through vacuum feeding system into horizontal plates in the reactor, which are heated by molten salts. When the biomass is broken down, the pyrolytic products are removed by vacuum pump (Mohan et al., 2006). Vacuum reactors are characterized by slow heating rate and rapid removal of pyrolysis vapours, thus maintaining short residence time for the pyrolysis vapours (Scott et al., 1999).Vacuum pyrolysis are usually carried out at 450^{o} C, 15kPa total pressure. The liquid yield obtained is between 55 – 60 wt % on dry basis, with higher char yield (Vamvuka, 2011). The advantage of these reactors is that large particle size could be pyrolysed, there is no need of fluidizing gas. However these reactors need vacuum pumps and large equipments, thus making the operation complicated and high-priced (Bridgwater, 2012). The first industrial scale vacuum pyrolysis was built by Ecosun bv (Netherlands) and Groupe PyroVac Inc (Canada), which mainly focused to produce phenol formaldehyde resins from the bio-oil (Vamvuka, 2011).

4.1.4. Ablative pyrolysis reactors

Ablative pyrolysis reactors have peculiar concept, in which heat is transferred to the biomass from heated surface (Scott et al., 1999). Biomass is pyrolysed when it comes in contact with hot surface under pressure. Thus, pressure controls the reaction rate and high pressure is obtained by centrifugal or mechanical motion of the hot surface (Bridgwater, 2012b). When the biomass is moved from the point of contact, the oil evaporates and could be collected similar to other reactors. The advantages of ablative reactors are, there is no heat transfer limitations thus large particle size could be used (Vamvuka, 2011). The heat transfer rate is limited by the rate of heat supplied to the reactor rather than the rate of heat absorbed by the biomass (Vamvuka, 2011). The disadvantages of these reactors are high char attrition, high degree of heat loss due to mechanically driven parts, thus causing complexity and scaling up is depend on the surface area than the volume which causes economic problems in scaling up (Briens et al., 2008).

4.1.5. Rotating cone reactors

In rotating cone reactors, sand or catalyst along with the biomass is introduced to the bottom of rotating cone containing heaters. The biomass is pyrolysed as they move up along the heated surface due to centrifugal force (Vamvuka, 2011; Bridgwater and Peacocke, 2000). The movement of the sand and biomass is caused by the rotating motion of the reactor. The vapors produced are condensed to bio-oil, while the sand and biochar are carried to a combustor reactor. The biochar is burned to heat the sand and the heated sand is introduced into the rotating cone (Bridgwater and Peacocke, 2000). Carrier gas requirement is minimal, but it needs a complex design which includes the rotating cone reactor, char combustor and a riser for sand (Bridgwater, 2012b). The rotating cone reactors were first constructed by University of Twente and further developed by British Technical Group (BTG) (Vamvuka, 2011).

4.1.6. Entrained flow reactors

Entrained flow reactors were first constructed by Georgia Tech Research Institute and further developed by Egemin (Vamvuka, 2011). In entrained flow reactors, the biomass is introduced into the bottom of the reactor which contains a stream of hot combustion gas. The hot gas is obtained by burning propane and air stoichiometrically (Bridgwater and Peacocke, 2000). Entrained flow reactors were not successful, due to heat transfer limitations. Heat is transferred to the biomass from the gas stream. High gas flow rates and fine particle size are needed to attain good heat transfer rate (Bridgwater, 2006)**.** Liquid yields were lower when compared to other reactors, with maximum yield of about 60 wt% on dry basis (Vamvuka, 2011).

4.2. Heat transfer and heating rate

Heat transfer and heating rate are interrelated factors and influenced by local factors (Kersten et al., 2005) and these are rate limiting step. In fluidized bed reactors there are two ways by which heat can be transferred to the biomass 1) gas to solid heat transfer 2) solid to solid heat transfer. The fluidization gas is heated before and thus can be used to transfer heat to the biomass through convection. The solid-solid heat transfer mainly occurs through conduction (Bridgwater et al., 1999). High heat transfer is needed to obtain high heating rate and maintain the endothermic reaction. Heat transfer takes place mainly through conduction (90%), small contribution through convection (10%) and radiation (1%) (Bridgwater et al., 1999). Heat is obtained from an external source until the reaction temperature is reached, then the byproducts (char and gas) could be burned in order to provide the required process heat (Vamvuka, 2011). Heating rate experiments are carried out only in fixed bed reactors or in oven using a single particle. These experiments have concluded that, low heating rates reduces the liquid yield (Kersten et al., 2005). High heating rates could be achieved by using biomass particle size less than 2-3mm (Bridgwater, 2012b).

4.3. Temperature

Pyrolysis yield have been reported for wide range of temperature for different biomass (Kersten et al., 2005). Most of them have reported increase in liquid yield, with decrease in char yield until optimum temperature is reached and further increase in temperature increased the gas yield in the expense of liquid yield (Kersten et al., 2005). Most of the biomass, yields maximum organic liquid in the temperature range of 475 - 525^{o}C, if the vapor residence time is within 0.2 – 0.6s. Secondary cracking of vapors takes place at higher temperature and longer residence time, thus reducing the liquid yield (Bridgwater et al., 1999).Thus, for experiments conducted above 500^{o} C, it is difficult to avoid secondary cracking of vapors (Neves et al., 2011). Secondary reaction slows down at temperature below 350^{o} C, but some reactions takes place even at low temperatures which causes instability in the properties of the bio-oil (Bridgwater and Peacocke, 2000). In order to obtain maximum liquid yield, two criteria should be followed 1) Temperature of reaction should be as minimum as possible 2) Temperature of products leaving the reactor should be lower than the reaction temperature (Scott et al., 1999). At higher temperature, the concentration of desired chemicals and the quality of the bio-oil decreases (Scott et al., 1999).

4.4. Vapor residence time

The pyrolysis vapor residence time is controlled by fluidizing gas flow rate. The apparent vapor residence time is calculated by dividing the volume of reactor by the flow rate (Agblevor et al., 2010a). At higher temperature, the pyrolysis vapours are cracked more, thus at higher temperature with longer residence time the vapour cracking increases further (Bridgwater and Peacocke, 2000). Thus, shorter residence time is required in order to increase the liquid yield and decrease the char and gas yield (Vamvuka, 2011).

Low liquid yield are obtained at long residence time are due to cracking and polymerization of vapors into gases and solids (Kersten et al., 2005). As the temperature and residence time increases, the molecular weight of the bio-oil decreases, due to secondary cracking (Bridgwater et al., 1999). Laboratory scale fluidization bed reactors can be operated at shorter residence time (0.5 s), but commercial scale reactors are operated at longer residence time (5 -10 s) (Briens et al., 2008). Scott et al., was able to obtain similar liquid yield and chemical composition at two different pyrolysis conditions.1) Higher temperature, short residence time (0.5 s), and 2) low temperature and longer residence time (up to 5 s) (Scott et al., 1999). This shows that the results obtained at higher temperature could be easily obtained at lower temperature with longer residence time.

4.5. Char and ash separation

The ash from the biomass is retained in the char, Thus ash is removed by effectively removing the char from the gas phase (Bridgwater and Peacocke, 2000). Vapor cracking rates cannot be calculated based on residence time and temperature basis alone, because the amount of char in the reactor is also reported to have a significant effect on the extent of cracking (Kersten et al., 2005). At reaction temperature, char acts as an effective pyrolysis vapor catalyst causing secondary cracking (Kersten et al., 2005; Neves et al., 2011). The presence of sodium and potassium has a large impact, while sulfur and phosphorous containing ammonium salts also affects the oil yield (Venderbosch and Prins, 2010). Char in the bio-oil at room temperature contributes to polymerization process, thus increasing the viscosity (Bridgwater and Peacocke, 2000). Hence, complete removal of char is very important. Char could be removed using cyclones (Vamvuka, 2011), but high quality liquid could be obtained by using hot gas filter (Hoekstra et al., 2009).

4.6. Liquid collection

Pyrolysis products after filtration of the char contain vapors and aerosols at very low concentration along with the inert gas. Thus, the partial pressures of condensable liquids are very low, which increases the cooling and condensation problems (Bridgwater and Peacocke, 2000). Thus care is needed to design and operate efficient heat exchange and liquid collection systems. In addition the large inert gas flow rate result in relatively large equipment thus increasing the cost (Bridgwater, 2012b). The vapors are condensed by direct contact with cooled surface and aerosols are effectively recovered by using electrostatic precipitator (Vamvuka, 2011).

5. Pyrolysis liquid

Pyrolysis liquid are usually referred as pyrolysis oil, bio-oil, wood oil, biocrude oil,etc and these appear to be dark brown to dark red in color with a smoky smell (Czernik and Bridgwater, 2004; Zhang et al., 2007). Pyrolysis liquid is a blend of oxygenated organic compound and water formed by depolymerization or breakdown of cellulose, hemicelluloses and lignin at high temperature (Vamvuka, 2011; Mohan et al., 2006). The oxygenated organic compound consist of alkenes, alcohols, ethers, sugars, aromatics, phenols, acids, ketones and aldehydes (Vamvuka, 2011). The physico-chemical properties of the bio-oil depend on the feedstock, operating conditions and the liquid collecting process (Venderbosch and Prins, 2010). The physico-chemical properties of bio-oil usually reported are acidity, viscosity, water content, elemental analysis, energy content, and chemical composition.

6. Properties of pyrolysis liquid

6.1. Acidity

The pH of bio-oil is usually between 2.0 - 3.0 which is due to the presence of considerable amount of organic acids which includes formic acid, acetic acid, and aromatic acids (Scott et al., 1999; Bridgwater and Peacocke, 2000). Thus, bio-oil are corrosive, which forces to change the construction materials in the engines and upgrading process (Zhang et al., 2007).

6.2. Water content

Water content in bio-oil is due to feedstock moisture (Czernik and Bridgwater, 2004) and decomposition of holocellulose and lignin (Scott et al., 1999). Moisture content in bio-oil has a wide spectrum (15% - 50%) depending on the feedstock and operating conditions (Bridgwater, 2006). Water content has both positive and negative effect; it lowers the heating value and flame temperature, yet it reduces the viscosity (Vamvuka, 2011). Phase separation occurs in the bio-oil, if excess amount of water is added. This shows that bio-oil is immiscible with water (Briens et al., 2008).

6.3. Viscosity and ageing

Bio-oil viscosity varies between 25cP -1000 cP at 40^{o}C depending on the quantity of lower molecular weight compound, water content, biomass, pyrolysis condition, age of bio-oil (Bridgwater and Peacocke, 2000; Mohan et al., 2006; Venderbosch and Prins, 2010). High viscosity of bio-oil is due to the existence of highly polar groups (Bridgwater et al., 1999). It was also found that the viscosity of bio-oil increases with time (Vamvuka, 2011). Viscosity could be decreased by preheating and by adding organic solvents like methanol, but this reduces the flash point (Vamvuka, 2011). The chemical reaction within the bio-oil, leading to polymerization could be the reason for increasing viscosity (Czernik and Bridgwater, 2004).

6.4. High heating value and oxygen content

Wood bio-oil has a heating value of about 17 MJ/Kg (with 25% water content), which is only 40% efficient when compared to fossil fuels (Bridgwater and Peacocke, 2000). The pyrolysis of oil plants yields bio-oil of higher heating value, when compared to wood (Zhang et al., 2007). The abundant amount of oxygen (35 - 40 wt %) present in the bio-oil is responsible for difference in the properties between bio-oil and fossil fuel (Czernik and Bridgwater, 2004). Pyrolysis oil are thus, low in energy content and immiscible with light hydrocarbons due to the large amount of oxygen content (Vamvuka, 2011). Pyrolysis carried out at high temperature reduces the oxygen content, at the expense of liquid yield (Czernik and Bridgwater, 2004).

7. Application of Bio-oil

7.1. Bio-oil for transport fuels

Bio-oil is mainly focused to be used as transportation fuel, which is a mixture of hydrocarbons. Thus, even after extracting the valuable chemicals, the remaining bio-oil can be used as fuel (Briens et al., 2008). Combustion carried out at elevated temperature with bio-oil and ethanol mixture (20:80) was normal without decrease in performance (Nguyen and Honnery, 2008). The fuel characteristic of different combination of bio-oil and diesel mixture was tested. The results showed that the fuel properties did not change significantly but only caused small increase in viscosity and density (Garcia-Perez et al., 2007). The drawback in the use of bio-oil, diesel mixture is the cost and energy needed for surfactant and emulsification (Czernik and Bridgwater, 2004). Bio-oil could be upgraded into transportation fuel by two main routes namely hydrotreating and catalytic vapor cracking. The fuel produced till today, could not compete with fossil fuel in terms of cost and energy. Currently, bio-oil upgrading to transport fuels does not look promising, but could be used as source for transport fuels in the near future (Czernik and Bridgwater, 2004).

7.2. Bio-oil for heat production (boiler, furnace)

Bio-oils have the advantage of easy transport, handling, and also could be used in existing technology with minor changes (Bridgwater et al., 1999). Furnace and boilers which are less efficient and could be operated with wide range of fuels are used for heat production (Czernik and Bridgwater, 2004). The presence of water and oxygenated compounds reduces the heating value of the bio-oil (Bridgwater and Peacocke, 2000; Mohan et al., 2006). Although, the flame combustion results shows that, heavy and light fuels used in broiler application could be substituted with pyrolysis oil (http://www.btgworld.com) (Mohan et al., 2006). Red arrow products, Wisconsin is using bio-oil to produce heat for more than 10 years (Czernik and Bridgwater, 2004). Research done at Finland by Neste and Oy (Gust and Oy, 1997), reported satisfactory operation with few comments a) needed some modification of burner and oiler. b) Fossil fuel needed for start up. c) Difference in combustion and emission, due to difference in properties of oil tested (Czernik and Bridgwater, 2004). The advantages of using bio-oil are, the emission were lower than fossil fuel burning; bio-oil combustion had longer flame than fossil fuel combustion (Bridgwater and Peacocke, 2000).

7.3. Bio-oil for power production (diesel engines)

Bio-oils could be used in diesel engines equipped with large cylinder bores, which can be operated on low grade fuels (Czernik and Bridgwater, 2004). Bio-oil is being tested in diesel engines by Motori, Italy; Kansas University, USA; MIT, USA; Pasquali, Italy; and Wartsila, Finland (Bridgwater and Peacocke, 2000). Bio-oils are used in modified diesel engines by PyTech, Germany (Fair et al., 2010). The results from these tests showed that there are some problems due to acidity, viscosity, lack of stability, low cetane value of bio-oil. Thus, modification of bio-oil and engines could address all the problems (Venderbosch and Prins, 2010).

7.4. Bio-oil for electricity production (gas turbines)

Bio-oil used in gas turbines was found to emit less pollutant, except carbon monoxide (Czernik and Bridgwater, 2004). Research were conducted by Orenda division of Magellan Aerospace Corporation, Canada; Rostock University, Germany; and ENEL Thermal Research Center, Italy (Venderbosch and Prins, 2010). The drawbacks of using bio-oil in turbines are deposits, corrosion of turbine blades and chambers (Briens et al., 2008). Orenda, reported successful operation of gas turbine, with filtered bio-oil (Bridgwater and Peacocke, 2000). Thus, finding solution to the problems is necessary in order to commercially use bio-oil in gas turbines.

7.5. Bio-oil for chemical production

Initially pyrolysis oils were the feedstock for the production of various chemicals, before finding the low cost feedstock from natural gas and crude oil (Czernik and Bridgwater, 2004). There are more than 300 compounds identified in bio-oil, but there is no evidence of high yield of particular chemical and the market for them (Bridgwater, 1996). Levoglucosan and Hydroxyacetaldehyde are two chemicals with significant concentration in bio-oil (Bridgwater, 1996) . The method for extraction of levoglucosan at pure level was patented (Bridgwater, 1996). The aqueous phase of bio-oil after adding water contains aldehydes and phenolic compounds which are used as browning agent and food flavors respectively (Czernik and Bridgwater, 2004). These products have been patented and commercialized by Red Arrow Products for more than 10 years (Underwood and Graham, 1989). The water insoluble portion of the bio-oil which are mainly derived from lignin degradation are referred to as pyrolytic lignin (Czernik and Bridgwater, 2004). Research is been carried out in order to replace phenol with pyrolytic lignin in phenol-formaldehyde resin, which is near commercialization (Czernik and Bridgwater, 2004; Venderbosch and Prins, 2010).

8. Biochar

Biochar which is the major product of slow pyrolysis, is produced by incomplete decomposition of organic compounds, particularly lignin (Vamvuka, 2011). The ash from the biomass is retained in the char (Bridgwater and Peacocke, 2000). Thus, biochar is a carbonaceous material with inorganic compounds, which is ashed to different degree based on the operating conditions (Vamvuka, 2011). The LHV of chars have been reported to be about 32MJ/kg and volatilities between 15 and 45% wt (Vamvuka, 2011). The biochar products are highly volatile, and thus auto ignited in temperature between 200^{o}C – 250^{o}C (Vamvuka, 2011). Biochar produced can be gasified to produce medium BTU gas, which can provide energy for heating or feedstock drying (Scott et al., 1999; Bridgwater et al., 2002). Biochar can be converted to commercial grade activated carbon, in the expense of 50% weight loss (Scott et al., 1999). Biochar, as a fuel, could be substituted for coke, in metallurgical processes, due to low metal concentration (Briens et al., 2008). The atmospheric carbon which is captured by the biomass, are trapped in the form of biochar. Thus, biochar acts as carbon negative or carbon sink (Lehmann et al., 2006). Biochar acts as a host for microbes, releases the nutrients and water slowly, thereby increasing the soil structure (Lehmann et al., 2006; Briens et al., 2008). Biochar applied to the soil, increases the soil fertility and crop production apart from capturing atmospheric carbon (Lehmann et al., 2006).

9. Gases

Non-condensable gases produced during pyrolysis process contain approximately 0.8% H_2, 53% CO_2, 39% CO and 6.7% light hydrocarbons (Vamvuka, 2011). The pyrolysis gases contains about 5% of energy in the biomass (Bridgwater, 2006). The pyrolysis gases has medium calorific value (Scott et al., 1999), which could be used for fluidization, to provide process heat or for drying the biomass (Bridgwater et al., 2002). Syngas could be used as a source for manufacturing all chemicals, including transportation fuels. In large plants the heat from the gases can be used to

produce electricity (Bridgwater, 2012b). Currently, the most interesting application of gases are power production, as it does not depend on the product quality (Bridgwater, 2006).

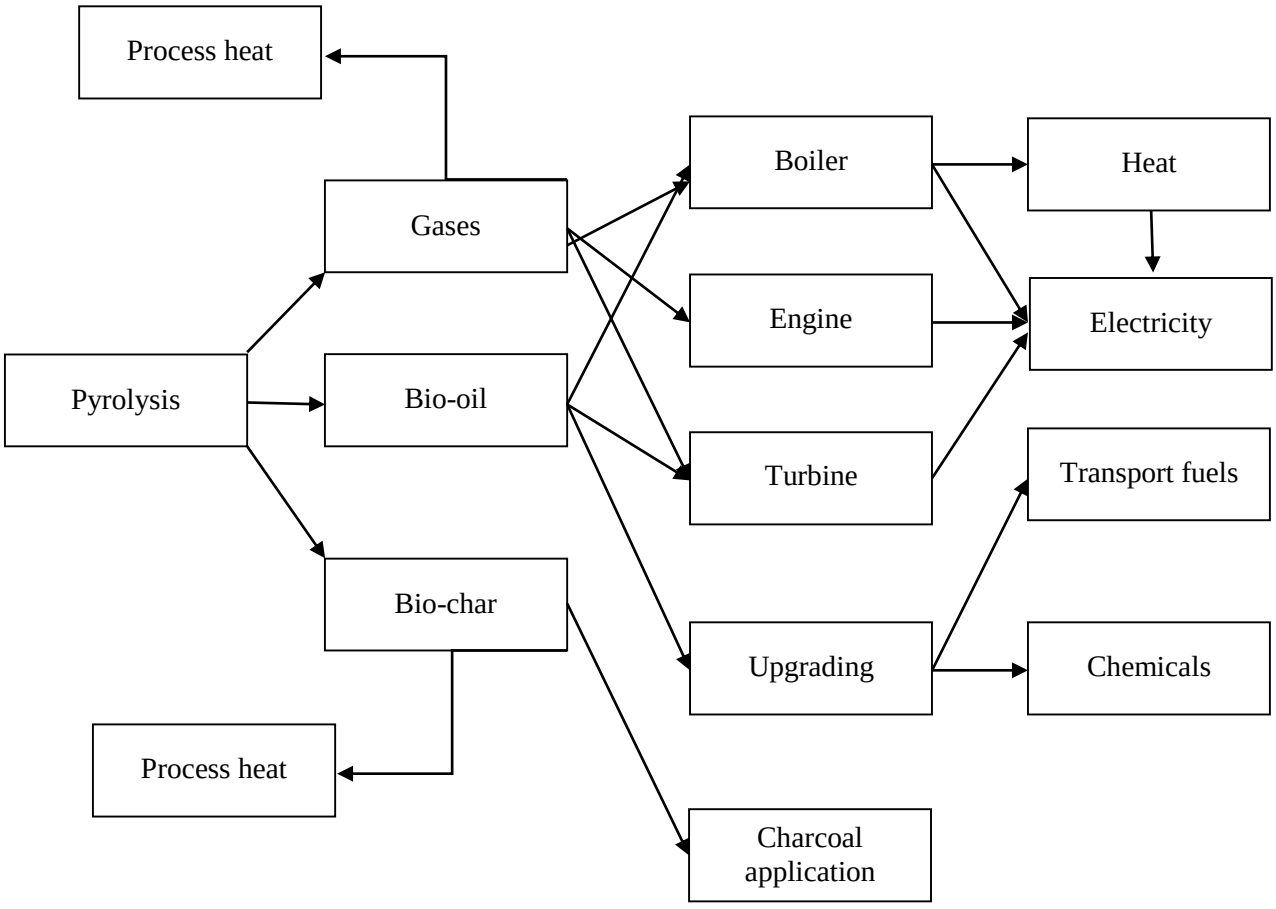

Fig. 1. 1. Application of pyrolysis products

10. Catalytic pyrolysis

Bio-oil produced from fast pyrolysis can be used as energy substituent or chemical feedstock, but the effective use of bio-oil is restricted due to drawbacks in the properties. Bio-oil produced from pyrolysis are highly acidic, viscous, oxygenated, and low in energy content (Bulushev and Ross, 2011). The comparison of bio-oil properties with conventional transportation fuel shows that bio-oil contains heavy compounds with long carbon chain, low H/C ratio and high O/C ratio

(Mohan et al., 2006; Perego and Bosetti, 2011; Bulushev and Ross, 2011). Thus, upgrading of bio-oil is crucial in order to use bio-oil as transportation fuels. The upgrading processes are mainly focused on removing the oxygenated compounds, which are responsible for reducing the quality of the bio- oil. The upgrading of bio-oil can be done by two methods namely hydrotreating and catalytic cracking. Hydrotreating are performed at a temperature of around 350^{o}C, under high pressure of hydrogen, in the presence of heterogeneous Co–Mo, Ni–Mo based catalysts (Elliott, 2007). Hydrotreating is an effective process for producing hydrocarbon rich fuel from bio-oil, by eliminating oxygen mainly through water and carbon dioxide (Perego and Bosetti, 2011). However the need for hydrogen input, high pressure, and catalyst deactivation makes hydroprocessing less attractive from economic point of view (Zhang et al., 2009a; French and Czernik, 2010).

Catalytic pyrolysis on the other hand is operated at atmospheric pressure, wide variety of catalyst available based on the product needed and can be integrated in the unit used for pyrolysis (Zhang et al., 2009a; French and Czernik, 2010; Park et al., 2011). The main aim of catalytic cracking is to reduce acidity, viscosity, oxygen content, increase heating value and produce low carbon chain compounds. Many different kinds of catalyst have been used in the past for biomass pyrolysis some of them are Si-SBA-15, Al-SBA-15 (Cho et al., 2011); ZSM-5 zeolite (López et al., 2011); H-ZSM-5-28 and H-ZSM-5-80 (Azeez et al., 2011); H-ZSM-5 (Agblevor et al., 2010b); nickel, cobalt, iron, and gallium-substituted ZSM-5 (French and Czernik, 2010); X-zeolite, Y-zeolite (Carlson et al., 2009); H-Beta zeolite (Aho et al., 2011); SN-27, MSN-15, MSM-15 (Azeez et al., 2011), Ni/Al2O3 catalyst (Rodjeen et al., 2006). However, zeolite based catalyst which contains the suitable porous structure and acidic properties are often used for biomass pyrolysis (Bulushev and Ross, 2011).

10.1. Zeolite

Zeolite based catalyst has been previously used in petrochemical industry and from late 1900's it is used in catalytic pyrolysis of biomass to upgrade the bio-oil (Park et al., 2011). The comparison of non-catalytic and catalytic pyrolysis showed that, catalytic pyrolysis decreased the organic fraction but, ZSM-5 gave high liquid yield compared to other forms of zeolite catalyst (Aho et al., 2008; Perego and Bosetti, 2011). In terms of bio-oil quality and catalyst stability HZSM-5 was concluded to be effective catalyst when compared to other forms of zeolite catalyst (Park et al., 2011). The study conducted to compare the catalytic effect of ZSM5, Y-zeolite, mordenite, silicate and silica alumina concluded that ZSM5 produced high yields of hydrocarbons, with higher proportion of aromatics than aliphatic hydrocarbons (Adjaye and Bakhshi, 1995). The composition of bio-oil from pyrolysis of cellulose, cellobiose, glucose and xilitol with different catalyst, showed that ZSM-5 resulted in high concentration of aromatics than aliphatics (Carlson et al., 2009). Catalytic upgrading of bio-oil with HZSM-5 and HY zeolites, showed that HZSM-5 produced highly deoxygenated oil with high energy content (Vitolo et al., 1999). The reaction which takes place during catalytic pyrolysis using HZSM-5 includes cracking, deoxygenation, aromatization and polymerization (Park et al., 2011). Thus, ZSM5 has been demonstrated to effectively transform pyrolysis vapors into upgraded bio-oils.

10.2. Red mud

From a commercial point of view, use of high-priced catalyst results in increasing the operational cost. Price of catalyst is an important factor when the economics of the process is considered (López et al., 2011). Thus the search of cheap catalyst is of at most interest. Red mud is a solid waste from bayer process, used for producing pure alumina from bauxite ore (Karimi et al., 2010). The amount of red mud produced depends on the process and the quality of the ore used (Sushil and Batra, 2008). Red mud are produced in large quantity (>70 x 10^6 ton / year) and

occupies vast area. Red mud are usually alkaline, and are classified as hazardous material (Sushil and Batra, 2008). Thus, efficient way of using red mud is of economic concern (Karimi et al., 2010). Red mud consists of different concentration of Fe_2O_3, SiO_3, Al_2O_3, TiO_2, CaO, MgO, K_2O, and Na2O which are present in bauxite ore and introduced during bayers process. Ferric oxide is present in large proportion compared to other compounds and responsible for the red color. The surface area of red mud is low and is between 20-30 m^2/g. Red mud which consists of metal oxides is a potential alternative catalyst in industrial scale (Sushil and Batra, 2008). Usage of Red mud as catalyst serves two purpose, namely 1) Effective usage of waste material 2) reduces the cost of catalyst in pyrolysis. Red mud has been used as hydrogenation and liquefaction catalyst, the results showed that they are not susceptible to catalyst poisons like sulfur (Sushil and Batra, 2008). The hydro-liquefaction of oil shale showed that, sulfur promoted red mud had better activity than original red mud and commercial metal supported catalyst (Metecan et al., 2003). Comparison of catalytic efficiency on pyrolysis of hazelnut shell concluded that metal oxides in red mud converted heavy molecular weight compounds to low molecular weight compounds (Gokdai et al., 2010). Red mud has been used as a catalyst for the pyrolysis of plastic waste (López et al., 2011), upgrading of hemp-seed oil (Karimi et al., 2010), degradation of vinyl chloride polymer (Yanik et al., 2001), hydro-liquefaction of biomass (Klopries et al., 1990). Thus, red mud has wide range of catalytic effect, but is low compared to noble metals (commercial catalyst). The lower catalytic activity of red mud is mainly due to low surface area and low concentration of specific metals. However, the catalytic effect of red mud could be improved by some physical or chemical treatments (Sushil and Batra, 2008). Red mud has not been extensively studied in catalytic pyrolysis of biomass and if found comparable to commercial catalyst, offers an advantage of reducing the cost of catalyst.

Currently, there is no detailed literature on 1) characterization and pyrolysis of pinyon juniper biomass, which is available in large quantity and 2) Red mud as catalyst on biomass pyrolysis. Hence, this research is mainly focuses on producing value added products from pinyon juniper biomass via pyrolysis and upgrading of the bio-oil, through catalytic pyrolysis using red mud as catalyst.

11. Objectives

The overall aim of this research is to explore the use of pinyon juniper biomass in conventional and catalytic pyrolysis and also study the effect of red mud on catalytic pyrolysis of biomass.

The specific objectives are

1. Biomass characterization of wood, bark and mixture of pinyon juniper biomass.
2. Determine the effect of temperature and different type (form) of biomass on pyrolysis yield.
3. Optimization of process parameters (temperature, flow rate, feed rate) for maximum liquid yield.
4. Comparison of conventional pyrolysis (sand) and catalytic pyrolysis (ZSM-5, red mud).

12. References

Adjaye, J., and Bakhshi, N.N., 1995. Production of hydrocarbon by catalytic upgrading of pyrolysis bio-oil. Fuel Processing Technology *45*, 185–202.

Agblevor, F.A., Besler, S., 1996. Inorganic compounds in biomass feedstocks. 1. Effect on the quality of fast pyrolysis oils. Energy & Fuels *10*, 293–298.

Agblevor, F.A., Besler, S., Wiselogel, A.E., 1995. Fast pyrolysis of stored biomass feedstocks. Energy Fuels *9*, 635–640.

Agblevor, F.A., Beis, S., Mante, O., Abdoulmoumine, N., 2010a. Fractional Catalytic Pyrolysis of Hybrid Poplar Wood. Ind. Eng. Chem. Res. *49*, 3533–3538.

Agblevor, F.A., Beis, S., Kim, S.S., Tarrant, R.,Mante, N.O., 2010b. Biocrude oils from the fast pyrolysis of poultry litter and hardwood. Waste Management *30*, 298–307.

Aho, A., Kumar, N., Eränen, K., Salmi, T., Hupa, M., Murzin, D.Y., 2008. Catalytic pyrolysis of woody biomass in a fluidized bed reactor: Influence of the zeolite structure. Fuel *87*, 2493–2501.

Aho, A., Tokarev, A., Backman, P., Kumar, N., Eränen, K., Hupa, M., Holmbom, B., Salmi, T., Murzin, D.Y., 2011. Catalytic pyrolysis of pine biomass over H-beta zeolite in a dual-fluidized bed reactor: effect of space velocity on the yield and composition of pyrolysis products. Top. Catal. *54*, 941–948.

Ansley, R.J., Wiedemann, H.T., Castellano, M.J., Slosser, J.E., 2006. Herbaceous restoration of juniper dominated grasslands with chaining and fire. Rangel. Ecol. Manag. *59*, 171–178.

Aro, R.S., 1971. Evaluation of Pinyon-Juniper Conversion to Grassland. J. Range Manag. *24*, 188–197.

Azeez, A.M., Meier, D., Odermatt, J., Willner, T., 2011. Effects of zeolites on volatile products of beech wood using analytical pyrolysis. J. Anal. Appl. Pyrolysis *91*, 296–302.

Babu, B.V., 2008. Biomass pyrolysis: a state-of-the-art review. Biofuels Bioprod. Biorefining *2*, 393–414.

Baughman, C., Forbis, T.A., Provencher, L., 2010. Response of two sagebrush sites to low-disturbance, mechanical removal of piñyon and juniper. Invasive Plant Sci. Manag. *3*, 122–129.

Biswas, A.K., Umeki, K., Yang, W., Blasiak, W., 2011. Change of pyrolysis characteristics and structure of woody biomass due to steam explosion pretreatment. Fuel Process. Technol. *92*, 1849–1854.

Blin, J., Volle, G., Girard, P., Bridgwater, T., Meier, D., 2007. Biodegradability of biomass pyrolysis oils: Comparison to conventional petroleum fuels and alternatives fuels in current use. Fuel *86*, 2679–2686.

Boateng, A.A., Hicks, K.B., Vogel, K.P., 2006. Pyrolysis of switchgrass (Panicum virgatum) harvested at several stages of maturity. J. Anal. Appl. Pyrolysis *75*, 55–64.

Brewer, C.E., Schmidt-Rohr, K., Satrio, J.A., Brown, R.C., 2009. Characterization of biochar from fast pyrolysis and gasification systems. Environ. Prog. Sustain. Energy *28*, 386–396.

Bridgwater, A.V., 1996. Production of high grade fuels and chemicals from catalytic pyrolysis of biomass. Catal. Today *29*, 285–295.

Bridgwater, A.V., 2012a. Upgrading biomass fast pyrolysis liquids. Environ. Prog. Sustain. Energy *31*, 261–268.

Bridgwater, A.V., 2012b. Review of fast pyrolysis of biomass and product upgrading. Biomass Bioenergy *38*, 68–94.

Bridgwater, A.V., Peacocke, G.V.C., 2000. Fast pyrolysis processes for biomass. Renew. Sustain. Energy Rev. *4*, 1–73.

Bridgwater, A.V., Meier, D., Radlein, D., 1999. An overview of fast pyrolysis of biomass. Org. Geochem. *30*, 1479–1493.

Bridgwater, A.V., Toft, A.J., Brammer, J.G., 2002. A techno-economic comparison of power production by biomass fast pyrolysis with gasification and combustion. Renew. Sustain. Energy Rev. *6*, 181–246.

Bridgwater, T., 2006. Biomass for energy. J. Sci. Food Agric. *86*, 1755–1768.

Briens, C., Piskorz, J., Berruti, F., 2008. Biomass valorization for fuel and chemicals production–a review. Int. J. Chem. React. Eng. *6*.

Brockway, D.G., Gatewood, R.G., Paris, R.B., 2002. Restoring grassland savannas from degraded pinyon-juniper woodlands: effects of mechanical overstory reduction and slash treatment alternatives. J. Environ. Manage. *64*, 179–197.

Brown, J.N., Brown, R.C., 2012. Process optimization of an auger pyrolyzer with heat carrier using response surface methodology. Bioresour. Technol. *103*, 405–414.

Bulushev, D.A., Ross, J.R.H., 2011. Catalysis for conversion of biomass to fuels via pyrolysis and gasification: A review. Catal. Today *171*, 1–13.

Butler, E., Devlin, G., Meier, D., McDonnell, K., 2011. A review of recent laboratory research and commercial developments in fast pyrolysis and upgrading. Renew. Sustain. Energy Rev. *15*, 4171–4186.

Carlson, T.R., Tompsett, G.A., Conner, W.C., Huber, G.W., 2009. Aromatic production from catalytic fast pyrolysis of biomass-derived feedstocks. Top. Catal. *52*, 241–252.

Chambers, J.C., Vander Wall, S.B., Schupp, E.W., 1999. Seed and seedling ecology of pinyon and juniper species in the pygmy woodlands of Western North America. Bot. Rev. *65*, 1–38.

Cho, H.J., Heo, H.S., Jeon, J.K., Park, S.H., Jeong, K.E., Park, Y.K., 2011. Catalytic conversion of wood waste to bio-oil using mesoporous SBA-15 catalyst. Rev Adv Mater Sci *28*, 150–153.

Czernik, S., Bridgwater, A.V., 2004. Overview of Applications of Biomass Fast Pyrolysis Oil. Energy Fuels *18*, 590–598.

Elliott, D.C., 2007. Historical developments in hydroprocessing bio-oils. Energy Fuels *21*, 1792–1815.

Evans, R.A., 1988. Management of Pinyon-Juniper Woodlands. USDA For. Serv. Rep. INT-249 Ogden UT.

Fair, A., Schweinle, D., Scholl, S., Becker, G., Meier, D., 2010. Life-cycle assesment of BTO-process with combined heat and power generation. Enviormental Prog. Sustain. Energy *29*, 193–202.

French, R., Czernik, S., 2010. Catalytic pyrolysis of biomass for biofuels production. Fuel Process. Technol. *91*, 25–32.

Garcia-Perez, M., Adams, T.T., Goodrum, J.W., Geller, D.P., Das, K.C., 2007. Production and Fuel Properties of Pine Chip Bio-oil/Biodiesel Blends. Energy Fuels *21*, 2363–2372.

Garcia-Perez, M., Wang, X.S., Shen, J., Rhodes, M.J., Tian, F., Lee, W.-J., Wu, H., Li, C.-Z., 2008. Fast Pyrolysis of Oil Mallee Woody Biomass: Effect of Temperature on the Yield and Quality of Pyrolysis Products. Ind. Eng. Chem. Res. *47*, 1846–1854.

Gerçel, H.F., Gerçel, ö., 2007. Bio-oil Production from an Oilseed By-product: Fixed-bed Pyrolysis of Olive Cake. Energy Sources Part Recovery Util. Environ. Eff. *29*, 695–704.

Gokdai, Z., Sinag, A., Yumak, T., 2010. Comparision of catalytic efficiency of synthesized nano tin oxide catalyst and various catalyst for the pyrolysis of hazelnut shell. Biomass Bioenergy *34*, 402–410.

Gust, S., Oy, N., 1997. Combustion experience of flash pyrolysis fuels in intermediate size boilers. Dev. Thermochem. Biomass Convers. *1*, 481–488.

Hodgkinson, K.C., Harrington, G.N., 1985. The case for prescribed burning to control shrubs in eastern semi-arid woodlands. Rangel. J. *7*, 64–74.

Hoekstra, E., Hogendoorn, K.J.A., Wang, X., Westerhof, R.J.M., Kersten, S.R.A., van Swaaij, W.P.M., Groeneveld, M.J., 2009. Fast pyrolysis of biomass in a fluidized bed reactor: in situ filtering of the vapors. Ind. Eng. Chem. Res. *48*, 4744–4756.

Ingram, L., Mohan, D., Bricka, M., Steele, P., Strobel, D., Crocker, D., Mitchell, B., Mohammad, J., Cantrell, K., Pittman, C.U., 2008. Pyrolysis of wood and bark in an auger reactor: physical properties and chemical analysis of the produced bio-oils. Energy Fuels *22*, 614–625.

Karimi, E., Briens, C., Berruti, F., Moloodi, S., Tzanetakis, T., Thomson, M.J., Schlaf, M., 2010. Red mud as a catalyst for the upgrading of hemp-seed pyrolysis bio-oil. Energy Fuels *24*, 6586–6600.

Kersten, S.R.A., Wang, X., Prins, W., van Swaaij, W.P.M., 2005. Biomass pyrolysis in a fluidized bed reactor. Part 1: literature review and model simulations. Ind. Eng. Chem. Res. *44*, 8773–8785.

Kim, K.H., Eom, I.Y., Lee, S.M., Choi, D., Yeo, H., Choi, I.-G., Choi, J.W., 2011. Investigation of physicochemical properties of biooils produced from yellow poplar wood (Liriodendron tulipifera) at various temperatures and residence times. J. Anal. Appl. Pyrolysis *92*, 2–9.

Klopries, B., Hodek, W., Bandermann, F., 1990. Catalytic hydroliquifaction of biomass with redmud and CoO-MoO3 catalyst. Fuel *69*, 448–455.

Knapp, P.A., Soule, P.T., 1999. Geographical distribution of an 18th-century heart rot outbreak in western juniper (Juniperus occidentalis spp. occidentalis Hook.). J. Arid Environ. *41*, 247–256.

Lehmann, J., Gaunt, J., Rondon, M., 2006. Bio-char Sequestration in Terrestrial Ecosystems – A Review. Mitig. Adapt. Strateg. Glob. Change *11*, 395–419.

Liu, Y., Zhao, X., Li, J., Ma, D., Han, R., 2012. Characterization of bio-char from pyrolysis of wheat straw and its evaluation on methylene blue adsorption. Desalination Water Treat. *46*, 115–123.

López, A., de Marco, I., Caballero, B.M., Laresgoiti, M.F., Adrados, A., Aranzabal, A., 2011. Catalytic pyrolysis of plastic wastes with two different types of catalysts: ZSM-5 zeolite and Red Mud. Appl. Catal. B Environ. *104*, 211–219.

Mante, O.D., Agblevor, F.A., McClung, R., 2011. Fluid catalytic cracking of biomass pyrolysis vapors. Biomass Convers. Biorefinery *1*, 189–201.

Metecan, I.H., Karayildirim, T., Yanik, J., Saglam, M., Yuksel, M., 2003. The effect of sulfur-promoted red mud catalysts on hydroliquefaction of oil shale. Oil Shale *20*, 69–79.

Miller, R.F., Bates, J.D., Svejcar, T.J., Pierson, F.B., Eddleman, L.E., 2005. Biology, ecology, and management of western juniper (Juniperus occidentalis). Tech. Bull. 152 Agric. Exp. Stn. Or. State Univ. Corvalis Or.

Miller, R.F., Tausch, R.J., 2001. The role of fire in juniper and pinyon woodlands: a descriptive analysis. KEM Galley TP Wilson Eds 15–30.

Miller, R.F., Wigand, P.E., 1994. Holocene changes in semiarid pinyon-juniper woodlands. BioScience *44*, 465–474.

Mohan, D., Pittman, C.U., Steele, P.H., 2006. Pyrolysis of wood/biomass for bio-oil: a critical review. Energy Fuels *20*, 848–889.

Mullen, C.A., Strahan, G.D., Boateng, A.A., 2009. Characterization of various fast-pyrolysis bio-oils by NMR spectroscopy. Energy Fuels *23*, 2707–2718.

Neves, D., Thunman, H., Matos, A., Tarelho, L., Gomez-Barea, A., 2011. Characterization and prediction of biomass pyrolysis products. Prog. Energy Combust. Sci. *37*, 611–630.

Nguyen, D., Honnery, D., 2008. Combustion of bio-oil ethanol blends at elevated pressure. Fuel *87*, 232–243.

Pandey, M.P., Kim, C.S., 2011. Lignin depolymerization and conversion: a review of thermochemical methods. Chem. Eng. Technol. *34*, 29–41.

Park, H.J., Jeon, J.-K., Suh, D.J., Suh, Y.-W., Heo, H.S., Park, Y.-K., 2011. Catalytic vapor cracking for improvement of bio-oil quality. Catal. Surv. Asia *15*, 161–180.

Pattiya, A., 2011. Bio-oil production via fast pyrolysis of biomass residues from cassava plants in a fluidized-bed reactor. Bioresour. Technol. *102*, 1959–1967.

Perego, C., Bosetti, A., 2011. Biomass to fuels: The role of zeolite and mesoporous materials. Microporous Mesoporous Mater. *144*, 28–39.

Petrus, L., Noordermeer, M.A., 2006. Biomass to biofuel,a chemical perspective. R. Soc. Chem. *8*, 861–867.

Pettersen, R.C., 1984. The chemical composition of wood. Am. Chem. Soc. Washington. DC 57–126.

Piskorz, J., Majerski, P., Radlein, D., Scott, D.S., Bridgwater, A.V., 1998. Fast pyrolysis of sweet sorghum and sweet sorghum bagasse. J. Anal. Appl. Pyrolysis *46*, 15–29.

Polley, H. Wayne, Johnson, H.B., Marino, B.D., Mayeux, H.S., 1993. Increase in C3 plant water-use efficiency and biomass glacial to present CO2 concentration. Nature *361*, 61–64.

Pu, Y., Kosa, M., Kalluri, U.C., Tuskan, G.A., Ragauskas, A.J., 2011. Challenges of the utilization of wood polymers: how can they be overcome? Appl. Microbiol. Biotechnol. *91*, 1525–1536.

Rodjeen, S., Mekasut, L., Kuchontara, P., Piumsomboon, P., 2006. Parametric studies on catalytic pyrolysis of coal-biomass mixture in a circulating fluidized bed. Korean J. Chem. Eng. *23*, 216–223.

Salehi, E., Abedi, J., Harding, T., 2011. Bio-oil from sawdust: effect of operating parameters on the yield and quality of pyrolysis products. Energy Fuels *25*, 4145–4154.

Sanderson, M.A., Agblevor, F., Collins, M., Johnson, D.K., 1996. Compositional analysis of biomass feedstocks by near infrared reflectance spectroscopy. Biomass Bioenergy *11*, 365–370.

Scholes, R.J., Archer, S.R., 1997. Tree-grass interactions in savannas. Annu. Rev. Ecol. Syst. *28*, 517–544.

Schröder, E., 2004. Experiments on the pyrolysis of large beechwood particles in fixed beds. J. Anal. Appl. Pyrolysis *71*, 669–694.

Scott, D.S., Majerski, P., Piskorz, J., Radlein, D., 1999. A second look at fast pyrolysis of biomass—the RTI process. J. Anal. Appl. Pyrolysis *51*, 23–37.

Sensoz, S., Angin, D., Yorgun, S., 2000. Biooil production from an oilseed crop: fixed-bed pyrolysis of rapeseed (Brassica napus L.). Energy Sources *22*, 891–899.

Sushil, S., Batra, V.S., 2008. Catalytic applications of red mud, an aluminium industry waste: A review. Appl. Catal. B Environ. *81*, 64–77.

Tausch, R.J., Chambers, J.C., Blank, R.R., Nowak, R.S., 1993. Differential establishment of perennial grass and cheatgrass following fire on an ungrazed sagebrush-juniper site. Wildland Shrub Arid Land Restor. Symp. Las Vegas NV Gen Tech Rep INT-GTR-315.

Underwood, G., Graham, R., 1989. Methods of using fast pyrolysis liquids as liquid smoke. US Pat. 4 876 108.

Vamvuka, D., 2011. Bio-oil, solid and gaseous biofuels from biomass pyrolysis processes-An overview. Int. J. Energy Res. *35*, 835–862.

Venderbosch, R.H., Prins, W., 2010. Fast pyrolysis technology development. Biofuels Bioprod. Biorefining *4*, 178–208.

Vitolo, S., Seggiani, M., Frediani, P., Ambrosini, G., Politi, L., 1999. Catalytic upgrading of pyrolytic oils to fuel over different zeolites. Fuel *78*, 1147–1159.

Wang, Y., Li, X., Mourant, D., Gunawan, R., Zhang, S., Li, C.-Z., 2012. Formation of aromatic structures during the pyrolysis of bio-oil. Energy Fuels *26*, 241–247.

Weisberg, P.J., Lingua, E., Pillai, R.B., 2007. Spatial patterns of pinyon–juniper woodland expansion in Central Nevada. Rangel. Ecol. Manag. *60*, 115–124.

West, N.E., Tausch, R.J., Tueller, P.T., 1998. A management-oriented classification of pinyon-juniper woodlands of the Great Basin. US Dep. Agric. For. Serv. Rocky Mt. Res. Stn. Ogden UT Gen. Tech. Rep. RMRS-GTR-12 495.

Westerhof, R.J.M., Brilman, D.W.F. (Wim), van Swaaij, W.P.M., Kersten, S.R.A., 2010. Effect of temperature in fluidized bed fast pyrolysis of biomass: oil quality assessment in test units. Ind. Eng. Chem. Res. *49*, 1160–1168.

Yanik, J., Uddin, M.A., Ikeuchi, K., Sakata, Y., 2001. The catalytic effect of red mud on the degradation of poly (vinyl chloride) containing polymer mixture into fuel oil. Polym. Degrad. Stab. *73*, 335–346.

Zhang, H., Xiao, R., Wang, D., Zhong, Z., Song, M., Pan, Q., He, G., 2009. Catalytic fast pyrolysis of biomass in a fluidized bed with fresh and spent fluidized catalytic cracking (FCC) catalysts. Energy Fuels *23*, 6199–6206.

Zhang, Q., Chang, J., Wang, T., Xu, Y., 2007. Review of biomass pyrolysis oil properties and upgrading research. Energy Convers. Manag. *48*, 87–92.

CHAPTER 2

BIOMASS CHARACTERIZATION AND PYROLYSIS OF PINYON JUNIPER BIOMASS

1. Abstract

Pinyon Juniper (PJ) biomass mixture consists wood and bark, in which wood is the main component of the mixture. In this study PJ wood, bark and mixture was characterized based on the proximate and ultimate analysis. Pyrolysis of PJ wood, bark and mixture was carried out at 475 ^{o}C in order to find the effect of the individual components on the product yield and the quality of bio-oil. Pyrolysis of PJ mixture was done at different temperature (475, 550, 600 ^{o}C) in order to find the effect of temperature on product yield and the quality of bio-oil. The results obtained for biomass characterization showed that the presence of bark in the mixture significantly affected the ash, carbon, nitrogen, oxygen, energy, carbohydrate, lignin and extractives content of PJ mixture biomass when compared to PJ wood. The pyrolysis of PJ wood, mixture and bark showed that the wood produced maximum organic yield followed by mixture and bark. The maximum char yield was obtained by bark followed by mixture and wood. Thus, the presence of bark in mixture reduces the liquid yield and increases the char yield. The Effect of temperature on the pyrolysis of PJ mixture showed that as the temperature increased the liquid and char yield decreased, while the gas yield increased. The increase in temperature also increased the viscosity of the bio-oil. The elemental composition and the energy content of the bio-oil were not affected much due to the increase in temperature. The results obtained showed that PJ biomass could be used as feedstock for biomass pyrolysis.

2. Introduction

Most of the world's energy need is supplied by fossil fuel. The depletion of fossil fuel and the concern on greenhouse gas effect on the environment, have forced to pay more concentration on renewable energy source (Bridgwater et al., 2002; Babu, 2008; Butler et al., 2011). Biomass is one of the renewable energy source and the only source for producing liquid fuel (Bridgwater et al., 1999). Pinyon Juniper woodlands are coniferous woodland which consists of different species of pinyon and juniper trees, and occupy about 47 million acres in Western United States (Evans, 1988; Chambers et al., 1999). The factors which contributed for the expansion of PJ woodlands are a) climate, b) livestock grazing, c) atmospheric CO_2, and d) fire (Miller et al., 2005; Ansley et al., 2006; Weisberg et al., 2007; Baughman et al., 2010). In recent years PJ woodlands are extensively studied due to the problems caused by them. PJ woodlands domination decreases the herbaceous vegetation, increase bare lands which in turn increases soil erosion and nutrition loss (Miller and Wigand, 1994; Brockway et al., 2002). Studies have shown that expansion of PJ woodlands have reduced the magnitude of precipitation (Miller et al., 2005), and increased soil erosion by four times (Carrara and Carroll, 2007). PJ woodlands increases the possibility of crown fires, which promotes the infiltration of exotic species (Tausch et al., 1993). Thus due to these problems land managing agencies are focusing on reducing the population of pinyon and junipers trees and restore the herbaceous vegetation (Ansley et al., 2006). Thus large amount of energy has to be invested in order to clear these woodlands. In order to account for the energy invested, the harvested biomass should be processed to produce high value products. The harvested biomass is a combination of wood and bark of different species of PJ trees. Currently, this biomass is used as fire woods, particle-flake boards, fences, and Christmas decoration trees. Honey lake power located in Wendell, California is one of the largest users of western junipers for power production, which could not account for the energy invested in harvesting (Miller et al., 2005). Thus technology for

processing lignocellulosic biomass into value added products should be investigated to solve the energy problem.

Pyrolysis is a promising technology for producing liquid fuel, which could be co-cracked with crude oil (Agblevor et al., 2012), and has not been investigated for PJ biomass. Pyrolysis is defined as thermo-chemical degradation of lignocellulosic biomass into solid, liquid and gaseous fuel in the absence of an oxidizing agent. Lignocellulosic biomass is mainly composed of cellulose (23-53%), hemicelluloses (20-35%), lignin (10-25%) and extraneous compounds (Petrus and Noordermeer, 2006). The components of the biomass are different from each other and undergo degradation at different temperatures (Bridgwater, 2012). Thus the difference in the structural component, the amount of oxygen and heteroatoms present affects the distribution of pyrolysis products (Akhtar and Saidina Amin, 2012). To investigate the effect of wood and bark in the pyrolysis of PJ biomass, the physical and chemical composition of biomass should be determined. The main objective of this chapter was to a) characterize Pinyon Juniper wood, bark and mixture, and predict their influence on pyrolysis products; b) Study the effect of wood, bark and mixture on product distribution, physical and chemical properties of the product produced from pyrolysis of PJ biomass; and c) Study the effect of temperature on the pyrolysis of PJ mixture biomass.

3. Material and Methods

3.1. Feedstock

Pinyon Juniper biomass mixture obtained from USA Bureau of Land Management consists of wood and bark. The wood and bark were separated manually (by hand), dried, and grounded until it passed through a 1mm sieve. The grounded biomass was then used for biomass characterization and pyrolysis experiments.

Fig. 2. 1. Photographs of various pinyon juniper fractions (a - PJ wood, b – PJ mixture, c – PJ bark)

3.2. Total solids in PJ biomass (Moisture content)

The moisture content of the biomass was determined according to ASTM E1756 - 08, standard method. Infrared moisture analyzer (Denver instruments, IR 60) was used to determine the moisture content. 2.0 g of biomass was placed in a tarred aluminum pan, and dried at 105^{o} C for 30 minutes. The moisture analyzer displays the result as mass percent total solid. Samples are analyzed in triplicates and the average value is reported as total solids in biomass.

3.3. Ash content of PJ biomass and bio-oil

The ash content of the biomass and bio-oil was determined using ASTM E1755-01 (2007), standard method. 1.0 g of sample was ashed at 575^{o} C for 3 h in lindberg blue M muffle furnace (Thermal Product Solutions, USA). After 3hrs, Samples were removed, cooled in a desiccator and weighed. The samples were again placed at 575^{o} C for 1 h, then removed, cooled in a desiccator and reweighed. The above step was repeated until the difference of mass after cooling was within 0.3 mg. samples were analyzed in triplicates and the average value were reported as ash content on moisture free basis. Ash content was calculated according to the equation (1).

$$\textbf{ash}\ (\%) = \frac{(\mathbf{m_{ash} - m_{cont}})\mathbf{X\ 100}}{(\mathbf{m_{od} - m_{cont}})} \qquad (1)$$

Where

Ash (%) = mass percent of ash, based on 105^{o}C oven dried mass of the biomass

m_{ash} = mass of ash and container, g

m_{cont} = mass of container, g

m_{od} = initial mass of 105^{o}C oven dried sample and container, g

3.4. Bulk density of PJ biomass

The bulk density of the biomass was determined using ASTM D1895-B, standard method. Biomass was allowed to flow freely, with the help of a funnel into a tarred 100 ml measuring cylinder. The weight of biomass used to fill the cylinder was measured and the bulk density was calculated using the equation (2).

$$\textbf{Bulk density}\left(\frac{\mathbf{g}}{\mathbf{cm^3}}\right) = \frac{\textbf{weight of the sample (g)}}{\textbf{volume of packed sample (cm}^3\textbf{)}} \quad (2)$$

3.5. Ultimate analysis of PJ biomass

The elemental composition (C, H, N, S, and O) of biomass and bio-oil was determined by using the organic elemental analyzer (Flash 2000 CHNS-O analyzer, Thermo Scientific Inc, MA, USA). The CHNS content were determined by combusting the sample in the presence of oxygen. The gases produced by combustion are passed through a layer filled with copper, separated by GC column and finally detected by thermal conductivity detector (TCD). Oxygen content is determined by pyrolysing the sample in a reactor containing nickel coated with carbon. The samples were analyzed thrice and averaged.

3.6. Higher heating value (HHV) of PJ biomass

The Heat of combustion of the samples (biomass, bio-oil) was determined by using IKA C2000 basic bomb calorimeter (IKA® Works Inc, NC, USA). 0.5 g of sample was combusted in oxygen

environment, under pressure. The heat produced during the combustion was used to calculate the energy content of the sample expressed in MJ/kg. The samples were analyzed thrice and the average value is represented as HHV of the samples.

3.7. Determination of extractives content of PJ biomass

Ethanol extractives of the biomass was determined by using ASTM E1690 - 08, standard method. The soxhlet apparatus was assembled with 10.0 g of biomass in the extraction thimble, 160 ml of 190 proof ethanol. The heating rate was adjusted so that at least four solvent exchanges take place in an hour. After extraction the ethanol was evaporated and the extractives content were weighed. The results are reported on moisture free basis.

3.8. Acid insoluble residue (lignin) of PJ biomass

The acid insoluble residue of the biomass was determined using ASTM E1721 – 01(2009), standard method. The extractive free biomass sample was used. The solid residue which remains after the primary (72% H_2SO_4) and secondary (4% H_2SO_4) hydrolysis represents the acid insoluble lignin content of the biomass.

3.9. TGA analysis of PJ biomass

Thermogravimetric analysis of biomass was done on TGA Q500 (TA instruments, DE, USA). 10.0 mg of biomass was heated unto 950^o C at a rate of 10^o C/min. The resulting graph displays the weight loss and derivative weight loss percent as a function of time. The samples were analyzed three times to check the reproducibility.

3.10. Pyrolysis of PJ biomass

Pyrolysis of biomass was carried out in bench scale fluidized bed reactor situated at the Thermochemical and biomass research laboratory located at USTAR Bioinnovations Center

described in Agblevor et al. (2010a) and Mante et al. (2011). The pyrolysis unit (Figure 2.2) consists of twin screw feeder (K-Tron, NJ, USA), fluidized bed reactor (equipped with 100µm gas distributor), hot gas filter (equipped with 10µm filter), two condensers (whose temperatures are maintained by water and ethylene glycol mixture), electrostatic precipitator (ESP), coalescing filter (2 µm), Micro GC (varian 490- GC, Varian Inc). The reactor was externally heated through a three-zone electric furnace. The bubbling fluid bed was sand (100 g), which was fluidized with nitrogen gas. The pyrolysis was conducted at around 475 ^{o}C, with PJ wood, mixture and bark to study the effect of different biomass. Pyrolysis was also carried out with PJ mixture at different temperature to find out the effect of temperature. The nitrogen flow rate was 18 L/min and the biomass feed rate was 300 g/h.

When the biomass is fed into the reactor through the feeder, heat is transferred into the biomass and broken down into solid (biochar) and gases (condensable vapors and non-condensable gases). Biochar produced was separated from the gases by hot gas filter maintained at 350^{o} C. The condensable vapors were condensed by passing through two condensers connected in series. Any condensable gases and aerosols that escaped from the condensers were captured by the ESP (maintained at 16 KV). The clean non-condensable gases (NCG) were then passed through a coalescing filter and a totalizer and then sampled online with Varian micro GC gas chromatographic analyzer. The excess gases were vented through a flare. The pyrolysis experiments were carried out from 120 min and the oils samples were collected at the end of the run. All experiments were conducted in triplicates to determine reproducibility.

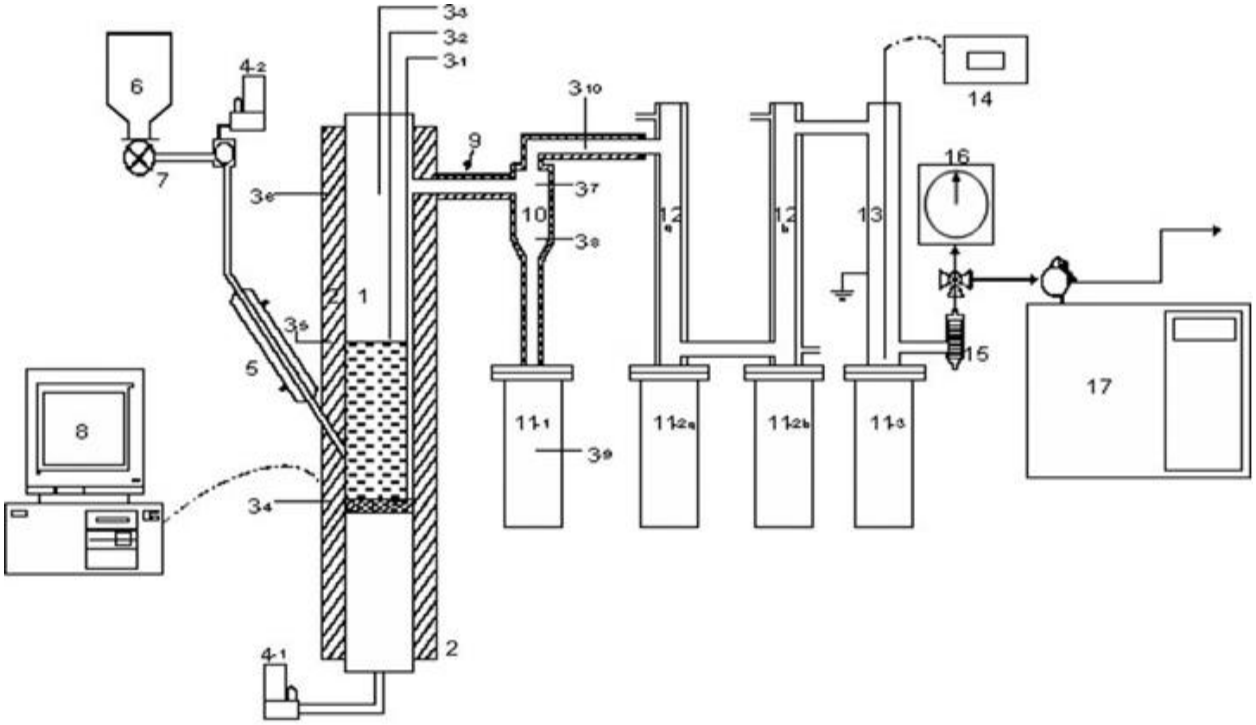

Fig. 2. 2. Laboratory scale bubbling fluidized bed reactor unit

(1-bubbling fluidized bed reactor, 2 - furnace, 3 - thermocouple, 4- mass flow controller, 5- jacketed air-cooled feeder tube, 6 - hopper, 7 – screw feeder, 8 - computer, 9 - insulation, 10 - hot gas filter, 11 - reservoir, 12 - condenser, 13 - ESP, 14 - AC power supply, 15 - filter, 16 – totalizer (mass flow meter), 17 - gas chromatograph)

3.11. Product distribution

All the reaction apparatus (reactor, hot gas filter, condensers, electrostatic precipitator, and filter) were weighed before and after each experiment. This enabled a gravimetric determination of the yield of various components. A fraction of the gases exiting the totalizer (0.1 L/min) was connected to Varian 490-microGC (Agilent Technologies, Santa Clara, CA, USA) for online analysis. The gases were automatically sampled every 7 min for the duration of the experiment. The micro GC was equipped with two modules, a 10 m Molsieve (MS) 5A column, and a 10 m porous polymer (PPU) column. Each module had a thermal conductivity detector. The MS was

used to analyze hydrogen, methane, and carbon monoxide. Carbon dioxide, C_1-C_5 hydrocarbons were analyzed on the PPU column.

3.12. Water content

Water content of the bio oil was determined using Karl Fischer titration. KF titrino 701 (Metrohm AG, Herisau, Switzerland) was used for determining the water content of bio-oil, by karl fischer titration. 50 ml of methanol was taken in the titration vessel, to which known amount of sample is added. The samples were dissolved in methanol and then titrated with KF reagent (Hydranal composite 5). The moisture content was calculated according to the equation (3).

$$\textbf{Moisture content}\ (\%) = \frac{\textbf{Titration volume}\ (\textbf{ml}) \times \textbf{titre}\left(\frac{\textbf{mg}}{\textbf{ml}}\right) \times \textbf{100}}{\textbf{sample quantity}\ (\textbf{g}) \times \textbf{1000}} \qquad (3)$$

3.13. Acidity of PJ biomass pyrolysis oils

The acidity of the bio-oil was determined using seveneasy pH meter s20 (Mettler Toledo AG, Switzerland). The probe was calibrated with standard buffers (pH 7, pH 4, and pH 10) before taking readings. The samples are mechanically stirred and readings are taken after 10 minutes of stabilization. The samples were analyzed in triplicates and the average value is reported as the pH of the sample.

3.14. Viscosity of PJ biomass pyrolysis oils

The viscosity of bio-oil was determined using Brookfield DV-II+ Pro viscometer (Brookfield Engineering Laboratories, Inc. MA, USA.). The system calibration was checked using standard viscosity fluids before taking readings. 7 ml of sample was placed in the sample chamber and then the spindle (Spindle SC4-18) is lowered into the sample. Viscosity readings were taken at 40^o C, with spindle speed ranging between 1 – 50 rpm depending on the sample. The average value at different spindle speed was reported as the viscosity of the sample.

3.15. FTIR of PJ biomass pyrolysis oils

Infrared spectroscopy was obtained using Avatar 360 FTIR spectrometer (Nicolet Instrument Corp, USA) equipped with a DTGS-KBR detector. Samples were analyzed over the range of (4000 – 650) cm^{-1}, with 128 scans and resolution of 4 cm^{-1}.The spectrum was analyzed using OMNIC 7.3 software.

3.16. 13C NMR analysis of PJ biomass pyrolysis oils

The ^{13}C-nmr spectra were recorded on a JOEL 300 MHz NMR spectrometer (JOEL Ltd, Tokyo, Japan). About 1.0 g of oil was dissolved in 0.6 ml dimethyl sulfoxide-d_6 (DMSO-d_6) in a 5 mm sample probe. The DMSO-d_6 containing 1% (v/v) tetramethylsilane (TMS) was obtained from Sigma Aldrich (Sigma Aldrich, St Louis, MO, USA). The observing frequency for the ^{13}C nucleus was 100.58 MHz, the pulse width was 10 μs, the acquisition time was 1.58 s, and the relaxation delay was 2 s. The spectra were obtained with 3000 scans and a sweep width of 20 kHz.

4. Results and discussion

4.1. Characterization of PJ biomass

The proximate, ultimate and component analysis of pinyon juniper biomass are listed in Table 2.1. The ash content of the bark was high (6.05±0.05 %) compared to wood (0.04±0.04 %). The high ash content in the bark is due to inorganic components plus windborne soil particles and grit trapped in the rhytidome (Harkin and Rowe, 1971; Ragland et al., 1991). Wood had higher bulk density (0.29 Kg/L) than bark (0.21 Kg/L). Low bulk density is not appealing, since burning rate of the fuel is directly proportional to the bulk density and also have a negative impact on handling, transportation and storage (Ryu et al., 2006). The carbon, hydrogen and oxygen content of bark were low, compared to wood. The nitrogen content in both wood and bark were low. The sulfur

content of wood and bark were below detectable limit. These results show that the production of NO_x and SO_x gases would be negligible. The low carbon and oxygen content in the bark are due to the high ash content (Corder, 1976). The energy content of wood (19.54±0.16 MJ/kg) was more than bark (17.18±0.05 MJ/kg). The high ash content of the bark attributes to the low energy content. The lignin content of bark was high and the carbohydrate concentration was low compared to wood. The results published on component analysis of biomass with and without bark, also showed that debarked wood had increased cellulose concentration and decreased lignin concentration (Serapiglia et al., 2009). Bark which is the outer part of the wood adapts itself to protect the tree and prevents water evaporation. The extractive content of bark was higher than wood. It is due to the fact that bark includes higher proportion of diverse extractives and phenolic compounds than wood (Serapiglia et al., 2009). Extractives act as intermediates in metabolism and as shield against insect and microbial invasion (Mohan et al., 2006). The comparison of bark properties with wood shows that the proximate and ultimate analyses are significantly different and have negative effect when considering bark as energy fuel. Thus, the amount of bark present in the mixture will affect the properties of pinyon juniper mixture. The ash, carbon, nitrogen, oxygen, energy and extractives content of pinyon juniper mixture are significantly different when compared to wood, which is caused due to the presence of bark in the mixture.

4.2. Thermogravimetric analysis of PJ biomass

The main aim of the TGA analysis of pinyon juniper mixture, wood and bark is to find 1) the degradation profile, 2) calculate the proximate analysis by monitoring the weight loss and compare it with proximate analysis done by standard methods. The plot between temperature and percent weight loss for PJ wood, mixture and bark at a heating rate of 10 ^{o}C/min are shown in the Fig 2.3. The initial weight loss observed below 125 ^{o}C corresponds to desorption of water molecule from the biomass. The major degradation region of PJ wood, mixture and bark was between (200 –

Table 2. 1. Proximate and ultimate analysis of PJ biomass (moisture free basis)

	Wood	Bark	Mixture
Proximate analysis			
Moisture (wt %)	7.55±0.06	7.71±0.04	6.95±0.46
Ash content (wt %)	0.50±0.04	6.56±0.05	2.74±0.08
Bulk density (kg/L)	0.29	0.21	0.26
Extractives (wt %)	5.84±0.93	12.63±1.35	7.06±0.41
Experimental HHV (MJ/kg)	21.14±0.16	18.62±0.05	19.91±0.22
Ultimate analysis			
Carbon %	53.43±0.11	48.88 ± 0.13	52.12±0.14
Hydrogen %	6.58±0.04	5.89± 0.09	6.52 ± 0.11
Nitrogen %	0.16±0.01	0.36± 0.04	0.29±0.01
Sulfur %	0	0	0
Oxygen% [a]	39.37±0.09	38.31 ± 0.25	38.33±0.11

a- by difference

550 ^{o}C). The degradation profile of wood, mixture and bark showed two weight loss regions between 220 – 600 ^{o}C. The lignocellulosic biomass usually comprises of three major components namely cellulose, hemicelluloses and lignin. Hemicelluloses which is characterized by amorphous and irregular shape degrades at low temperature 180 – 260^{o} C; cellulose which has crystalline structure degrades between 250 – 380^{o} C; and lignin which is a complex aromatic hetropolymer degrades in a wide range of temperature 280 – 500^{o} C (Mohan et al., 2006; Cheng et al., 2012). The lignin degradation showed two peaks, thus the degradation of lignin is unstable and makes it

difficult for analysis (Sait et al., 2012). The major weight loss region for wood was from 220-390 ^{o}C, whereas for mixture and bark it was from 200-390 ^{o}C and corresponds mainly to the degradation of hemicelluloses, cellulose and part of lignin. The weight loss corresponding to these regions were 65.38%, 62.07%, and 50.02% for wood, mixture and bark respectively. The second weight loss region has a broad range (390-600 ^{o}C) corresponding to the degradation of lignin. The results obtained are in accordance with the thermal data released (Gaur and Reed, 1995). The weight loss obtained after 80 % weight loss is mainly due to devolatilization of char formed during the pyrolysis of PJ wood, mixture and bark (Park et al., 2009). Table 2.2 shows the moisture, volatiles, fixed carbon and ash content of the biomass calculated from the weight loss curve. Wood had high volatile content when compared to mixture and bark. The residue left at 475 ^{o}C was about18.54, 20.78, and 29.39 % for wood, mixture, and bark respectively. Thus this shows that bark contains more lignin compared to wood and mixture. The residue which was left at 950 ^{o}C includes the ash and fixed carbon and was about 14.68, 16.54, and 19.73 % for wood, mixture, and bark respectively.

The differential thermogravimetric (DTG) thermogram for PJ wood, bark and mixture biomass at a heating rate of 10 ^{o}C/min is shown in the Fig 2.4. The DTG thermogram showed one peak for wood, two peaks for bark and mixture below 115 ^{o}C. These peaks correspond to water evaporation from the biomass. The second peak observed in mixture and bark is mainly due to the increased lignin content, since lignin is difficult to dehydrate (Mohan et al., 2006; Cheng et al., 2012). The maximum conversion of the biomass took place between 250-400 ^{o}C, which is mainly due to degradation of hemicelluloses, cellulose and part of lignin (Sait et al., 2012). The maximum decomposition rate was observed at 352, 348, 348 ^{o}C for PJ wood, mixture and bark respectively. The height of the decomposition peak obtained around 350 ^{o}C showed that PJ wood has more cellulose and hemicelluloses content followed by PJ mixture and bark. The maximum decomposition peak had a small shoulder peak, which is attributed to the decomposition of

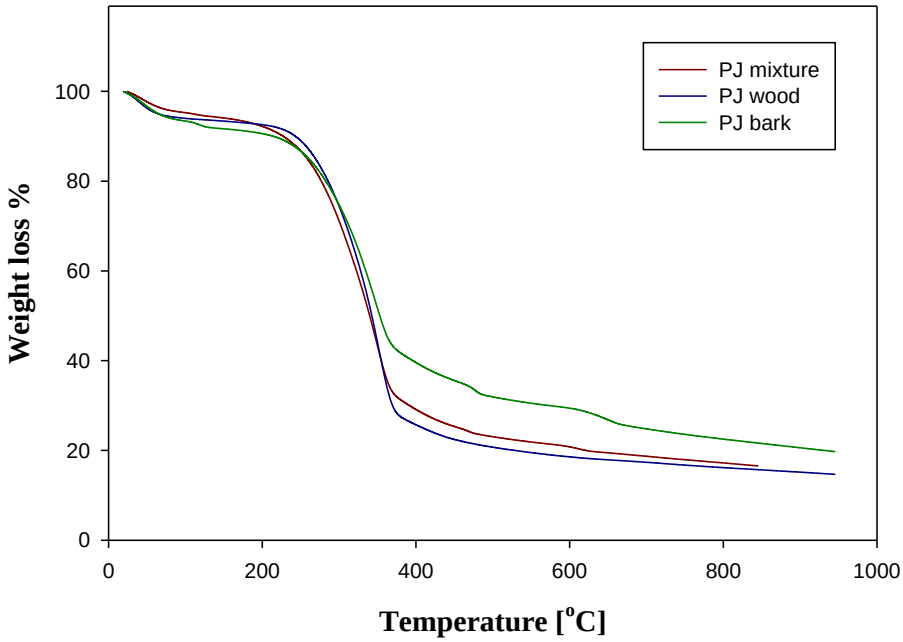

Fig. 2. 3. Weight loss curve for PJ wood, mixture and bark at a heating rate of 10 ºC/min

Table 2. 2. Proximate analysis from TGA weight loss thermogram of PJ wood, mixture and bark

	Wood	Mixture	Bark
Moisture (wt %)	7.55	7.58	7.08
Volatiles (200-950 ºC)	77.78	76.51	72.56
Fixed carbon	14.17	13.17	13.8
Ash	0.5	2.74	6.56

hemicelluloses (Park et al., 2009). Two peaks were found in the region 450-675 ºC in mixture and bark which was not found in the wood. The first peak and the second peak accounts for 1 and 4% weight loss for bark and mixture respectively. These peaks are mainly due to the presence of inorganic compounds which degrades at particular temperatures. More analysis has to be done in

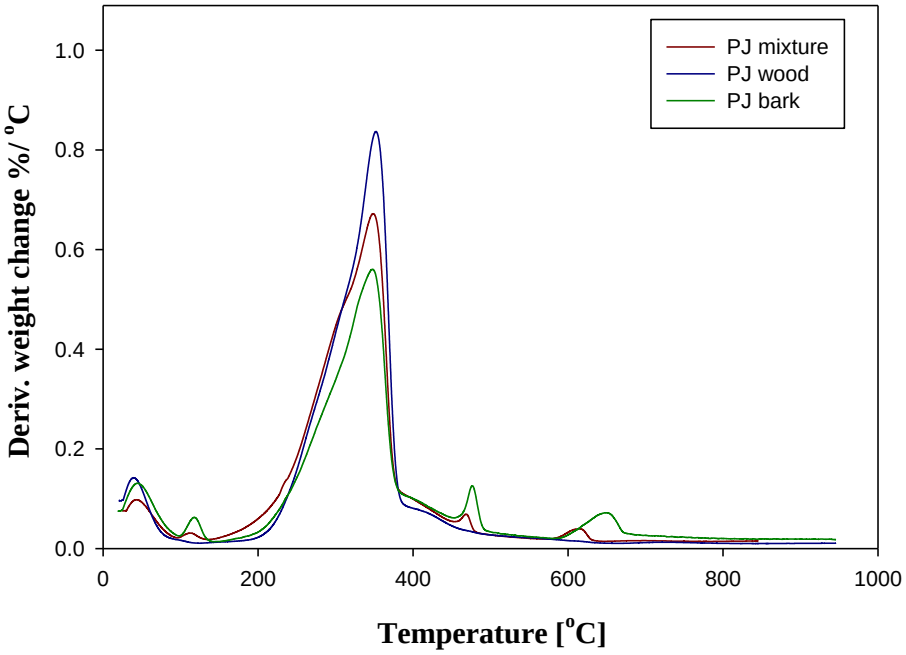

Fig. 2. 4. DTG curve of PJ wood, mixture and bark at a heating rate of 10 ºC/min

order to explain more about these peaks.

4.3. Effect of PJ wood, mixture and bark on pyrolysis product yield

The product yield obtained from the pyrolysis of pinyon juniper wood, mixture and bark are summarized in the Table 2.3. Wood had a total liquid yield of 63.62%, which comprises of 40.75% organics and 22.88% of water. The char and the gas yield was 20.61% and 15.78%, respectively. Mixture which comprises of wood and bark had a total liquid of 57.23%, which includes 36.42% organics and 20.81% water. The char and the gas yield for mixture was 25.68% and 17.60%, respectively. The bark which was separated from the wood had a total liquid yield of 47.49%, which contains 25.54% organics and 21.95% water. The char and the gas yield for bark was 33.80% and 18.72%, respectively. These results show that the pyrolysis product yields are affected by the presence of bark. The liquid content in the bark decreased due to the high ash content, since the

Table 2. 3. Pyrolysis product distribution of PJ wood, mixture and bark

	Product distribution (wt %)				
	Total liquid	Organic	Water	Char	Gas*
PJ wood	63.62±2.07	40.75±2.67	22.88±1.2	20.61±0.88	15.78±1.19
PJ mixture	57.23±1.54	36.42±0.65	20.81±0.89	25.68±2.34	17.60±0.22
PJ bark	47.49	25.54	21.95	33.80	18.72

* - by difference

inorganic content in the biomass catalyze biomass degradation and produces more char, thus reducing the liquid yield (Yaman, 2004; Butler et al., 2011). Bark had the maximum char yield, succeeded by mixture and wood. Increase in char yield in bark, is due to the fact that bark has more ash and lignin content. The residue produced from the TGA (Fig 2.3) also proves that the presence of bark increases the char yield. There was not much difference in the gas yield.

4.4. Effect of wood and mixture on physiochemical properties of ESP oil

The bio-oil collected in the condensers and ESP comprises of organics and water. The liquid collected in the first condenser was brown in color, with low viscosity due to high water content. The liquid collected in the second condenser was yellowish in color, and the quantity obtained was very low when compared to first condenser and ESP. The liquid collected in ESP was dark brown in color, viscous compared to condenser oil, with low water content. The chemical composition of liquid collected in the first condenser and ESP were similar. Thus, the oil from the ESP was used for measuring the physiochemical properties since the moisture content was very low. The bio-oil produced from pyrolysis of bark was very viscous and stuck to the walls of the ESP. Thus, the oil was collected by washing the ESP with methanol. The oil was then obtained by evaporating the

solvent. The physiochemical properties of bio-oil obtained from PJ wood and mixture are shown in the Table 2.4. Due to effective condensation the water content of the bio-oil was minimal. The viscosity of wood (482 cP) was lower when compared to the mixture (598 cP). This showed that the presence of bark in the mixture is responsible for increasing the viscosity. Ingram et al. (2008), showed that pine and oak bark produced high viscous bio-oil when compared to pine and oak wood bio-oil. Thus, the viscosity of the bio-oil is affected by the presence of bark in the mixture. The main reason for the increase in viscosity is due to increase in the phenolic compounds produced from the lignin content of the biomass (Fahmi et al., 2008). The pH, elemental composition and the energy content of the bio-oils from wood, mixture were similar. The results from the product yield and properties of bio-oil shows that bark was responsible for reducing the quality and quantity of the bio-oil produced.

Table 2. 4. Physicochemical properties of ESP oil produced from PJ wood, bark and mixture pyrolysis

	Wood	**Mixture**
Water content (wt %)	3.20±0.79	4.29±0.49
pH	2.89±0.16	3.12±0.12
Dynamic Viscosity (cP)	482.91±13.02	598.26±17.39
Carbon (%)	60.29±0.60	60.79±0.14
Hydrogen (%)	6.92±0.09	7.43±0.26
Nitrogen (%)	0.41±0.12	0.36±0.18
Oxygen (%)	31.38	31.42
Ash content (wt %)	<DL	<DL
HHV (MJ/Kg)	26.14±0.37	26.27±1.74

4.5. Effect of pyrolysis temperature on PJ mixture biomass pyrolysis product yield

The material balances of pyrolysis obtained at different temperatures (475, 550, 600 ^{o}C) are represented in the Table 2.5. As the temperature increases from 475 to 600 ^{o}C, the total liquid yield, which is the sum of organics and water yield decreased from 59% to 51%. Water content obtained at different temperatures did not vary significantly. Water produced during pyrolysis is mainly due to the decomposition of carbohydrates (cellulose and hemicelluloses) (Westerhof et al., 2010). Cellulose decomposes in a temperature range of 250 – 380^{o}C and hemicellulose degrades in a temperature range of 180 – 260^{o}C (Westerhof et al., 2010). There was no significant difference in water yield as the temperature increased from 475 to 600^{o}C, since degradation of carbohydrates takes place below 475^{o} C. The organic yield decreased from 38% to 31% as temperature increased. The decrease in liquid yield, particularly organic yield (Fig 2.5) is due to secondary cracking of pyrolysis vapors at high temperature (Gerçel and Gerçel, 2007; Salehi et al., 2011). The char yield also reduced as the temperature increased, which could be due to greater primary decomposition of pinyon juniper biomass, or due to secondary decomposition of char residues. The gas yield increased from 17% to 29% as the temperature was increased from 475 to 600^{o}C. The increase in gas yield are mainly attributed to greater primary cracking of biomass and secondary cracking of pyrolysis vapors, and char (Gerçel and Gerçel, 2007). Thus the maximum organic yield, which corresponds to bio-oil, was obtained at 475 ^{o}C.

4.6. Effect of pyrolysis temperature on the properties of PJ bio-oil

The physiochemical properties of the ESP oil, which is a representation of the organics obtained during the pyrolysis of pinyon juniper mixture biomass, at different temperatures are represented in the Table 2.6. The pH of the ESP oil showed a slight increase from 3.05 to 3.27 as the temperature increased from 475 to 600 ^{o}C. The dynamic viscosity of the oil increased from 439 to 776 cP as the

Table 2. 5. Effect of pyrolysis temperature on pyrolysis product yield

Temperature (ºC)	Product distribution (wt %)				
	Total liquid	Organic	Water	Char	Gas*
475	59.03±1.13	38.32±2.04	20.71±1.04	23.91±0.47	17.07±0.53
550	57.13±0.85	35.76±1.43	21.38±0.60	21.18±0.37	21.69±0.47
600	51.86±0.90	31.43±0.39	20.43±1.29	18.71±0.70	29.44±1.6

* - by difference

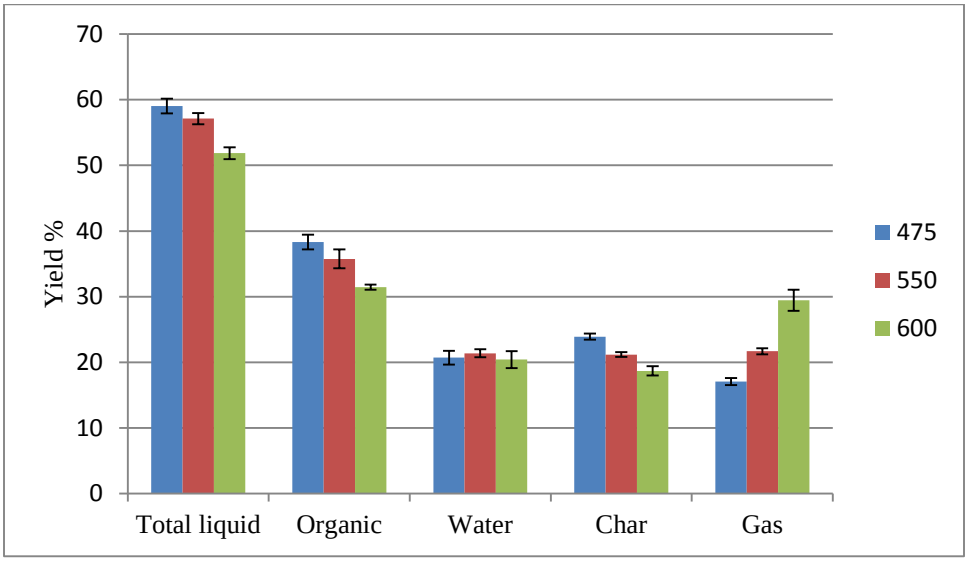

Fig. 2. 5. Effect of pyrolysis temperature on pyrolysis product yield

temperature increased from 475 to 550 ºC. At the same time the organic yield decreased from 38.32 to 35.76% (Table 2.5), this shows that as the temperature increases the lighter molecular compounds are further cracked to form non-condensable gases and also due to the increase of lignin derived compounds in the bio-oil. Thus, the oil is left with heavier molecule which increased the viscosity. The increase in temperature could also promote polymerization, causing the viscosity to

increase. As the temperature was further increased from 550 to 600°C, the dynamic viscosity was not significantly different, but was slightly lesser. The main reason is due to enhanced vapor cracking, which converts heavy molecular weight compounds to light molecular weight compound in the expense of organic yield (Westerhof et al., 2010). The elemental analysis of oil collected at different temperature showed that there was no significant difference in the carbon, hydrogen, nitrogen, and oxygen content. The oil had high carbon (61%) and hydrogen content, when compared to the biomass (49%). The oxygen content of the oil (32%) was lower than the biomass (44%), which is due to the rejection of oxygen in the form of CO, CO_2 and H_2O during pyrolysis. The energy content of the bio-oil which is depended on the elemental composition was not significantly affected as the temperature increased.

Table 2. 6. Physicochemical properties of ESP oil produced at different pyrolysis temperatures

	475 °C	550 °C	600 °C
Water content (wt %)	3.58±0.54	3.85±0.30	3.92±0.17
pH	3.05±0.12	3.24±0.18	3.27±0.20
Dynamic Viscosity (cP)	439.79±28.28	740.45±24.24	776.98±27.24
Carbon (%)	61.03±0.33	60.22±0.69	60.96±0.92
Hydrogen (%)	7.29±0.17	7.26±0.19	7.26±0.10
Nitrogen (%)	0.40±0.04	0.44±0.05	0.49±0.08
Oxygen (%)	31.28±0.24	32.09±0.86	31.29±1.02
Ash content (wt %)	<DL	<DL	<DL
HHV (MJ/Kg)	26.27±28.28	26.53±0.51	26.43±0.54

The energy content of the biomass and the pyrolysis oil were 19 and 26 MJ/kg respectively. The increase in energy content of bio-oil is due to increase in carbon, and hydrogen content and decrease in oxygen content.

The functional groups present in the bio-oil are characterized by integrating the ^{13}C NMR spectrum. The ^{13}C NMR spectrum of bio-oil produced at different temperatures is shown in the Fig 2.6. The difference in chemical properties of the bio-oil can be found by observing the changes in the intensity of the chemical shift between 0 to 210 ppm. The semi quantitative analysis were done by allotting the chemical shifts in the spectrum to different functional groups based on the analysis reported in (Mante et al., 2011). The comparison between the bio-oil spectra produced at different temperature showed that there was not much difference in the aromatic, aldehyde, ketones and carbohydrate degradation region. The aliphatic region increased as the temperature increased, which is attributed to increased demethoxylation of lignin moieties which resulted in more alkylation reaction. The semi quantitative analysis of bio-oil produced at different temperatures (Table 2.7) supported the conclusion made above.

The results obtained showed that 475 ^{o}C, was the optimum temperature for producing maximum bio-oil yield and for producing less viscous oil as other properties are not much affected by increasing the temperature. The properties of bio-oil obtained from PJ biomass is comparable with the bio-oil produced from pine (Westerhof et al., 2010), hybrid poplar (Mante et al., 2011) and other biomass used in fluidized bed reactor. This proves that PJ biomass could be used in pyrolysis process for producing valuable products.

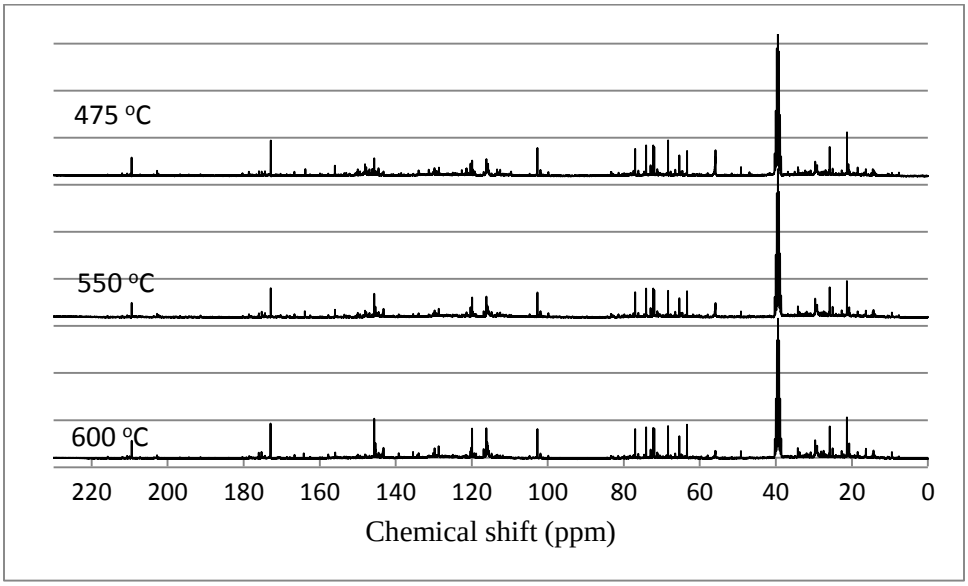

Fig. 2. 6. ^{13}C NMR spectrum of PJ bio-oil produced at different pyrolysis temperature

Table 2. 7. Carbon distribution in PJ bio-oil produced at different pyrolysis temperature

	475 °C	550 °C	600 °C
Aliphatics	34.26	40.98	41.52
Methoxyl in lignin	7.70	4.65	2.39
Carbohydrate degradation	20.78	21.45	20.21
Aromatics	34.02	29.76	32.17
Carboxylic acids	2.64	2.45	2.95
Ketones and aldehydes	0.60	0.71	0.77

5. Conclusion

PJ wood, bark and mixture biomass was characterized and their effect on pyrolysis was studied. Biomass characterization showed that bark had high ash content and low bulk density, which had a negative effect while considering as a fuel source. The presence of bark in the mixture affected

the ash, carbon, nitrogen, oxygen and energy content of PJ mixture when compared to PJ wood. Pyrolysis of PJ wood, bark and mixture showed that bark reduced the bio-oil yield, increased the char yield and viscosity of the bio-oil produced. The effect of temperature on the pyrolysis of PJ mixture showed that less viscous bio-oil was produced at the temperature (475 ^{o}C) which produced maximum bio-oil yield. The results obtained show that PJ biomass can be effectively used in pyrolysis process for producing value added products.

6. References

Agblevor, F.A., Beis, S., Mante, O., Abdoulmoumine, N., 2010. Fractional catalytic pyrolysis of hybrid poplar wood. Ind. Eng. Chem. Res. 49, 3533–3538.

Agblevor, F.A., Mante, O., McClung, R., Oyama, S.T., 2012. Co-processing of standard gas oil and biocrude oil to hydrocarbon fuels. Biomass Bioenergy 45, 130–137.

Akhtar, J., Saidina Amin, N., 2012. A review on operating parameters for optimum liquid oil yield in biomass pyrolysis. Renew. Sustain. Energy Rev. 16, 5101–5109.

Ansley, R.J., Wiedemann, H.T., Castellano, M.J., Slosser, J.E., 2006. Herbaceous restoration of juniper dominated grasslands with chaining and fire. Rangel. Ecol. Manag. 59, 171–178.

Babu, B.V., 2008. Biomass pyrolysis: a state-of-the-art review. Biofuels Bioprod. Biorefining 2, 393–414.

Baughman, C., Forbis, T.A., Provencher, L., 2010. Response of two sagebrush sites to low-disturbance, mechanical removal of piñyon and juniper. Invasive Plant Sci. Manag. 3, 122–129.

Bridgwater, A.V., 2012. Upgrading biomass fast pyrolysis liquids. Environ. Prog. Sustain. Energy 31, 261–268.

Bridgwater, A.V., Meier, D., Radlein, D., 1999. An overview of fast pyrolysis of biomass. Org. Geochem. 30, 1479–1493.

Bridgwater, A.V., Toft, A.J., Brammer, J.G., 2002. A techno-economic comparison of power production by biomass fast pyrolysis with gasification and combustion. Renew. Sustain. Energy Rev. 6, 181–246.

Brockway, D.G., Gatewood, R.G., Paris, R.B., 2002. Restoring grassland savannas from degraded pinyon-juniper woodlands: effects of mechanical overstory reduction and slash treatment alternatives. J. Environ. Manage. 64, 179–197.

Butler, E., Devlin, G., Meier, D., McDonnell, K., 2011. A review of recent laboratory research and commercial developments in fast pyrolysis and upgrading. Renew. Sustain. Energy Rev. 15, 4171–4186.

Carrara, P.E., Carroll, T.R., 2007. The determination of erosion rates from exposed tree roots in the Piceance Basin, Colorado. Earth Surf. Process. 4, 307–317

Chambers, J.C., Vander Wall, S.B., Schupp, E.W., 1999. Seed and seedling ecology of pinyon and juniper species in the pygmy eoodlands of Western North America. Bot. Rev. 65, 1–38.

Cheng, K., Winter, W.T., Stipanovic, A.J., 2012. A modulated - TGA approach to the kinetics of lignocellulosic biomass pyrolysis/combustion. Polym. Degrad. Stab. 97, 1606–1615.

Corder, S.E., 1976. Properties and uses of bark as an energy source. Proc. XVI IUFRO World Congr. Oslo Nor.

Evans, R.A., 1988. Management of pinyon-juniper woodlands. USDA For. Serv. Rep. INT-249 Ogden UT.

Fahmi, R., Bridgwater, A., Donnison, I., Yates, N., Jones, J., 2008. The effect of lignin and inorganic species in biomass on pyrolysis oil yields, quality and stability. Fuel 87, 1230–1240.

Gaur, S., Reed, T.B., 1995. An atlas of thermal data for biomass and other fuels. Natl. Renew. Energy Lab. Gold. Colo. Technical report: NRELA'P-433-7965.

Gerçel, H.F., Gerçel, ö., 2007. Bio-oil production from an oilseed by-product: fixed-bed pyrolysis of olive cake. Energy Sources Part Recovery Util. Environ. Eff. 29, 695–704.

Harkin, J.M., Rowe, J.W., 1971. Bark and its possible uses. USDA For. Serv. Res. Note FPL–091.

Ingram, L., Mohan, D., Bricka, M., Steele, P., Strobel, D., Crocker, D., Mitchell, B., Mohammad, J., Cantrell, K., Pittman, C.U., 2008. Pyrolysis of wood and bark in an auger reactor: physical properties and chemical analysis of the produced bio-oils. Energy Fuels 22, 614–625.

Mante, O.D., Agblevor, F.A., McClung, R., 2011. Fluid catalytic cracking of biomass pyrolysis vapors. Biomass Convers. Biorefinery 1, 189–201.

Miller, R.F., Wigand, P.E., 1994. Holocene changes in semiarid pinyon-juniper woodlands. BioScience 44, 465–474.

Miller, R.F., Bates, J.D., Svejcar, T.J., Pierson, F.B., Eddleman, L.E., 2005. Biology, ecology, and management of western juniper (Juniperus occidentalis). Tech. Bull. 152 Agric. Exp. Stn. Or. State Univ. Corvalis Or.

Mohan, D., Pittman, C.U., Steele, P.H., 2006. Pyrolysis of wood/biomass for bio-oil: a critical review. Energy Fuels 20, 848–889.

Park, H.J., Park, Y.-K., Dong, J.-I., Kim, J.-S., Jeon, J.-K., Kim, S.-S., Kim, J., Song, B., Park, J., Lee, K.-J., 2009. Pyrolysis characteristics of oriental white oak: kinetic study and fast pyrolysis in a fluidized bed with an improved reaction system. Fuel Process. Technol. 90, 186–195.

Petrus, L., Noordermeer, M.A., 2006. Biomass to biofuel, a chemical perspective. R. Soc. Chem. 8, 861–867.

Ragland, K.W., Aerts, D.J., Baker, A.J., 1991. Properties of wood for combustion analysis. Bioresour. Technol. 37, 161–168.

Ryu, C., Yang, Y.B., Khor, A., Yates, N.E., Sharifi, V.N., Swithenbank, J., 2006. Effect of fuel properties on biomass combustion: part I. experiments—fuel type, equivalence ratio and particle size. Fuel 85, 1039–1046.

Sait, H.H., Hussain, A., Salema, A.A., Ani, F.N., 2012. Pyrolysis and combustion kinetics of date palm biomass using thermogravimetric analysis. Bioresour. Technol.

Salehi, E., Abedi, J., Harding, T., 2011. Bio-oil from Sawdust: effect of operating parameters on the yield and quality of pyrolysis products. Energy Fuels 25, 4145–4154.

Serapiglia, M.J., Cameron, K.D., Stipanovic, A.J., Smart, L.B., 2009. Analysis of biomass composition using high-resolution thermogravimetric analysis and percent bark content for the selection of shrub willow bioenergy crop varieties. Bioenerg 2, 1–9.

Tausch, R.J., Chambers, J.C., Blank, R.R., Nowak, R.S., 1993. Differential establishment of perennial grass and cheatgrass following fire on an ungrazed sagebrush-juniper site. Wildland Shrub Arid Land Restor. Symp. Las Vegas NV Gen Tech Rep INT-GTR-315.

Weisberg, P.J., Lingua, E., Pillai, R.B., 2007. Spatial Patterns of Pinyon–Juniper Woodland Expansion in Central Nevada. Rangel. Ecol. Manag. 60, 115–124.

Westerhof, R.J.M., Brilman, D.W.F. (Wim), van Swaaij, W.P.M., Kersten, S.R.A., 2010. Effect of temperature in fluidized bed fast pyrolysis of biomass: oil quality assessment in test units. Ind. Eng. Chem. Res. 49, 1160–1168.

Yaman, S., 2004. Pyrolysis of biomass to produce fuels and chemical feedstocks. Energy Convers. Manag. 45, 651–671.

CHAPTER 3

PARAMETRIC STUDIES ON THE PYROLYSIS OF PINYON JUNIPER BIOMASS

1. Abstract

In this study effect of temperature, feed rate and gas flow rate on the total liquid, organic, water, char and gas yield was studied using Response surface methodology (RSM). The ranges of operating parameters used in this study are temperature (400 – 550 ^{o}C), gas flow rate (12 – 24 L/min) and feed rate (150 – 450 g/hr). Mathematical model which includes linear, quadratic and interaction term was developed using Box-Behnken design to show how each response is related to the explanatory factors. The experimental design and data analysis were performed using statistical analysis system software (SAS 9.0). Analysis of variance (ANOVA) at 95% confidence interval was used to find the statistically significant term affecting the responses. The developed model was statistically significant and definite in predicting the response. The factors which affect the yields significantly are as follows: temperature had positive effect on water and gas yield and negative effect on total liquid, organic and char yield; Gas Flow rate had positive effect on total liquid and organic yield and negative yield on water and char yield; The feed rate had negative effect on total liquid, organic and water. The total liquid yield ranged between 50.05 - 59.05 wt%, the organic yield ranged between 33.41 - 38.09 wt%, the water yield ranged between 17.00 - 22.64 wt%, the char yield ranged between 18.97 - 35.39 wt% and the gas yield ranged between 9.72 - 27.91 wt%. The results show that each response is affected by different factor level combinations, and maximum yield for each response was obtained at different factors level.

2. Introduction

Pinyon Juniper (PJ) trees are widely spread across Western United States due to climatic change, overgrazing, fire suppression and recent increase in atmospheric CO_2 (Miller and Wigand, 1994; Ansley et al., 2006; Weisberg et al., 2007; Baughman et al., 2010). The wide spread of PJ woodlands has a negative effect by converting high-priority habitat types into woodlands. Thus, efforts are being taken to remove PJ trees and restore the herbaceous vegetation. PJ resources in the past have been used as firewood, fence posts, medicines, pine nuts, chips for particle-flake board. Interior paneling, frame molds, Christmas tree, for flavoring gin and small scale electricity production (Miller et al., 2005). The most consistent usage of PJ woodland was personal use of firewood or marketed as firewood. Utilization of PJ biomass for renewable energy is a logical way for making the highly energy intense harvesting to be self-sustainable. PJ biomass which is available in large quantity could be used as potential feed stock in fast pyrolysis for producing fuel and chemical feedstock.

Fast pyrolysis is an efficient way of producing value added products from biomass. In the previous chapter it is shown that PJ biomass could be effectively used as a feedstock for fast pyrolysis. Fast pyrolysis product are affected by number of factors which includes reactor configuration, heat transfer, heating rate, temperature, vapor residence time, secondary cracking of vapors, char separation, and liquid collection (Bridgwater et al., 1999). The process parameters temperature, gas flow rate and feed rate controls heat transfer, heating rate, vapor residence time and secondary cracking of vapors plays a vital role in determining the (distribution) quantity and quality of the products. Temperature plays an important role in braking down the biomass by providing the necessary energy. Lignocellulosic biomass is mainly composed of cellulose (23-53%), hemicelluloses (20-35%), lignin (10-25%) and extraneous compounds (Petrus and Noordermeer, 2006). The components of the biomass are different from each other and undergo

degradation at different temperatures (Bridgwater, 2012). Cellulose degrades at temperature range of 310 – 430 ^{o}C, hemicelluloses at a range of 250 – 400 ^{o}C and lignin in a wide temperature range 300 – 500 ^{o}C (Bulushev and Ross, 2011). Thus suitable temperature should be selected to obtain maximum liquid yield. Gas flow rate determines the apparent vapor residence time of the pyrolysis vapors (Piskorz et al., 1998). The apparent vapor residence time is defined as empty reactor volume divided by the inlet gas flow rate at operating conditions (Scott et al., 1999). The pyrolysis vapors are susceptible to secondary cracking and polymerization at high vapor residence time and thus low residence time are usually needed to obtain maximum liquid yield (Olukcu et al., 2002). Biomass feed rate plays an important role in controlling the heat transfer rate. High heating rates are required to rapidly degrade the biomass to produce volatiles. Thus optimizations of process parameters are essential for maximizing the liquid yield obtained from fast pyrolysis of biomass. Maximum liquid product could be achieved by using moderate temperature, low residence time and rapid removal and quenching of pyrolysis vapors (Butler et al., 2011). Optimization of process parameters have been carried out for different biomass. Pattiya, (2010) concluded that the optimum pyrolysis temperature for maximum organic yield from stalk and rhizome of cassava plants pyrolysis was around 500 ^{o}C. Kim et al. (2011) concluded that maximum liquid yield for yellow poplar wood was obtained at a temperature of 500 ^{o}C and residence time of 1.9s. Salehi et al. (2011) showed that temperature and particle size had significant effect on bio-oil production, but the effect of residence time was negligible. Thus it shows that optimum process parameters, varies for different biomass.

Although much research has been carried out in fast pyrolysis to optimize the process parameters using different biomass, there is no information on how the process parameters affect the product distribution on PJ biomass pyrolysis. The aim of this research is to study the effect of temperature, gas flow rate and feed rate on total liquid, char and gas yield from fast pyrolysis of PJ

mixture in bubbling fluidized bed reactor. The parameters used in this study are temperature (400, 475, 500 ºC), gas flow rate (12, 18, 24 L/min) and feed rate (150, 300, 450 g/hr).

3. Materials and methods

3.1. Feedstock

Pinyon Juniper biomass obtained from USA Bureau of Land Management consists of wood and bark mixed together. The biomass were dried in laboratory condition and ground until it passed through 1mm sieve. The ground biomass was then used for the optimization studies.

3.2. Design of experiments

Response surface methodology (RSM) is a combination of mathematical and statistical technique, to optimize the response which is affected by several variables. RSM was first established by Box and Wilson (1951). The basic approach of RSM is to perform screening experiments to find the explanatory factors which affect the response and then a complicated design is used to find out second degree regression model, which could be used to optimize the explanatory factors.

In this study response surface methodology was carried out to find out the main effect and interaction effect of the operating parameters. Box Behnken experimental design with three factors (temperature, gas flow rate, feed rate), and three levels (low, medium, high) were used to study the effect on the responses (Total liquid, organic, water, char, and gas yield). The different levels used for the optimization of parameters using Box Behnken design are shown in Table 3.1. Screening experiments were done in order to select the levels for the temperature. Feed rate (g/h) which corresponds to weight hourly space velocity (WHSV) of 1.5, 3.0, 4.5 and gas flow rate (L/min) which corresponds to vapor residence time of 0.75, 1.0, 1.5 s were selected.

Table 3. 1. Factor levels used for different factors

	Levels		
	Low (-1)	Medium (0)	High (1)
Temperature (°C), A	400	475	550
Gas flowrate (L/min), C	12	18	24
Feedrate (g/h), B	150	300	450

The experimental design and data analysis were performed using statistical analysis system software (SAS 9.0) provided by SAS Institute Inc, NC, USA. A total of 15 experiments shown in (Table 3.2), which includes 3 center points were generated and analyzed. Statistical analysis of the response variables was done using analysis of variance (ANOVA) on 95% confidence interval. ANOVA analysis was used to find the statistically significant term affecting the responses. Second order regression model which includes linear, quadratic and interaction term explains how the response is related to the explanatory variables. It is usually expressed as

$$y = \beta_0 + \beta_1 A + \beta_2 B + \beta_3 C + \beta_{11} A^2 + \beta_{22} B^2 + \beta_{33} C^2 + \beta_{12} AB + \beta_{13} AC + \beta_{23} BC + \varepsilon \quad (4)$$

Equation (4) represent the second order regression model, where y is the response; A, B, C represents the linear terms namely temperature, gas flow rate and feed rate respectively; A^2, B^2, C^2 represents the quadratic terms; AB, AC, BC represents the interaction term; β_0, β_1, β_2, β_3, β_{11}, β_{22}, β_{33}, β_{12}, β_{13}, β_{23} represents the regression co-efficient for linear, quadratic and interaction terms.

3.3. Pyrolysis of pinyon juniper biomass

Pyrolysis of biomass was carried out in bench scale fluidized bed reactor situated at the Thermochemical and biomass research laboratory located at USTAR Bioinnovations Center. The pyrolysis unit has been described in chapter 2 (section 3.10). The process parameters investigated

were temperature (400, 475, 550 ^{o}C), WHSV (1.5, 3.0, 4.5 h^{-1}) and vapor residence time (0.75, 1.0, 1.5s).

4. Results and discussion

The parameters and levels used in the experimental design are shown in Table 3.1. The process parameters were selected based on the previous research and preliminary experiments conducted. Research on lignocellulosic biomass pyrolysis showed that maximum liquid yield was obtained in a temperature range of 400–600^{o}C, and vapor residence times within the range of 0.1–2 s (Vamvuka, 2011). Thus the temperature investigated was from 400 to 550 ^{o}C, gas flow rate corresponding to vapor residence time from 0.75 to 1.5 s and depending on the reactor and feeder configuration feed rate from 150 to 450 g/h was selected. Statistical analysis was done using SAS 9.0, at 95 % confidence interval. The results from the ANOVA table (F value and p value) were used to find the reliability of the model, lack of fit and significant effect of each term on the response. The regression analysis was done to find the relationship between the dependent variable and independent variable. The coefficient of determination (R^2) is used to define how much percentage of variation in the response is explained by the model Table 3.2 shows the combination of parameters used in each experiment and their corresponding yields.

4.1. Total liquid

The ANOVA table at 95 % confidence interval and the model equation, for the total liquid yield is shown in the Table 3.3 and equation (5). The p-value obtained for the fitted model and lack of fitness, shows that the regression model (p value = 0.0024) was statistically significant and the lack of fit (p value = 0.1515) was statistically insignificant. R^2 value of 0.97 was obtained for the model, which implied that 97% of variability in the total liquid yield was explained by the model.

Table 3. 2. Response surface methodology, Box Behnken coded design

Temperature (°C)	Gas flow rate (L/min)	Feed rate (g/hr)	Total liq (wt %)	Organic (wt %)	Water (wt %)	Char (wt %)	Gas (wt %)
-1	0	-1	57.83	37.77	20.06	30.4	11.77
0	0	0	58.64	37.02	21.62	25.42	15.94
0	-1	-1	56.81	36.32	20.48	27.28	15.91
-1	1	0	55.44	38.09	17.35	31.9	12.66
-1	-1	0	54.69	35.44	19.24	35.59	9.72
1	0	1	54.74	34.71	20.03	21.66	23.6
0	0	0	59.05	37.3	21.75	24.83	16.13
0	0	0	58.32	36.88	21.44	24.24	17.44
1	1	0	53.12	35.25	17.87	18.97	27.91
0	-1	1	54.51	34.97	19.54	28.23	17.27
1	-1	0	50.05	33.41	16.64	23.83	26.12
-1	0	1	55.39	35.99	19.40	31.31	13.3
1	0	-1	56.74	35.16	21.58	22.94	20.32
0	1	-1	58.62	37.96	20.66	24.14	17.25
0	1	1	54.75	36.75	18.10	25.77	19.48

This showed that the model assumptions were met and the conclusions made are valid. Thus based on the results and analysis, a quadratic equation (5) was formulated to explain the dependency of the response on the factors.

In the model equation (5), positive coefficient implies that as the factors increase response increases and negative coefficient implies that as the factors increase, the response decreases. The equation showed that terms B, AB, AC had positive coefficient and terms A, C, BC had negative terms. Thus the linear term gas flow rate and interaction terms of temperature with gas flow rate

(AB) and temperature with feed rate had negative effect on total liquid yield. While, the linear terms

Table 3. 3. ANOVA table for total liquid yield

Term	Sum of squares	DF	Mean of squares	F value	Prob > F
Model	87.47	9	9.72	18.82	0.0024
A	5.61	1	5.61	10.64	0.0098
B	5.07	1	5.07	9.62	0.127
C	14.07	1	14.07	26.67	0.0006
A^2	32.41	1	32.41	61.47	<0.0001
AB	0.83	1	0.83	1.60	0.2612
AC	0.05	1	0.05	0.09	0.7718
B^2	32.47	1	32.47	61.57	<0.0001
BC	0.62	1	0.62	1.19	0.3245
C^2	0.67	1	0.67	1.30	0.3060
Lack of fit	2.31	3	0.77	5.76	0.1515
Pure error	0.27	2	0.13		
Total	90.05	14			

$$\text{Total liquid} = 58.93 - 0.84A + 0.80B - 1.33C - 2.92A^2 + 0.46AB + 0.11AC - 2.92B^2 - 0.39BC + 0.43C^2 \quad (5)$$

temperature, feed rate and interaction term gas flow rate with feed rate had negative effect on the total liquid yield. The p-value obtained for different factors shows that the linear terms temperature, gas flow rate, feed rate, and quadratic terms temperature, and gas flow rate significantly affected the liquid yield.

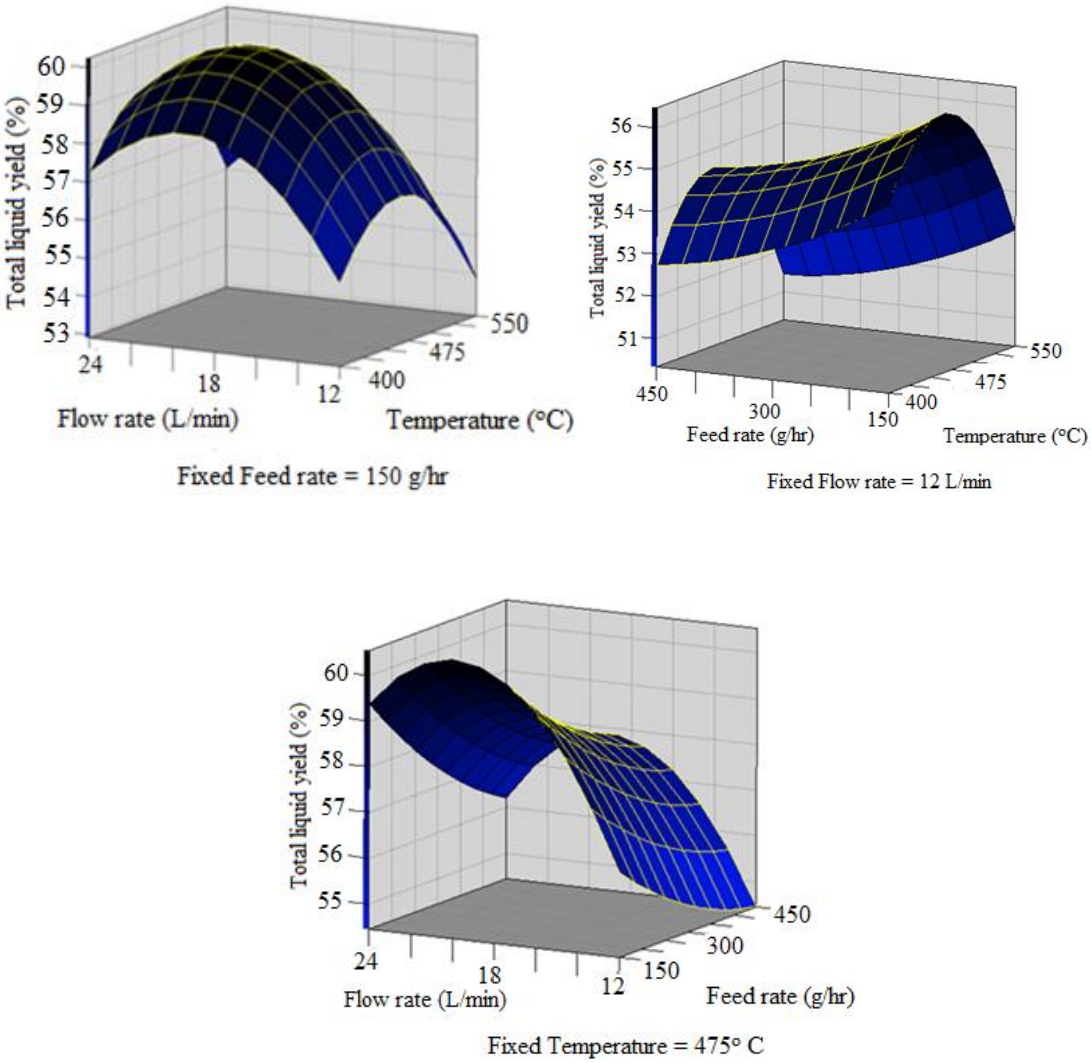

Fig. 3. 1. a) Effect of temperature and gas flow rate on total liquid yield, b) Effect of temperature and feed rate on total liquid yield and c) Effect of gas flow rate and feed rate on total liquid yield.

The regression model could be graphically represented in the form of interaction plots. The interaction plot (Fig 3.2a) suggests that as the temperature increased from 400 to 475 ºC, the liquid yield increased and further increasing the temperature to 550 ºC, decreased the liquid yield. The low yield of total liquid obtained at lower temperature was due to the inefficiency of reaction temperature to break down the biomass into pyrolysis vapors and low yield at high temperature is

due to secondary cracking of pyrolysis vapors (Park et al., 2009; Calonaci et al., 2010; Salehi et al., 2011). Ngo et al., 2013, showed that low temperature was not able to completely decompose the biomass, thus reducing the liquid yield.

The interaction plot also showed that as the gas flow rate increased from 12L to 18 L/min the total liquid increased and further increase in gas flow rate reduced the total liquid yield. Gas flow rate controls the residence time of pyrolysis vapors, which in turn controls secondary reaction like secondary cracking, repolymerization of pyrolysis vapors (Kersten et al., 2005). At low gas flow rate, the total liquid yield was reduced due to secondary reactions such as secondary cracking, re-polymerization and re-condensation (Salehi et al., 2011). At higher gas flow rate these secondary reactions were avoided, thus increasing the liquid yield, but further increasing the gas flow rate decreases the total liquid yield due to reduced condensation capacity by increasing the vapor pressure of the vapors (Mante and Agblevor, 2011). Similar results were reported in the pyrolysis of saw dust and olive bagasse (Şensöz et al., 2006; Salehi et al., 2009). The interaction plot between temperature and feed rate (Fig 3.2b) shows that, as the feed rate increased from 150 – 450 g h^{-1}, the liquid yield decreased. Feed rate which affects the heat transfer efficiency and the residence time had a negative effect on the total liquid yield. Thus as the feed rate, increased the total liquid yield decreased both at low and high temperatures. At low temperature, increase in feed rate caused inefficient heat transfer thus increasing the char yield and at high temperature there was more gasification, thus producing more gas yield.

The interaction plot between gas flow rate and feed rate (Fig 3.2c) at fixed temperature shows that as the feed rate increased, the liquid yield decreased at different gas flow rates. This showed that pinyon juniper biomass needs high heat transfer rates for breaking down into pyrolysis vapors. Increase in gas flow rate increased the liquid yield and further increase in gas flow rate at different feed rates decreased the liquid yield.

4.2. Organic liquid (OL) production

The ANOVA table at 95 % confidence interval and the model equation, for the organic liquid portion is shown in Table 3.4 and equation (6). The p-value obtained in ANOVA table shows that the regression model (p value = 0.0004) is statistically significant and the lack of fitness (p value = 0.348) is statistically insignificant. Thus, the model assumptions were met and the conclusions made are valid. The R^2 value showed that 98.58% of variability in the organic yield was explained by the model. Based on the results and analysis, a quadratic equation was formulated to explain the dependency of organic yield on the factors.

Table 3. 4 ANOVA table for organic yield

Term	Sum of squares	DF	Mean of squares	F value	Prob > F
Model	25.55	9	2.84	38.55	0.0004
A	9.59	1	9.59	133.09	<0.0001
B	7.82	1	7.82	108.51	<0.0001
C	2.87	1	2.87	39.79	0.0002
A^2	4.08	1	4.08	56.59	<0.0001
AB	0.16	1	0.16	2.23	0.1958
AC	0.44	1	0.44	6.14	0.0383
B^2	0.77	1	0.77	10.69	0.0114
BC	0.01	1	0.01	0.07	0.8067
C^2	0.04	1	0.04	0.54	0.4972
Lack of fit	0.28	3	0.09	2.02	0.3484
Pure error	0.09	2	0.05		
Total	25.92	14			

$$OL\ yield = 37.07 - 1.1A + 0.99B - 0.60C - 1.06A^2 - 0.20AB + 0.33AC - 0.46B^2 + 0.04BC - 0.10C^2 \quad (6)$$

The model equation showed that the terms B, AC, BC had positive coefficient and the terms A, C, A^2, AB, B^2, C^2 had negative coefficient. This showed that linear term gas flow rate and interaction term temperature with feed rate had positive effect on the OL yield. The terms temperature, feed and interaction terms (temperature with gas flow rate and gas flow rate with feed rate) had negative effect on the OL yield. Thus, increase in temperature and feed rate reduced the OL yield, while increase in gas flow rate increased the OL yield. The p value obtained for the individual and interaction terms shows that the linear terms temperature, gas flow rate, feed rate, and the interaction term temperature with feed rate affect the OL yield significantly.

The interaction plot between temperature and gas flow rate (Fig 3.3a) suggest that increase in gas flow rate at different temperature increases the OL yield. The plot also shows that high OL yields were obtained at moderate temperature (475 ^oC) and high gas flow rates (24 L/min) and low OL yields were obtained at high temperature (550 ^oC) and low gas flow rates (12L/min). The decrease in OL yields at high temperature and low gas flow rates are mainly due to secondary cracking of pyrolysis vapors, which increased the gas yield. The plot between temperature and feed rate (Fig 3.3b) shows that, as temperature increased at different feed rate, OL yield increased, but decreased with further increase in temperature. Feed rate had a negative effect on OL yield at different temperature; this shows that pinyon juniper biomass needs high heat transfer rate for converting into pyrolysis vapors. The decrease in the OL yield due to increase in feed rate was high

at low temperature (400 ºC) compared to high temperature (550 ºC). The plot between feed rate and gas

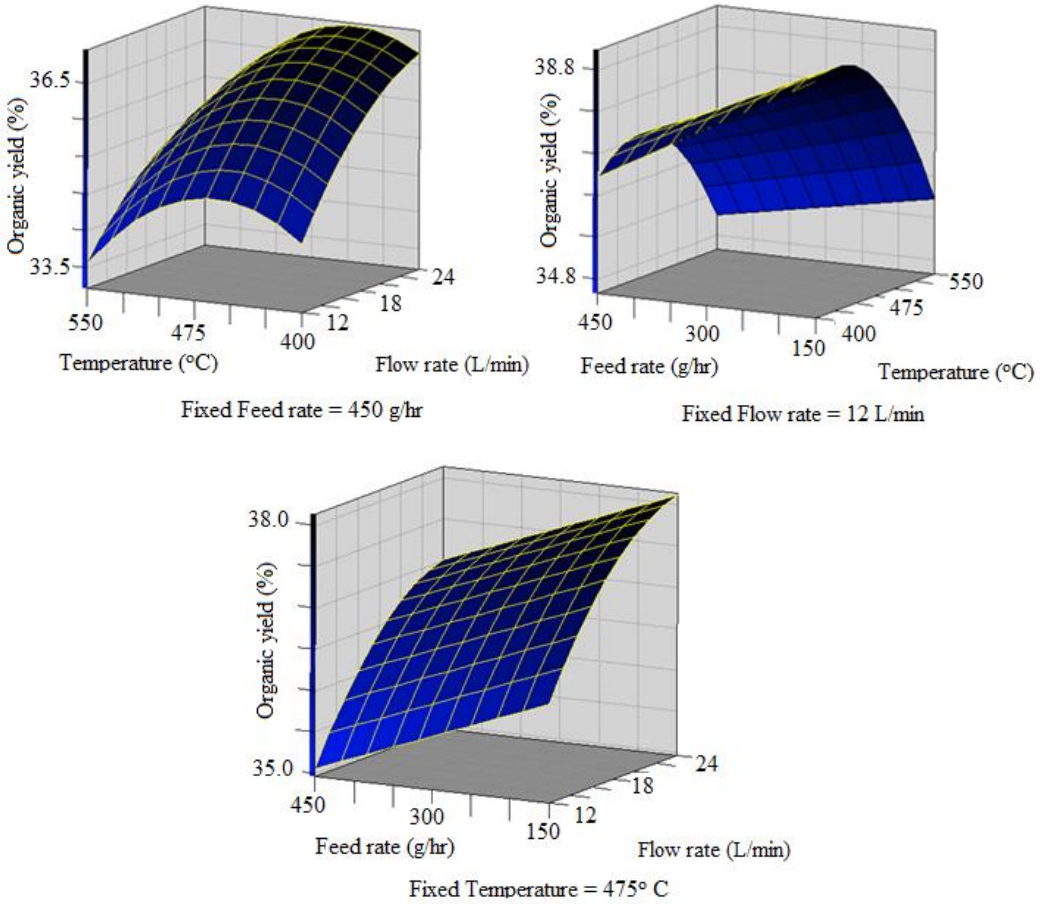

Fig. 3. 2. a) Effect of temperature and gas flow rate on OL yield, b) Effect of temperature and feed rate on OL yield and c) Effect of gas flow rate and feed rate on OL yield.

flow rate (Fig 3.3c) showed that OL yield increased as the gas flow rate increased at different feed rates, which showed that low residence time favored OL production. The low residence time reduced secondary cracking and repolymerization reactions.

4.3. Water

The analysis of variance (ANOVA) at 95 % confidence interval and the model equation, for the water yield is shown in Table 3.5 and equation (7). The p-value obtained in ANOVA table shows that the regression model (p value = 0.0002) was statistically significant and the lack of fit (p value = 0.0740) was statistically insignificant. Thus, the model assumptions were met and the conclusions made were valid. The R^2 value showed that 97.98% of variability in the water yield could be explained by the model. A quadratic equation was formulated to explain the dependency of water yield on the factors.

The model equation showed that the terms A, AB, C^2 had positive coefficient, thus increasing these terms increased the water yield and the terms B, C, A^2, B^2, AC, and BC had negative coefficient,This showed that increasing the linear term temperature and the interaction term temperature with gas flow rate would increase the water yield. The increase in the linear term gas flow rate and feed rate and the interaction terms (temperature with feed rate and gas flow rate with feed rate) showed decrease in the water yield. The graphical representation of the model is showed in the form of interaction plots. The p value obtained for the individual and interaction terms showed that gas flow rate and feed rate were significant linear terms and temperature and gas flow rate have significant interaction effect on char yield.

Table 3. 5 ANOVA table for water yield

Term	Sum of squares	DF	Mean of squares	F value	Prob > F
Model	49.44	9	5.49	24.46	0.0013
A	0.54	1	0.54	2.29	0.1832
B	1.93	1	1.93	8.60	0.0326
C	4.09	1	4.09	18.21	0.0080
A^2	13.04	1	13.04	58.06	0.0006
AB	6.55	1	6.55	29.18	0.0029
AC	0.20	1	0.20	0.88	0.3908
B^2	22.15	1	22.15	98.63	0.0002
BC	0.65	1	0.65	2.89	0.1501
C^2	1.09	1	1.09	4.85	0.0788
Lack of fit	1.07	3	0.36	14.79	0.0740
Pure error	0.05	2	0.02		
Total	50.56	14			

Water yield = $21.60 + 0.26A – 0.49B -0.72C – 1.88 A^2 + 1.28 AB - 0.22 AC – 2.45 B^2 -0.40 BC + 0.54C^2$ (7)

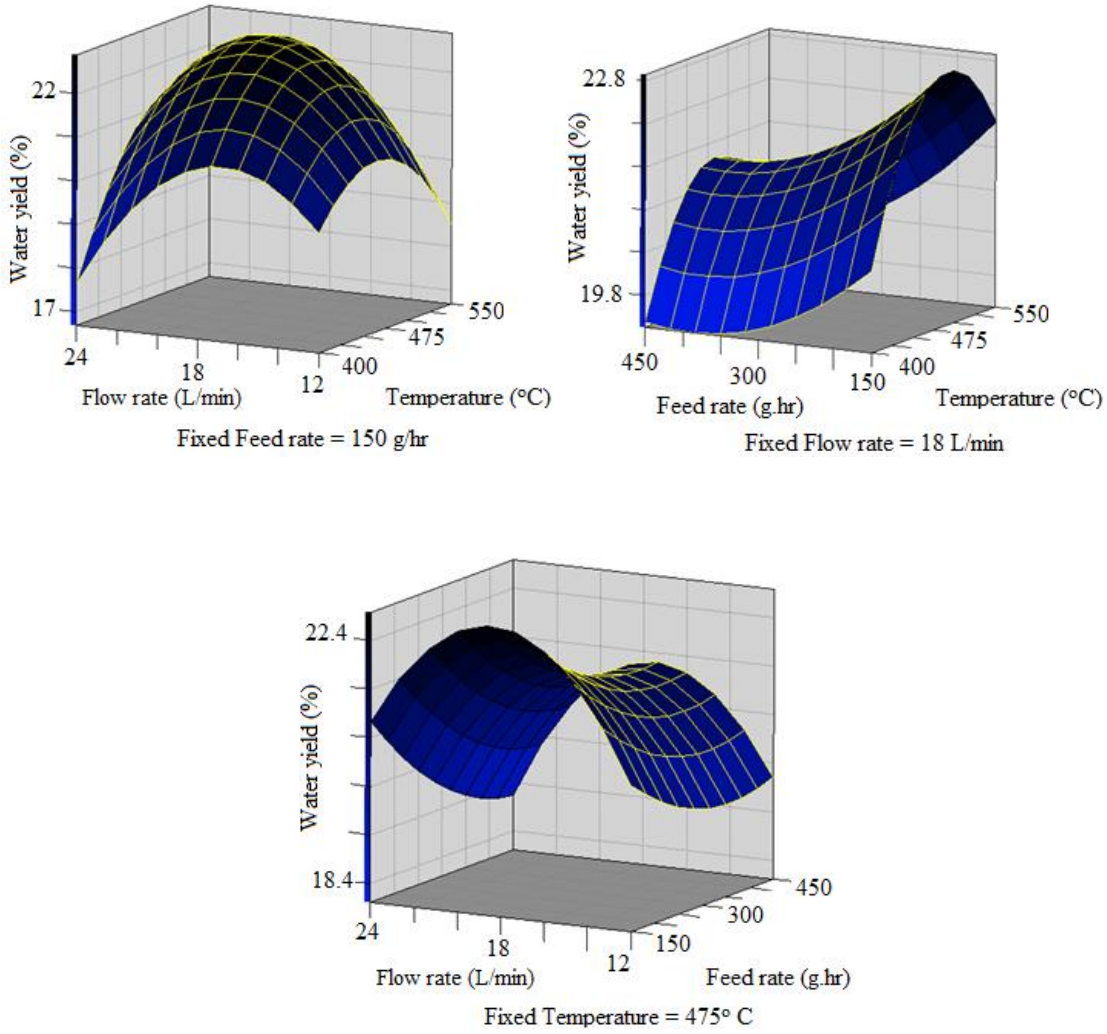

Fig. 3. 3. a) Effect of temperature and gas flow rate on water yield, b) Effect of temperature and feed rate on water yield and c) Effect of gas flow rate and feed rate on water yield.

The interaction plot between temperature and gas flow rate (Fig 3.4a) showed that as the temperature increased the water yield increased, but decreased with further increase in the temperature for all gas flow rates. The plot also shows that maximum water yield was obtained at medium gas flow rate and further increasing the gas flow rate decreased the water yield. The decrease in water yield as the gas flow rate increases was due to reduced time spent by the biomass in the reaction zone. The interaction plot between temperature and feed (Fig 3.4b) showed that the

increase in the feed rate decreased the water yield, due to insufficient heat transfer to the biomass for converting the biomass and organic vapors into water (Salehi et al., 2009). The water production was enhanced at moderate temperature and at higher temperature the water production had reduced marginally. Results from fast pyrolysis has shown that dehydration reaction is elevated at low temperature (Pattiya, 2011b).

4.4. Char production

ANOVA table at 95 % confidence interval and the model equation, for the char production is shown in Table 3.6 and equation (8). The p-value obtained in ANOVA table showed that the regression model (0.0042) was statistically significant and the lack of fit (0.1075) was statistically insignificant. This shows that the model assumptions were met and the conclusions made are valid. The R^2 value showed that 96.40% of variability in the char yield could be explained by the model. The quadratic equation explains the dependency of char yield on the different factors.

The model equation (8), suggests that the factors B, BC have positive sign and factors A, B, AB, and AC have negative sign. This suggests that the feed rate and the interaction term with gas rate has positive effect, thus as these factors increase char yield was increased. The factors temperature, gas flow rate and interaction terms (temperature with gas flow rate and temperature with feed rate) have negative effect, thus increasing these factors decreased the char yield. The model equation also suggests that temperature plays a major role in controlling the char yield. The p value obtained for the individual and interaction terms showed that the linear tem temperature and the interaction term of temperature and gas flow rate significantly affect the char yield.

Table 3. 6. ANOVA table for char yield

Term	Sum of squares	DF	Mean of squares	F value	Prob > F
Model	255.60	9	28.40	14.89	0.0042
A	216.32	1	216.32	105.98	<0.0001
B	24.33	1	24.33	11.92	0.0048
C	0.61	1	0.61	0.32	0.5960
A^2	7.84	1	7.84	4.11	0.0984
AB	0.47	1	0.47	0.25	0.6409
AC	1.20	1	1.20	0.63	0.4638
B^2	5.63	1	5.63	2.95	0.1464
BC	0.12	1	0.12	0.06	0.8153
C^2	0.31	1	0.31	0.16	0.7033
Lack of fit	8.84	3	2.95	8.47	0.1075
Pure error	0.70	2	0.35		
Total	265.12	14			

Char yield = $24.83 – 5.20A – 1.74B + 0.28C + 1.46A^2 – 0.34AB – 0.55AC +1.24B^2 + 0.17BC + 0.29C^2$

(8)

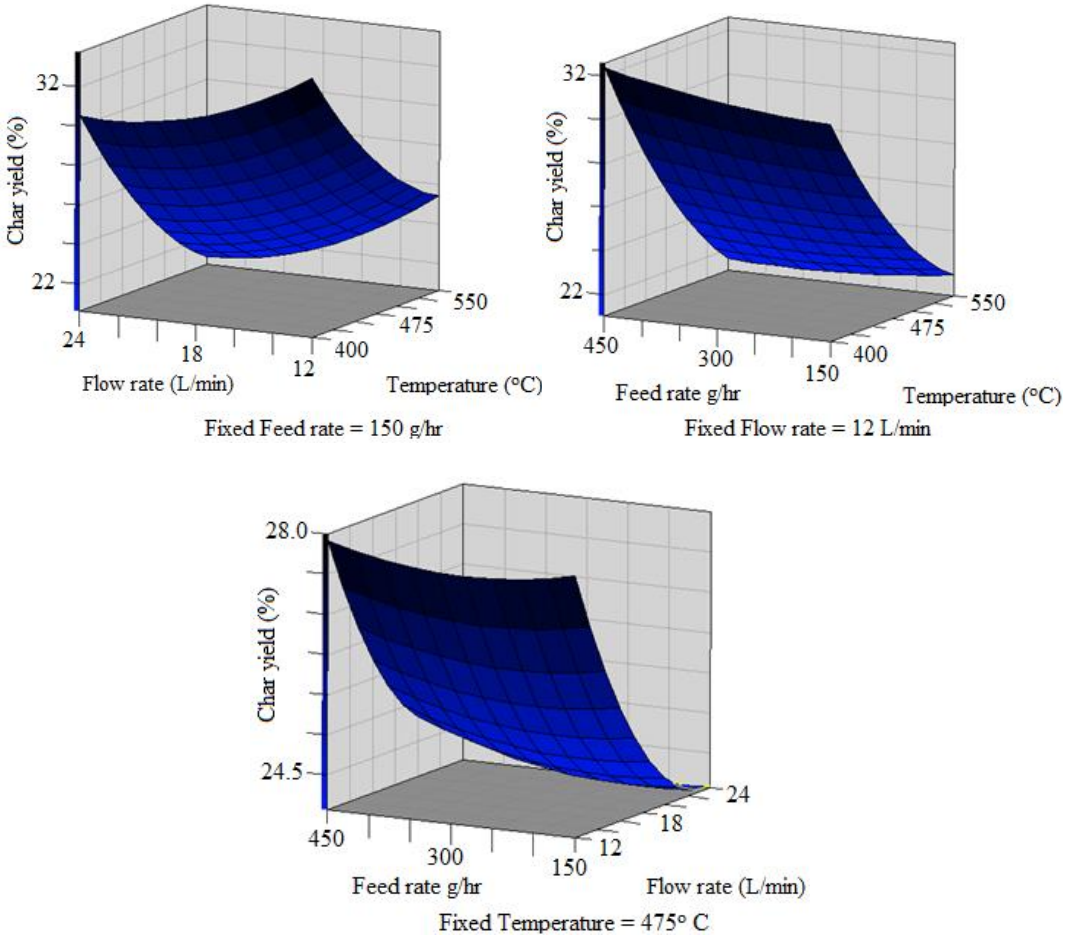

Fig. 3. 4. a) Effect of temperature and gas flow rate on char yield, b) Effect of temperature and feed rate on char yield and c) Effect of gas flow rate and feed rate on char yield.

The interaction plot between temperature and gas flow rate (Fig 3.5a) showed that at constant temperature, increase in gas flow rate decreased the char yield. Increase in gas flow rate decreases the residence time of pyrolysis vapors spent in the reaction zone. The low residence time reduces secondary reaction such as re-polymerization, which is responsible for reducing the char yield. Increase in gas flow rate also increases temperature control problem, which leads to increase in the gas yield. The plot also shows that at fixed gas flow rate, increase in temperature decreased the char yield. The decrease of char yield at high temperature is due to greater thermal degradation of biomass or secondary cracking of the char residues (Gerçel and Gerçel, 2007; Pattiya, 2010; Zhang

et al., 2009b). The interaction plot between feed rate and gas flow rate (Fig 3.5c) showed that at fixed gas flow rate, increase in feed rate increased the char yield but was not significant. Increase in feed rate caused temperature control problems, which in turn increased the gas yield.

4.5. Non condensable gas

ANOVA table at 95 % confidence interval and the model equation, for the char production is shown in Table 3.7 and equation (9). The p-value obtained in ANOVA table showed that the regression model (p value = <0.001) was statistically significant and the lack of fit (p value = 0.3090) was statistically insignificant. Thus, the model assumptions were met and the conclusions made were valid. The R^2 value showed that 94.05% of variability in the gas yield was explained by the model.

Table 3. 7. ANOVA table for gas yield

Term	Sum of squares	DF	Mean of squares	F value	Prob > F
Model	350.61	9	38.96	8.78	0.0138
A	318.78	1	318.78	76.74	<0.0001
B	8.57	1	8.57	1.93	0.2232
C	8.82	1	8.82	1.99	0.2175
A^2	5.18	1	5.18	1.17	0.3291
AB	0.33	1	0.33	0.08	0.7957
AC	0.77	1	0.77	0.17	0.6950
B^2	7.39	1	7.39	1.67	0.2533
BC	0.19	1	0.19	0.04	0.8445
C^2	0.72	1	0.72	0.16	0.7044
Lack of fit	20.84	3	6.95	10.41	0.0889
Pure error	1.33	2	0.68		
Total	372.78	14			

$$\text{Gas yield} = 16.50 + 6.31A + 1.035B + 1.05C + 1.19A^2 - 0.29AB + 0.44AC + 1.42B^2 + 0.22BC - 0.44C^2 \quad (9)$$

The model equation shows that term A, B, C, AC, and BC has positive sign and terms AB has negative sign. Thus linear terms temperature, feed rate, gas flow rate and interaction terms temperature with feed rate and gas flow rate with feed rate had a positive effect on gas yield and increasing these terms increased the gas yield. The interaction term temperature with gas flow rate had a negative effect on the gas yield, thus increasing this term decreased the gas yield. The p value obtained for the individual and interaction terms showed that only temperature was significantly affecting the gas yield.

Fig 3.6 a, b, c shows the interaction plot of different factors on gas yield. The interaction plot between temperature and gas flow rate (Fig 3.6a) showed that, as the temperature increased the gas yield increased at different gas flow rates and increase in gas flow rate at different temperature did not show much difference in the gas yield. As explained in the influence of char yield section, increase in temperature causes greater biomass degradation or secondary degradation of the char formed, which increased the gas yield. The interaction plot between feed rate and gas flow rate (Fig 3.6c) showed that as the gas flow rate is increased from 12L/min to 18 L/min, there was a decrease in the gas yield, but further increase to 24 L/min increased the gas yield. The interaction plot also showed that increase in feed rate increased the gas yield. Thus, increasing the gas flow rate and feed rate to higher levels caused temperature control problem due to the capacity of the reactor. The interaction plot between temperature and feed rate (Fig 3.6b) also showed that temperature had a positive effect on gas yield.

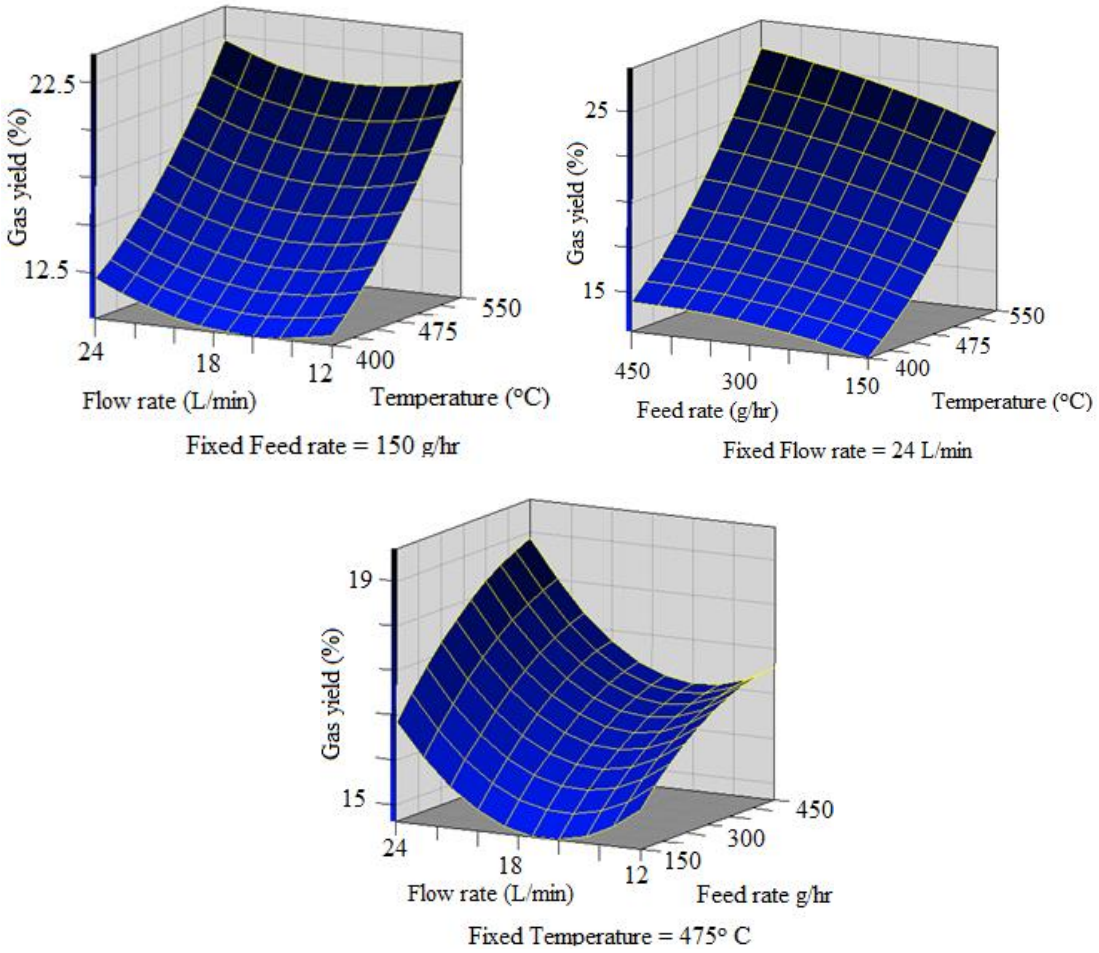

Fig. 3. 5. a) Effect of temperature and gas flow rate on gas yield, b) Effect of temperature and feed rate on gas yield and c) Effect of gas flow rate and feed rate on gas yield.

5. Conclusions

Fast pyrolysis of PJ biomass was carried out in fluidized bed reactor to study the effect of temperature, gas flow rate and feed rate on pyrolysis yield. Response surface methodology was conducted with the help of box behnken design in order to optimize the factors for desired yields. The total liquid, organic, char and gas yields are affected by the individual, quadratic and interaction terms of the factors. The results obtained showed that temperature had positive effect on water and gas yield and negative effect on total liquid, organic and char yield; gas flow rate had positive effect

on total liquid and organic yield and negative yield on water and char yield; the feed rate had negative effect on total liquid, organic and water.

The total liquid yield ranged between 59.05 wt% – 50.05 wt%. The maximum liquid yield was obtained at (475 ^{o}C, 18 L/min, 300 g h^{-1}) and minimum obtained at (550 ^{o}C, 12 L/min, 300 gh^{-1}). The organic yield ranged between 38.09 wt% and 33.41 wt%, with maximum organic yield obtained at (400 ^{o}C, 24 L/min, 300 g h^{-1}) and minimum obtained at (550 ^{o}C, 12 L/min, 300 g h^{-1}). The water yield ranged between 22.64 wt% and 17.00 wt%, with maximum water yield obtained at (550 ^{o}C, 12 L/min, 300 g h^{-1}) and minimum obtained at (475 ^{o}C, 24 L/min, 450 g h^{-1}). The char yield ranged between 35.39 wt% and 18.97 wt%, with maximum char yield obtained at (400 ^{o}C, 12 L/min, 300 g h^{-1}) and minimum obtained at (550 ^{o}C, 24 L/min, 300 g h^{-1}). The gas yield ranged between 27.91 wt% and 9.72 wt%, with maximum gas yield obtained at (550 ^{o}C, 24 L/min, 300 g h^{-1}) and minimum obtained at (400 ^{o}C, 12 L/min, 300 g h^{-1}). Thus, the result from this study could be used for maximizing the yield of bio-oil, biochar or gas.

6. References

Ansley, R.J., Wiedemann, H.T., Castellano, M.J., Slosser, J.E., 2006. Herbaceous restoration of juniper dominated grasslands with chaining and fire. Rangeland Ecology & Management. 59, 171–178.

Baughman, C., Forbis, T.A., Provencher, L., 2010. Response of two sagebrush sites to low-disturbance, mechanical removal of piñyon and juniper. Invasive Plant Sci. Manag. 3, 122–129.

Box, G.E.., Wilson, K.B., 1951. On the experimental attainment of optimum conditions. J. R. Stat. Soc. Ser. B Methodol. 13, 1–45.

Bridgwater, A.V., 2012. Upgrading biomass fast pyrolysis liquids. Environ. Prog. Sustain. Energy 31, 261–268.

Bridgwater, A.V., Meier, D., Radlein, D., 1999. An overview of fast pyrolysis of biomass. Org. Geochem. 30, 1479–1493.

Bulushev, D.A., Ross, J.R.H., 2011. Catalysis for conversion of biomass to fuels via pyrolysis and gasification: a review. Catal. Today 171, 1–13.

Butler, E., Devlin, G., Meier, D., McDonnell, K., 2011. A review of recent laboratory research and commercial developments in fast pyrolysis and upgrading. Renew. Sustain. Energy Rev. 15, 4171–4186.

Calonaci, M., Grana, R., Barker Hemings, E., Bozzano, G., Dente, M., Ranzi, E., 2010. Comprehensive kinetic modeling study of bio-oil formation from fast pyrolysis of biomass. Energy Fuels 24, 5727–5734.

Gerçel, H.F., Gerçel, ö., 2007. Bio-oil production from an oilseed by-product: fixed-bed pyrolysis of olive cake. Energy Sources Part Recovery Util. Environ. Eff. 29, 695–704.

Kersten, S.R.A., Wang, X., Prins, W., van Swaaij, W.P.M., 2005. Biomass pyrolysis in a fluidized bed reactor. part 1: literature review and model simulations. Ind. Eng. Chem. Res. 44, 8773–8785.

Kim, K.H., Eom, I.Y., Lee, S.M., Choi, D., Yeo, H., Choi, I.-G., Choi, J.W., 2011. Investigation of physicochemical properties of biooils produced from yellow poplar wood (Liriodendron tulipifera) at various temperatures and residence times. J. Anal. Appl. Pyrolysis 92, 2–9.

Mante, O.D., Agblevor, F.A., 2011. Parametric study on the pyrolysis of manure and wood shavings. Biomass Bioenergy 35, 4417–4425.

Miller, R.F., Wigand, P.E., 1994. Holocene changes in semiarid pinyon-juniper woodlands. BioScience 44, 465–474.

Miller, R.F., Bates, J.D., Svejcar, T.J., Pierson, F.B., Eddleman, L.E., 2005. Biology, ecology, and management of western juniper (Juniperus occidentalis). Tech. Bull. 152 Agric. Exp. Stn. Or. State Univ. Corvalis Or.

Ngo, T.-A., Kim, J., Kim, S.-S., 2013. Fast pyrolysis of palm kernel cake using a fluidized bed reactor: design of experiment and characteristics of bio-oil. J. Ind. Eng. Chem. 19, 137–143.

Olukcu, N., Yanik, J., Saglam, M., Yuksel, M., 2002. Liquefaction of beypazari oil shale by pyrolysis. J. Anal. Appl. Pyrolysis 64, 29–41.

Park, H.J., Park, Y.-K., Dong, J.-I., Kim, J.-S., Jeon, J.-K., Kim, S.-S., Kim, J., Song, B., Park, J., Lee, K.-J., 2009. Pyrolysis characteristics of oriental white oak: kinetic study and fast pyrolysis in a fluidized bed with an improved reaction system. Fuel Process. Technol. 90, 186–195.

Pattiya, A., 2011. Bio-oil production via fast pyrolysis of biomass residues from cassava plants in a fluidized-bed reactor. Bioresour. Technol. 102, 1959–1967.

Petrus, L., Noordermeer, M.A., 2006. Biomass to biofuel, a chemical perspective. R. Soc. Chem. 8, 861–867.

Piskorz, J., Majerski, P., Radlein, D., Scott, D.S., Bridgwater, A.V., 1998. Fast pyrolysis of sweet sorghum and sweet sorghum bagasse. J. Anal. Appl. Pyrolysis 46, 15–29.

Salehi, E., Abedi, J., Harding, T., 2009. Bio-oil from sawdust: pyrolysis of sawdust in a fixed-bed system. Energy Fuels 23, 3767–3772.

Salehi, E., Abedi, J., Harding, T., 2011. Bio-oil from Sawdust: effect of operating parameters on the yield and quality of pyrolysis products. Energy Fuels 25, 4145–4154.

Scott, D.S., Majerski, P., Piskorz, J., Radlein, D., 1999. A second look at fast pyrolysis of biomass—the RTI process. J. Anal. Appl. Pyrolysis 51, 23–37.

Şensöz, S., Demiral, İ., Ferdi Gerçel, H., 2006. Olive bagasse (Olea europea L.) pyrolysis. Bioresour. Technol. 97, 429–436.

Vamvuka, D., 2011. Bio-oil, solid and gaseous biofuels from biomass pyrolysis processes- an overview. Int. J. Energy Res. 35, 835–862.

Weisberg, P.J., Lingua, E., Pillai, R.B., 2007. Spatial patterns of pinyon–juniper woodland expansion in Central Nevada. Rangel. Ecol. Manag. 60, 115–124.

Zhang, H., Xiao, R., Huang, H., Xiao, G., 2009. Comparison of non-catalytic and catalytic fast pyrolysis of corncob in a fluidized bed reactor. Bioresour. Technol. 100, 1428–1434.

CHAPTER 4

CATALYTIC PYROLYSIS OF PINYON JUNIPER USING RED MUD AND HZSM-5 AS CATALYST

1. Abstract

Pinyon and juniper are invasive woody species in Western United States that occupy over 47 million acres of land. The US Bureau of Land Management (BLM) has embarked on harvesting these woody species to make room for range grasses for grazing. The major application of harvested pinyon-juniper (PJ) is low value firewood. Thus, there is a need to develop new high value products from this woody biomass to reduce the cost of harvesting. We investigated the fractional catalytic pyrolysis of PJ using both HZSM-5 catalyst and red mud at 475^{o} C in a fluidized bed reactor at atmospheric pressure. Both the HZSM-5 and the red mud were effective catalysts for producing low viscosity pyrolysis oils. The red mud catalyzed oils had a lower viscosity (141 cP @40 ^{o}C) than the HZSM-5 catalyzed oils (222 cP @40 ^{o}C). In both cases the yields of liquids ranged from 42 to 49 wt%. The mechanisms of catalysis by the two catalysts were quite different. The HZSM-5 rejected oxygen mostly as carbon monoxide (CO) and water and produced lower amounts of carbon dioxide (CO_2), in contrast the red mud produced more CO_2 and less CO. However, both catalysts produced similar amounts of water. The char yields from both catalysts were similar but the total gas yields were slightly different. The higher heating value of the red mud catalyzed oil (29.46 MJ/kg) was slightly higher than that catalyzed by HZSM-5 (28.55 MJ/kg). Thus, red mud can be used to achieve similar catalytic pyrolysis results as HZSM-5 catalysts.

2. Introduction

Pinyon juniper woodlands occupy about 47 million acres in the Western United States which includes states of Arizona, California, Colorado, Idaho, Nevada, New Mexico, Oregon, Utah, and Wyoming (Evans, 1988; Chambers et al., 1999). The tree species associated with pinyon juniper woodlands are extremely variable, with complex distribution and patterns (West et al., 1998). The juniper trees found in the pinyon juniper woodlands consists of following species, alligator juniper (*Juniperus deppeana* Steud.), one-seed juniper *(Juniperus monosperma* (Engelm.) Sarg.), western juniper *(Juniperus occidentalis* Hook.), Utah juniper (*Juniperus osteosperma* (Torr.) Little), and Rocky Mountain juniper *(Juniperus scopulorum* Sarg.). The pinyon trees consists of following species, Mexican pinyon (Pinus cembroides Zucc.), pinyon (Pinus edulis Engelm.), and singleleaf pinyon (Pinus monophylla Torr. and Frem.) (Chambers et al., 1999).

PJ woodlands domination decreases the herbaceous vegetation, increase bare lands which in turn increases soil erosion and nutrition loss (Miller and Wigand, 1994; Brockway et al., 2002). Studies have shown that expansion of PJ woodlands have reduced the magnitude of precipitation (Miller et al., 2005), and increased soil erosion by four times (Carrara and Carroll, 2007). PJ woodlands increases the potential of crown fires, which promote the infiltration of exotic species (Tausch et al., 1993). Thus, land managing agencies are focusing on reducing the population of PJ woodlands by bulldozing, chaining (Ansley et al., 2006), hand cutting, mechanical removal (Baughman et al., 2010) , and prescribed fire (Ansley et al., 2006; Baughman et al., 2010). The harvested material is therefore a mixture of several species bundled together which are used for low value applications. Western junipers are used as firewood and chips for particle-flake board. The production of naval stores from PJ woodlands is of great interest since they contain four times more resin than douglas-fir.

Catalytic pyrolysis is an emerging technology that has the potential of producing liquid fuels from biomass feedstocks. The major advantage of the catalytic pyrolysis process is the improvement in the property and stability of the pyrolysis oils because of cracking of the reactive species into either low molecular weight organics or gasification of some of this reactive species to carbon oxides and C1 to C5 hydrocarbons. The most effective catalysts used for biomass conversion to liquids are mostly acidic zeolite catalysts and modification of these catalysts. Although they produce relatively stable pyrolysis oils they also generate considerable quantities of water, carbon oxides, and char/coke. This combination of gaseous products, char and water constitute loss of carbon and reduction in the overall carbon efficiency. Thus, there is a pressing need to develop new catalysts that improve carbon efficiency and yet produce stable pyrolysis oils.

Red mud or red sludge is the solid residue from the processing of bauxite to alumina using the Bayer process. Red mud is a complex mixture of metallic oxides such as ferric oxide, aluminum oxide, titanium dioxide, magnesium oxide, calcium oxide, silicon oxide, and other minor compounds, in addition to the residual sodium hydroxide used in the extraction process. This material has been investigated by several researchers for various catalytic applications such as hydrodechlorination (Ordonez et al., 2001), hydrogenation of anthracene (Alvarez et al., 1995, 1999), pyrolysis of waste plastics and waste oils (Cakici et al., 2004; López et al., 2011), hydrogenation and liquefaction of rye straw (Klopries et al., 1990), upgrading of hemp-seed pyrolysis oils, and acetic acid (Karimi et al., 2010). In most of these applications red mud was activated through acid treatment and other modifications. However, there has not been any systematic investigation of using red mud as fractional catalytic pyrolysis catalysts. In this paper we report the investigation of red mud as a catalyst for conversion of pinyon juniper into pyrolysis oils for higher value applications.

3. Experimental methods

3.1. Biomass

Pinyon juniper (PJ) biomass feedstock chips were harvested in Nevada and supplied by P&P Ventures. The pinyon pine and juniper trees are usually harvested together, thus in order to represent the mixture pinyon pine and juniper wood were manually mixed in ratio of 50: 50 wt %. Wood samples were dried to equilibrium moisture content under ambient laboratory conditions and then ground in Wiley mill (model 4) until all the biomass passed through 1-mm screen. The biomass was characterized on the basis of moisture (ASTM E1756 - 08, standard method), ash content (ASTM E1755-01 (2007), standard method), bulk density (ASTM D1895-B, standard method), elemental analysis and energy content.

Table 4. 1. Composition and calorific value of PJ wood

Moisture (wt %)	7.55±0.06
Ash content (wt %)	0.46±0.04
Carbon %	53.43±0.11
Hydrogen %	6.58±0.04
Nitrogen %	0.16±0.01
Sulfur %	0
Oxygen% [a]	39.37±0.09
Experimental HHV (MJ/kg)	19.54±0.16

3.2. Catalysts

A commercial catalyst, ZSM5 was obtained in sodium form from BASF catalysts LLC (Iselin, NJ, USA). ZSM5 was calcined at 550^{o} C for 5 hr, to convert ZSM5 into protonated form (HZSM5). The catalyst was sieved to obtain particular particle size (125 – 180 µm). The catalyst was characterized based on acidity and Brunauer–Emmett–Teller (BET) surface area analyzer

(Quantachrome Instruments, Boyton Beach, FL). The acidity of the catalyst was determined by VTT technical research centre of Finland, based on temperature programmed ammonia desorption (NH_3-TPD). The red mud which was supplied by Sherwin Alumina Co LLC, (Gregory, TX), was dried at ambient laboratory conditions, ground with mortar and pestle and sieved to appropriate particle size (150-180 μm) for fluidized bed pyrolysis studies. The chemical composition of the red mud was determined using X-ray diffraction (XRD) (PANanalytic X'Pert Pro XRD spectrometer, PANalytical Inc, Westborough, MA) and X-ray fluorescence (XRF) (Philips PW2404 XRF spectrometer, PANalytical Inc, Westborough, MA) and surface area was determined using Quantachrome BET surface analyzer.

3.3. BET surface area

The BET surface area of the fresh and spent catalyst was measured using Quantachrome BET surface analyzer (Quantachrome Instruments, Boyton Beach, FL). 0.5 g of samples were degassed at 220^o C for 3 h and then used in the experiment. The BET surface area was calculated based on nitrogen adsorption/ desorption from the surface of the sample.

3.4. XRD and XRF analysis

The chemical composition of red mud was obtained from XRF analysis and was confirmed by XRD analysis. The XRD and XRF analysis of fresh and spent catalyst were analyzed by Analytics Laboratory in department of geology (Utah State University, UT). The XRD data was measured between 5◦ to 150◦ interval in 2θ using a 0.02^o step size.

3.5. Pyrolysis of biomass

The pyrolysis of the biomass feedstocks were conducted in a 2-inch fluidized bed reactor described in Agblevor et al, Mante et al. Thus, the ground biomass was fed into a hopper and conveyed by K-Tron screw feeder into an entrainment zone where it was entrained by nitrogen carrier gas and

through an air-cooled feeder tube into the bubbling fluid bed. The bubbling fluid bed was either sand or catalyst (100 g) depending on the desired outcome. The pyrolysis was conducted at 475^{o} C at atmospheric pressure. The fluidizing gas was nitrogen at a flow rate of three times the minimum fluidization velocity for catalytic (6.5 L/min) and noncatalytic pyrolysis (15 L/min). The biomass feed rate was 150 g/h and weight hourly space velocity was 1.5 h^{-1}. The pyrolysis products exiting the reactor were first separated with a hot gas filter to collect the solid residue and some entrained catalyst. The vapors and non-condensable gases exiting the hot gas filter were then passed through two ethylene glycol collected condensers maintained at 10 ^{o}C and 4 ^{o}C respectively to condense the pyrolysis vapors. The non-condensable gases and aerosols were then passed through an electrostatic precipitator maintained at 20-30 kV to condense the aerosols. The clean non-condensable gases (NCG) were then passed through a coalescing filter and a totalizer and then sampled online with Varian microGC gas chromatographic analyzer. The excess gases were vented through a flare.

All the reaction apparatus (reactor, hot gas filter, condensers, electrostatic precipitator) were weighed before and after each experiment. This enabled a gravimetric determination of the yield of various components. The pyrolysis times were 120 to 180 min. In order to determine the catalyst activity, oils samples were collected at 60 min intervals and their viscosities measured. Additionally the gaseous products were analyzed every 5 min to follow the composition of the gases which is related to the catalyst activity. All experiments were conducted in triplicates to determine reproducibility. In addition, some red mud catalysts was regenerated after the first run and reused for the pyrolysis.

3.6. Gas analysis

A fraction of the gases exiting the totalizer (0.1 L/min) was connected to Varian 490-microGC (Agilent Technologies, Santa Clara, CA) for online analysis. The gases were automatically sampled every 3.25 min for the duration of the experiment. The microGC was equipped with two modules, a 10 m Molsieve (MS) 5A column, and a 10 m porous polymer (PPU) column. Each module had a thermal conductivity detector. The MS was used to analyze hydrogen, methane, and carbon monoxide. Carbon dioxide, C_1-C_5 hydrocarbons were analyzed on the PPU column.

3.7. Bio-oil analysis

Catalytic pyrolysis oil samples (biocrude) were characterized for organic elemental composition (CHNOS) using ThermoFischer Scientific Flash 2000 organic elemental analyzer; the higher heating value (HHV) was determined using IKA C2000 basic bomb calorimeter (IKA® Works Inc, NC) according to ASTM D2015. The pH was measured using Mettler Toledo pH Meter and probe (Mettler-Toledo GmbH, Switzerland). The pH data were obtained after 5-10 min stabilization of the mechanically stirred oil. The dynamic viscosity of the oils was measured at 40 ^{o}C using DV-II + Pro viscometer (Brookfield Engineering Laboratory, Inc, Middleboro, MA). A Metrohm 701KF Titrino (Brinkmann Instruments Inc, NY) and 703 titration stand setup were used for the volumetric Karl Fischer titration. Hydranal Composite 5™ reagent was sued for the titration. 50 ml methanol was placed in the titration vessel and conditioned. About 60-100 mg of the oil sample was loaded into a hypodermic plastic syringe and weighed. The sample was injected into the titration solvent and the syringe was reweighed. The water content was titrated volumetrically and the percentage mass recorded.

The ^{13}C-nmr spectra were recorded on a JOEL 300 MHz NMR spectrometer (JOEL Ltd, Tokyo, Japan). About 1.0 g of oil was dissolved in 0.7 ml dimethyl sulfoxide-d_6 (DMSO-d_6) in a 5 mm sample probe. The DMSO-d_6 containing 1% (v/v) tetramethylsilane (TMS) was obtained from

Sigma Aldrich (Sigma Aldrich, St Louis, MO). The observing frequency for the ^{13}C nucleus was 100.58 MHz, the pulse width was 10 µs, the acquisition time was 1.58 s, and the relaxation delay was 2 s. The spectra were obtained with 4000 scans and a sweep width of 200 kHz.

4. Results and Discussion

4.1. Catalyst characterization

The protonated ZSM5 catalyst was sieved to a particle size of 150-180 µm and had BET surface area of 115 m^2/g. The HZSM5 had a total acidity of 2.39 mmol g^{-1}, which was a combination of weak and strong acid sites. The red mud water slurry had a pH 9 and the dry ground material used for the experiments had a particle size of 150-180 µm and a BET surface area of 30 m^2/g. The XRF analysis showed that red mud was a mixture of metal oxides and is comprised of Fe_2O_3 (53.98), Al_2O_3 (13.53), SiO_2 (8.91), CaO (8.87), TiO_2 (6.18), Na_2O (5.83). The presence of these oxides was further confirmed with XRD analysis (Fig 4.2). There was no special activation of the red mud before being used, thus, the reported effect is on as received basis. The red mud samples were however heated in the reactor for almost two hours to get to a stable pyrolysis temperature before each experiment.

4.2. Pyrolysis product distribution

In order to determine the effect of HZSM5 and red mud on pyrolysis of PJ biomass, pyrolysis was carried out with sand and catalysts. The effect of sand, HZSM5 and red mud on product distribution is shown in Table 4.2 for pyrolysis carried out for 2 hours. The liquid products were segregated in three condensers. Most of the aqueous fraction was found in the first condenser whereas the oil collected in the electrostatic precipitator (ESP) had low moisture content. However, the properties of the oils collected in the condensers were similar to those from the ESP oil. The results show that both HZSM5 and red mud reduced the liquid yield, specifically the organic yield compared to sand.

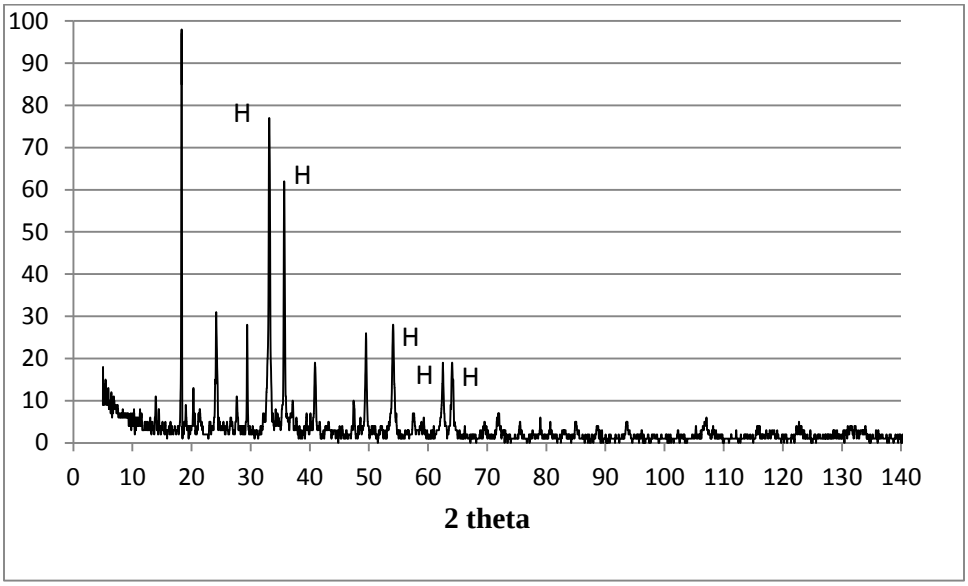

Fig. 4. 1. XRD spectrum of fresh red mud sample (H= hematite, M= magnetite)

The reduction in the organic yield was mainly due to extensive cracking of the pyrolysis vapors by the catalyst. The conversion of organic liquid to water and char by the catalyst was relatively low compared to the amount of gas produced. The water yields of HZSM5 and red mud were only slightly different from sand. Due to the reduction in organic content, the water content of the liquid product of HZSM5 and red mud was about 50 % compared to 33% for sand. In the case of the silica sand (sand) pyrolysis, the aqueous phase was miscible with the organic fraction whereas in the cases of HZSM-5 and red mud the aqueous phases were immiscible with the organic phases because the oils were more deoxygenated, which made them less polar than the sand pyrolysis oil. The char/coke yields for the HZSM-5 and the red mud were similar but slightly higher than that for the sand. These char/coke yields were relatively low and followed trends reported by Agblevor et al, because, in this process, the species in contact with the catalyst are unstable pyrolysis intermediates, whereas in traditional pyrolysis upgrading systems, the compounds in contact with the catalyst are stable molecules that promote coke formation. The pyrolysis medium

Table 4. 2 Pyrolysis product distribution using different pyrolysis medium

	Product distribution (wt %)				
	Total liquid	organic	Water	Char/coke	Gas*
Sand	60.31±0.05	40.15±0.51	20.16±0.55	22.49±0.39	17.21±0.34
HZSM-5	49.34±0.14	25.92±0.11	23.42±0.25	20.98±0.32	29.69±0.18
Red mud	44.37±1.02	20.85±1.0	23.53±0.02	23.50±0.21	32.14±1.23

greatly influenced the gas yield. The sand produced the least amount of gas whereas the red mud produced the highest amount of gas.

4.3. Physicochemical properties of bio oil obtained from catalytic and non catalytic pyrolysis

The ESP captured most of the oil product with minimal water content, thus this fraction was used for the characterization studies. The oil phase from the condenser had similar properties like the ESP oil and therefore data from the ESP oils are representative of the total oils produced from this process. The physical properties of the oils from the ESP are shown in Table 4.3. Clearly it can be seen that the moisture content of the ESP oils were very low because of the efficient condensation in the ethylene glycol cooled condensers. The pH of red mud oil was slightly higher than those of the sand and HZSM-5 oils, this is mainly due to decarboxylation reaction. The densities of the red mud oils were also slightly lower than those of the sand and HZSM-5 oils although they were all higher than the density of water. The dynamic viscosities of the oils showed dramatic differences. The red mud oils were about seven times less viscous than the sand oils whereas the HZSM-5 was only two and half times less viscous. This major difference was obviously due to the cracking of the oils by the red mud and the HZSM-5 which resulted in the high gas production (Table 4.2). The relative carbon content of the red mud oils were 14% higher than that of the sand oil and oxygen content of the red mud oils were 25% lower than those of the

sand oil (Table 4.3). The hydrogen content of the red mud pyrolysis oil were also slightly higher than that of the sand oil and HZSM5 oils probably because most of the oxygen was rejected as carbon dioxide and less as water. There were also significant differences in the higher heating value (HHV) of the oils. Both the red mud and HZSM-5 oils had much higher HHV than the sand oil.

Table 4. 3 Physicochemical properties of ESP oil produced from catalytic and non-catalytic pyrolysis

	Sand	**HZSM5**	**Red mud**
Water content (wt %)	2.81±0.15	1.72±0.08	1.45±0.08
pH	2.75	2.80±0.10	3.56
Density	1.22±0.02	1.19±0.04	1.14±0.01
Dynamic Viscosity (cP)	686.02±27.52	213.68±10.14	96.99±19.54
Carbon (%)	58.11±0.07	62.79±0.10	65.13±0.05
Hydrogen (%)	6.72±0.04	6.86±0.04	7.17±0.01
Nitrogen (%)	0.13±0.02	0.27±0.03	0.21±0.02
Oxygen (%)	35.04	30.08	27.49
HHV (MJ/Kg)	24.87±0.37	28.55±0.23	29.46±0.62

The functional groups present in the bio-oil were characterized by integrating the ^{13}C NMR spectrum. The ^{13}C NMR spectra of sand, HZSM5 and red mud are shown in the Fig 4.3. The chemical shifts in the spectrum were assigned to different functional groups based on the analysis reported in (Mante et al., 2011).

The comparison between HZSM5 and red mud pyrolysis oils spectra showed that the later was more effective in the reduction of carbohydrate degradation products. The aromatic compounds produced by red mud were different from those from HZSM5, and there were also more aliphatic

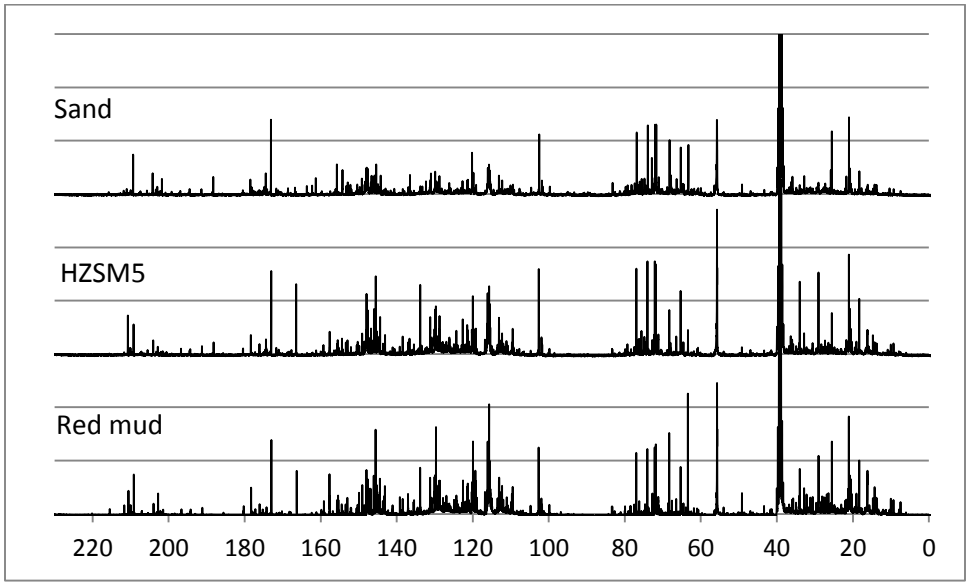

Fig. 4. 2. ^{13}C NMR spectrum of bio-oil produced from catalytic and non-catalytic pyrolysis

carbon signals in red mud pyrolysis oils than the HZSM5 oils. The increased aliphatic signal intensity was attributed to increased demethoxylation of lignin moieties which resulted in more alkylation reaction and production of methanol. The methanol signal at 50 ppm was much higher for red mud oil than the other two oils (Fig 4.3).

The semi-quantitative analysis of the ^{13}C-NMR functional groups show that pyrolysis with sand produced more highly oxygenated compounds since the pyrolysis oil produced had higher amounts of carbohydrate degradation products, alcohol, ethers, methoxylated phenols, carboxylic groups, aldehydes, and ketones (Table 4.4). The catalytic pyrolysis oils had lower concentration of carbohydrate degradation product, alcohol and ethers, while aliphatic and aromatic products were relatively higher than that from sand. The carboxylic acids, ketones and aldehydes concentration were also relatively lower than that of sand.

Table 4. 4. Carbon distribution in catalytic and non-catalytic pyrolysis bio-oil (NMR integration)

	Sand	ZSM5	Red mud
Aliphatics	17.70	20.21	26.03
Methoxyl in lignin	8.22	6.72	5.04
Levoglucosan	30.04	16.08	12.45
Aromatics	38.03	53.74	53.93
Carboxylic acids	3.73	1.99	1.51
Ketones and aldehydes	2.29	1.26	1.05

4.4. Gas analysis

The gas yields obtained from catalytic and non-catalytic pyrolysis on weight basis are shown in Table 4.5. The pyrolysis gas components were similar for all the pyrolysis media, but varied in their individual concentrations. The results obtained showed that all the pyrolysis gases contained hydrogen, CO, CO_2 and C_1-C_5 hydrocarbons, with CO and CO_2 constituting 84 - 92% of the gas yield. Catalytic pyrolysis (experiments with HZSM5 and red mud) had substantially increased the concentration of carbon oxides and hydrocarbons, compared to non-catalytic pyrolysis. The Hydrogen concentration of red mud was slightly higher than HZSM5, which was closer to sand. The concentrations of hydrocarbons also increased for catalytic pyrolysis, when compared to non-catalytic pyrolysis. Butane accounts for about 39% of hydrocarbons for both catalysts and methane accounts for 27% and 37% of hydrocarbons in HZSM5 and red mud respectively.

Table 4. 5. Yield of gases produced using different pyrolysis medium

Gases	Sand	ZSM5	Red mud
	% yield (N_2 free basis)		
Hydrogen	0.14±0.02	0.19±0.02	0.49±0.12
Methane	0.50±0.05	1.21±0.08	1.59±0.16
Carbon monoxide	5.41±0.81	14.27±0.56	9.21±0.27
Carbon dioxide	10.30±0.34	10.85±0.05	18.51±0.41
Ethane	0.09±0.01	0.67±0.02	0.36±0.01
Propane	0.31±0.02	0.64±0.01	0.37±0.04
N-butane	0.25±0.14	2.06±0.05	1.37±0.24
N-pentane	0.21±0.02	0.27±0.06	0.23±0.03
Total	17.21±1.37	29.69±1.01	32.14±1.28

The main difference in the gas yields between the HZSM5 and red mud is in the concentration of carbon oxides. HZSM5 produced more CO, while red mud produced more CO_2. The difference in the carbon oxide contents of the gases may be due to differences in reaction pathway. In the case of sand, the carbon oxides production was attributed to thermal cracking whereas in the case of HZSM5 and red mud, there appeared to be catalytic cracking. The catalytic rejection of oxygen from the biomass appeared to be through production of H_2O, CO, and CO_2. The catalytic CO and CO_2 production from biomass pyrolysis could be through decarbonylation, ketonization, decarboxylation or all the three pathways. In the case of HZSM5 it appeared the decarboxylation reaction was dominant producing more CO and CO_2. The results obtained are in agreement with

(Stefanidis et al., 2011), who reported that acidic catalyst favored decarbonylation reaction to produce CO.

In the case of red mud catalysis, the CO_2 production was more pronounced than CO. The CO_2 production from the red mud was attributed to catalytic activity instead of thermal cracking because the organic liquids produced had lower oxygen, higher carbon, and lower viscosity than those produced from the sand (Table 4.3). The higher CO_2 production may be due to reduction of hematite to magnetite or due to decarboxylation reaction. The higher CO_2 production from red mud catalyzed pyrolysis could be due to contribution from the reduction of hematite to magnetite. Jozwiak et al. 2007, reported that under low hydrogen and CO concentration at 150-400^o C and atmospheric pressure, hematite was reduced to magnetite with the subsequent release of CO_2 as shown in equation (4) and (5). The pyrolysis gas composition showed the presence of both H_2 and CO and the red mud after pyrolysis had magnetic properties, thus it is plausible that some of CO_2 originated from the reduction of hematite to magnetite.

$$3Fe_2O_3 + H_2 = 2Fe_3O_4 + H_2O \quad (10)$$

$$3Fe_2O_3 + CO = 2\ Fe_3O_4 + CO_2 \quad (11)$$

The XRD data of the red mud after the pyrolysis also confirmed the formation of magnetite. The contribution of CO_2 from the reduction of hematite to magnetite was presumed minimal because reaction (5) is very rapid and the CO_2 will be released within few minutes of the start of the pyrolysis. Furthermore, the red mud regeneration data also supported such assertion, because the catalyst after regeneration was completely reduced to magnetite form and yet the CO/CO_2 ratio was similar to that of the fresh catalyst pyrolysis. During the red mud catalytic pyrolysis, the catalyst was partially transformed into magnetite/hematite and regeneration did not cause any phase change in the catalyst because of the oxidative nature of the process.

Oxygen rejection as H_2O was similar for the two catalysts since the H_2O yields were similar and higher than that of the sand. The hydrogen yield also varied according to the pyrolysis media. The highest hydrogen production was from the red mud medium whereas the sand produced the lowest amount of hydrogen. The concentrations of hydrocarbons also increased for catalytic pyrolysis compared to non-catalytic pyrolysis. Butane accounted for about 39% of hydrocarbons for both catalysts and methane accounted for 27% and 37% of hydrocarbons in HZSM-5 and red mud, respectively.

Oxygen rejection from the pyrolysis product was probably through decarboxylation reaction because the relative amounts of carboxylic acids and ketones were lower for red mud oil than for the HZSM5 and sand oils (Table 4.4). In the ^{13}C-NMR spectra, the carboxylic acid signal for red mud oil was less than one half that from sand oil. Oxygen rejection through CO_2 has been reported as through ketonization reaction, which converted carboxylic acids to ketones and released CO_2 (Deng et al., 2009; Gaertner et al., 2009). Thus, if high CO_2 production from the red mud reaction proceeded through ketonization pathway, the ketone there should have been an increase in ketone signal and decrease in the carboxylic signal in the ^{13}C NMR spectrum relative to the sand, but this was not observed. This shows that the high CO_2 production in red mud catalyzed reaction is mainly through decarboxylation reaction.

4.5. Catalyst deactivation

The Activity of the catalyst is monitored with the variation of CO and CO_2 concentration over time (Agblevor and Besler-Guran, 2002; Agblevor et al., 2010a). The CO/CO_2 ratio variation (wt% basis) for sand, HZSM5 and red mud are shown in Fig 4.4. The average CO/CO_2 ratio for sand was constant at about 0.61 throughout the pyrolysis process. The ratio of CO/CO_2 for HZSM5 was high during the first hour (1.8-1.4) and gradually decreased to 1.0 during the second hour with a total average of 1.31. Thus, the catalyst was highly active during the first 60 minutes, but the activity

decreased sharply during the second hour and remained constant thereafter. Since the CO/CO_2 ratio did not decreased to the value of the sand, this suggested that there was some residual activity in the catalyst. During the first 60 min of pyrolysis, no significant amount of oil accumulated in the ESP and most of the oil was produced during the deactivated equilibrium phase of the catalyst. Furthermore, we observed that as the catalyst deactivated, the viscosity of the pyrolysis oil increased. The final oil collected after 120 min had a viscosity about threefold less than that of the sand pyrolysis oil Table 4.3.

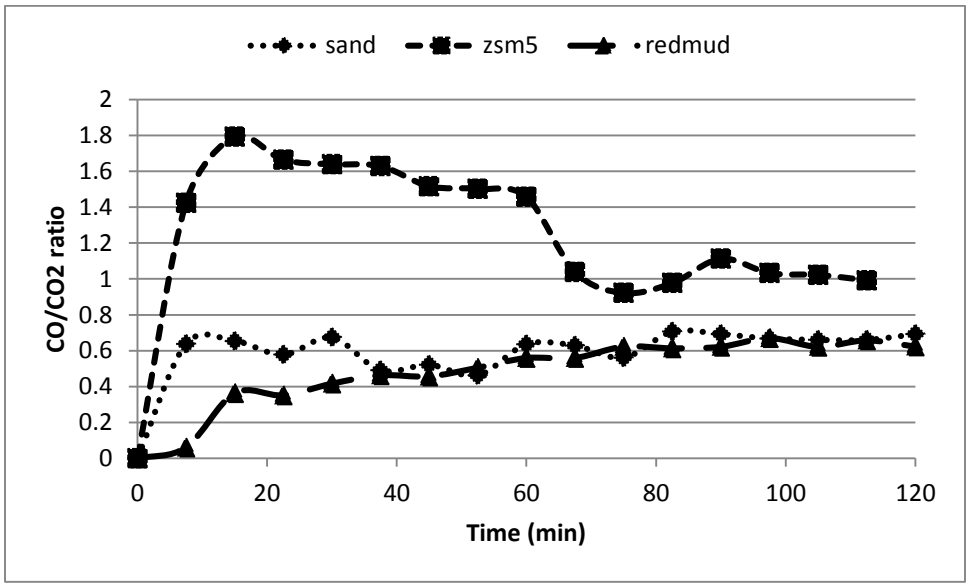

Fig. 4. 3. Variation of CO/CO_2 ratio with time using various pyrolysis media (sand, HZSM5, and red mud)

Red mud produced more CO_2, and thus the CO/CO_2 was below 1.0 throughout the experiment. During the first 60 minutes CO/CO_2 ratio was lower than sand, but the ratio increased gradually and was only slightly lesser than sand. Even though the CO/CO_2 ratios of sand and red mud were similar after 60 min of pyrolysis, the properties of the pyrolysis oils were significantly different. The red mud oil was about seven times less viscous than the sand pyrolysis oil, which suggests that the reaction pathway was different from that of sand.

After 3 h of continuous pyrolysis using red mud, the CO/CO_2 ratio and the viscosity of the oil suggested that the catalyst had deactivated significantly. The catalyst was then regenerated by burning the char/coke deposit in a muffler furnace at 550 °C for 5 h. The regenerated catalyst had magnetic properties which suggested that the hematite (Fe_2O_3) has been reduced to magnetite (Fe_3O_4) under pyrolysis condition. To verify that the change was not due to the regeneration process, freshly discharged catalyst from the pyrolysis reactor was tested for magnetic activity (after cooling), which was positive. The formation of magnetite was further confirmed by comparing the XRD spectra of fresh red mud and regenerated red mud (Fig 4.5). Both hematite and magnetite have 2 theta signals at 35.2, but for the regenerated catalyst this signal intensity increased significantly. Furthermore, only magnetite has signals at 2 theta signal at 30 and hematite has 2 theta signal at 33 (Suber et al., 2005). The signals for both hematite and magnetite were detected in the regenerated catalyst conforming that some of the hematite was converted under the pyrolysis conditions.

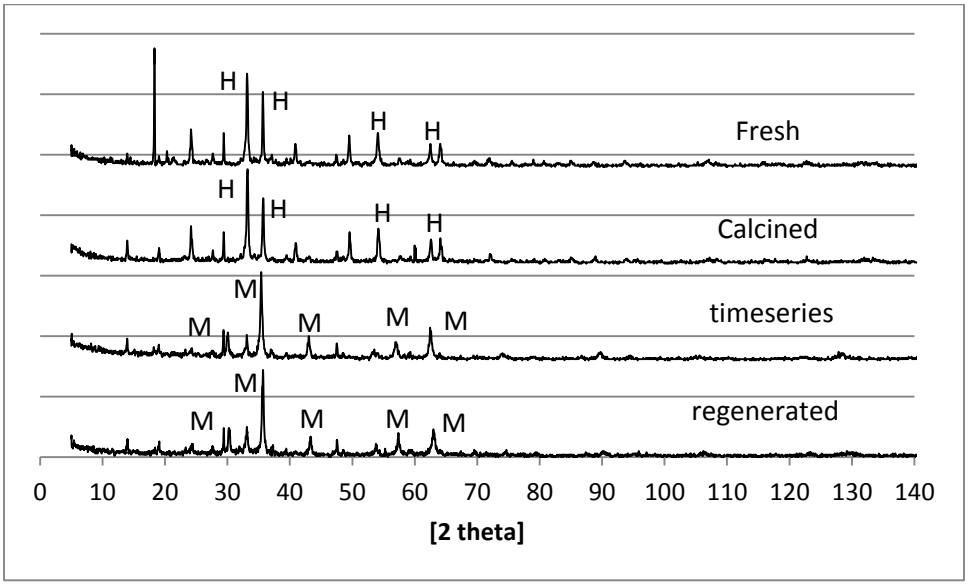

Fig. 4. 4. Comparison of XRD pattern of different red mud samples (H= hematite, M= magnetite)

The HZSM5 catalyst was most effective during the first 60 min, and then when its activity reduced, it was no longer effective in decomposing the long chain molecules and the viscosity of the oil increased with pyrolysis time on stream. The other disadvantage of the HZSM5 was the production of large quantities of gas during the early stages of the pyrolysis when the catalyst was extremely active and thus reducing the liquid yield. The rejection of oxygen was also through the production of CO which led to excessive loss of carbon and thus reducing the overall carbon efficiency of the process.

Although the red mud pyrolysis process also generated large quantities of gas similar to HZSM5 pyrolysis, this gas was rich in CO_2. The viscosity of the pyrolysis oil generated from red mud catalytic process also increased during the pyrolysis time on stream. However, the increase was less rapid then the HZSM5. Both catalysts appeared to reach a steady or equilibrium state during which the rejection of carbon oxides did not vary much with time on stream. The major advantage of red mud oil also appeared to be slightly better than the HZSM5 oils. Furthermore, red mud is a waste product of the Bayer alumina process and could therefore be procured at minimal cost and hence improve the economics of the process.

Red mud could therefore be potentially used to replace HZSM5 for catalytic biomass pyrolysis.

Thus, red mud showed good catalytic property compared to HZSM5, in terms of physical and chemical property of the bio-oil. In order to investigate how long the red mud was active and the effect of regeneration, experiments were carried out with fresh and regenerated catalyst for 180 minutes continuously. The bio-oil and gases were analyzed periodically in order to monitor the catalytic activity.

The pyrolysis product distributions of fresh and regenerated red mud were similar. The physicochemical properties of ESP oil from fresh and regenerated red mud collected at 60 min intervals during the pyrolysis are shown in Table 4.6. There was not much difference in pH,

densities, elemental composition and energy content of the bio-oil collected at different time for fresh red mud. However the viscosity of the bio-oil increased with time, this shows that fresh red mud lost some of its activity to break down larger molecules.

Table 4. 6. Physicochemical properties of ESP oil produced from fresh and regenerated red mud pyrolysis

	Fresh red mud			**Regenerated red mud**		
	60 min	**120 min**	**180 min**	**60 min**	**120 min**	**180 min**
Water content (wt %)	0.67±0.11	0.93±0.08	0.99±0.07	1.80±0.08	1.42±0.02	1.15±0.02
pH	3.41±0.04	3.58±0.06	3.49±0.10	3.76±0.05	3.65±0.06	3.58±0.05
Density (g/cm3)	n/d	1.26±0.11	1.19±0.10	n/d	1.14±0.15	1.14±0.18
Dynamic Viscosity(cP)	n/d	101.16±8.79	120.25±6.91	n/d	99.34± 6.44	122.81±9.7
Carbon (%)	67.63±0.41	67.10±0.21	67.16±0.09	66.03±0.23	66.47±0.08	66.55±0.02
Hydrogen (%)	7.02±0.12	7.09±0.05	7.13±0.02	7.21±0.04	7.23±0.01	7.27±0.03
Nitrogen (%)	0.31±0.03	0.29±0.05	0.28±0.03	0.24±0.01	0.25±0.02	0.23±0.01
Oxygen (%)	25.04	25.52	25.43	26.55	26.05	25.95

The physicochemical properties of ESP oil from Regenerated red mud showed that there was not much difference in pH, density, elemental composition and energy content of the oils collected at different time intervals. As observed in the fresh red mud, the viscosity of bio-oil from regenerated red mud also increased with time. Thus, with fresh and regenerated red mud, there was not much difference in the physical properties.

The chemical compositions of the bio-oils from fresh and regenerated red mud were analyzed with the help of ^{13}C NMR spectrum. Fig 4.6 and Fig 4.7 shows the ^{13}C NMR spectrum of fresh and regenerated red mud collected at different time intervals. The semi-quantitative integration of the

^{13}C NMR spectra is shown in the Table 4.7. Clearly, the data showed that the two oils were similar in the relative concentration of the most functional groups, thus suggesting that the catalyst activity was fully restored after the regeneration. Furthermore, the variation in the CO/CO_2 ratio (Fig 4.8) of the fresh and regenerated red mud also supported the assertion that the regenerated catalyst had similar activities like the fresh red mud. However, the regeneration was for only one cycle, so the number of times red mud could be regenerated before the red mud deactivates permanently is not clear.

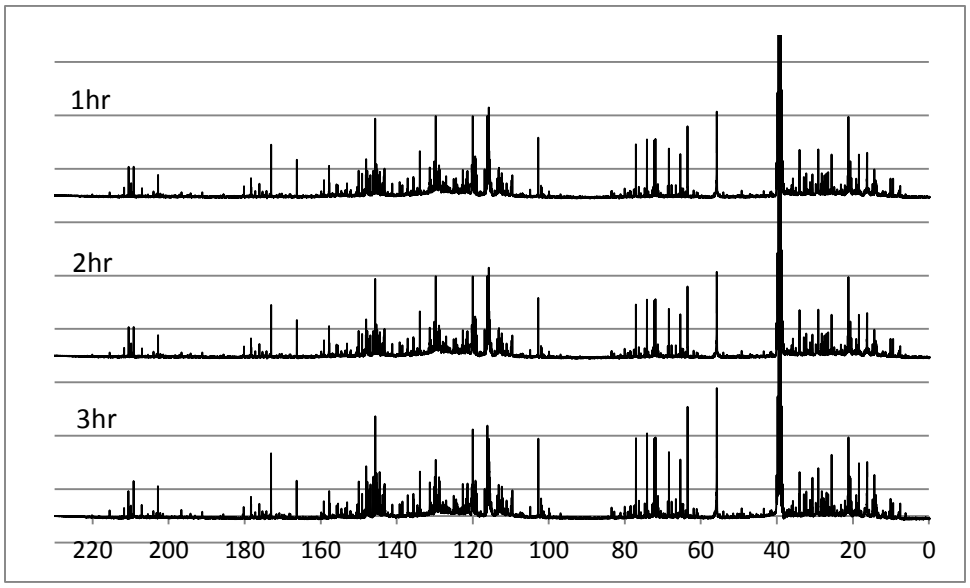

Fig. 4. 5. ^{13}C NMR spectrum of fresh red mud pyrolysis bio-oil collected at different time intervals

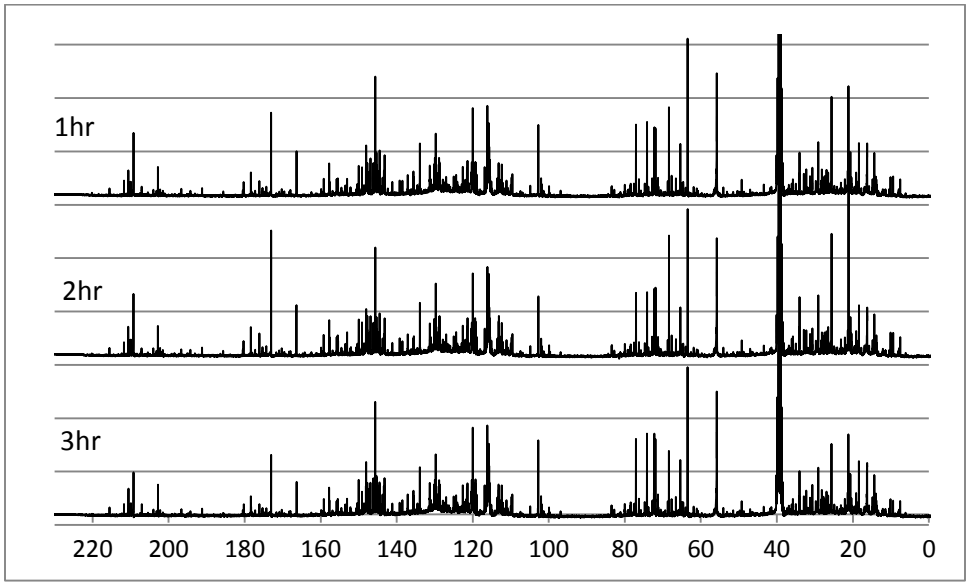

Fig. 4. 6. ^{13}C NMR spectrum of regenerated pyrolysis red mud bio-oil collected at different time intervals

Table 4. 7. Carbon distribution in fresh and regenerated red mud pyrolysis bio-oil

	Fresh red mud			Regenerated red mud		
	1 hr	2 hr	3 hr	1 hr	2 hr	3 hr
Aliphatics	22.77	26.16	21.68	23.58	23.02	22.93
Methoxyl in lignin	3.85	4.61	5.37	5.14	5.16	5.51
Levoglucosan	9.95	10.61	12.74	11.69	11.48	13.66
Aromatics	60.57	55.79	57.39	56.72	56.82	55.37
Carboxylic acids	1.57	1.75	1.72	1.49	2.30	1.49
Ketones and aldehydes	1.28	1.08	1.09	1.38	1.23	1.04

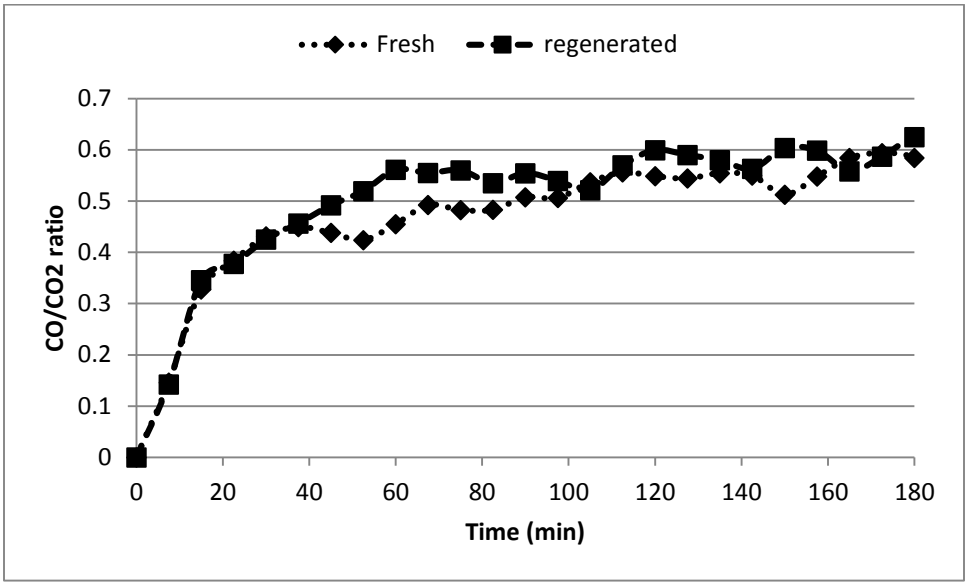

Fig. 4. 7. Variation of CO/CO_2 ratio with time using fresh and regenerated red mud

5. Conclusion

Pyrolysis of pinyon/juniper biomass was demonstrated using silica sand, HZSM5, and red mud as effective pyrolysis media. The HZSM5 and red mud had catalytic effect on the pyrolysis of the feedstock resulting in oils with much lower viscosity than the oils produced using silica sand as the pyrolysis medium. The pyrolysis oils generated using the red mud had viscosity that were seven times lower than the oils produced using silica sand. The reaction pathway of the red mud were quite different from that of the HZSM5 and silica sand. Red mud rejected oxygen from the biomass pyrolysis vapors probably through decarboxylation reaction instead of decarbonylation reaction observed for the HZSM5. The red mud appeared to be stable and regenerable for catalytic pyrolysis reaction.

6. References

Agblevor, F.A., Besler-Guran, S., 2002. Fractional pyrolysis of biomass for high-valued products. Fuel Chem. Prepr. 47(1), 374–375.

Agblevor, F.A., Beis, S., Mante, O., Abdoulmoumine, N., 2010. Fractional catalytic pyrolysis of hybrid poplar wood. Ind. Eng. Chem. Res. 49, 3533–3538.

Alvarez, J., Rosal, R., Sastre, H., Diez, F.V., 1995. Characterization and deactivation of sulfided red mud as hydrogenation catalyst. Appl. Catal. Gen. 128, 259–273.

Alvarez, J., Ordonez, S., Rosal, R., Sastre, H., Diez, F.V., 1999. A new method for enhancing the performance of red mud as a hydrogenation catalyst. Appl. Catal. Gen. 180, 399–409.

Ansley, R.J., Wiedemann, H.T., Castellano, M.J., Slosser, J.E., 2006. Herbaceous restoration of juniper dominated grasslands with chaining and fire. Rangel. Ecol. Manag. 59, 171–178.

Baughman, C., Forbis, T.A., Provencher, L., 2010. Response of two Sagebrush sites to low-disturbance, mechanical removal of piñyon and juniper. Invasive Plant Sci. Manag. 3, 122–129.

Brockway, D.G., Gatewood, R.G., Paris, R.B., 2002. Restoring grassland savannas from degraded pinyon-juniper woodlands: effects of mechanical overstory reduction and slash treatment alternatives. J. Environ. Manage. 64, 179–197.

Cakici, A.I., Yanik, J., Ucar, S., Karayildirim, T., Anil, H., 2004. Utilization of red mud as catalyst in conversion of waste oil and waste plastics to fuel. J. Mater. Cycles Waste Manag. 6, 20–26.

Carrara, P.E., Carroll, T.R., 2007. The determination of erosion rates from exposed tree roots in the piceance basin, Colorado. Earth Surf. Process. 4, 307–317.

Chambers, J.C., Vander Wall, S.B., Schupp, E.W., 1999. Seed and seedling ecology of Pinyon and juniper species in the pygmy woodlands of Western North America. Bot. Rev. 65, 1–38.

Deng, L., Fu, Y., Guo, Q.-X., 2009. Upgraded acidic components of bio-oil through catalytic ketonic condensation. Energy Fuels 23, 564–568.

Evans, R.A., 1988. Management of pinyon-juniper woodlands. USDA For. Serv. Rep. INT-249 Ogden UT.

Gaertner, C.A., Serrano-Ruiz, J.C., Braden, D.J., Dumesic, J.A., 2009. Catalytic coupling of carboxylic acids by ketonization as a processing step in biomass conversion. J. Catal. 266, 71–78.

Jozwiak, W.K., Kaczmarek, E., Maniecki, T.P., Ignaczak, W., Maniukiewicz, W., 2007. Reduction behavior of iron oxides in hydrogen and carbon monoxide atmospheres. Appl. Catal. Gen. 326, 17–27.

Karimi, E., Briens, C., Berruti, F., Moloodi, S., Tzanetakis, T., Thomson, M.J., Schlaf, M., 2010. Red mud as a catalyst for the upgrading of hemp-seed pyrolysis bio-oil. Energy Fuels 24, 6586–6600.

Klopries, B., Hodek, W., Bandermann, F., 1990. Catalytic hydroliquifaction of biomass with redmud and CoO-MoO3 catalyst. Fuel 69, 448–455.

López, A., de Marco, I., Caballero, B.M., Laresgoiti, M.F., Adrados, A., Aranzabal, A., 2011. Catalytic pyrolysis of plastic wastes with two different types of catalysts: ZSM-5 zeolite and red mud. Appl. Catal. B Environ. 104, 211–219.

Mante, O.D., Agblevor, F.A., McClung, R., 2011. Fluid catalytic cracking of biomass pyrolysis vapors. Biomass Convers. Biorefinery 1, 189–201.

Miller, R.F., Wigand, P.E., 1994. Holocene changes in semiarid pinyon-juniper woodlands. BioScience 44, 465–474.

Miller, R.F., Bates, J.D., Svejcar, T.J., Pierson, F.B., Eddleman, L.E., 2005. Biology, ecology, and management of western juniper (Juniperus occidentalis). Tech. Bull. 152 Agric. Exp. Stn. Or. State Univ. Corvalis Or.

Ordonez, S., Sastre, H., Diez, F., 2001. Catalytic hydrodechlorination of tetrachloroethylene over redmud. J. Hazard. Mater. B81, 103–114.

Stefanidis, S.D., Kalogiannis, K.G., Iliopoulou, E.F., Lappas, A.A., Pilavachi, P.A., 2011. In-situ upgrading of biomass pyrolysis vapors: Catalyst screening on a fixed bed reactor. Bioresour. Technol. 102, 8261–8267.

Suber, L., Imperatori, P., Ausanio, G., Fabbri, F., Hofmeister, H., 2005. Synthesis, Morphology, and magnetic characterization of iron oxide nanowires and nanotubes. J. Phys. Chem. B 109, 7103–7109.

Tausch, R.J., Chambers, J.C., Blank, R.R., Nowak, R.S., 1993. Differential establishment of perennial grass and cheatgrass following fire on an ungrazed sagebrush-juniper site. Wildland Shrub Arid Land Restor. Symp. Las Vegas NV Gen Tech Rep INT-GTR-315.

West, N.E., Tausch, R.J., Tueller, P.T., 1998. A management-oriented classification of pinyon-juniper woodlands of the Great Basin. US Dep. Agric. For. Serv. Rocky Mt. Res. Stn. Ogden UT Gen. Tech. Rep. RMRS-GTR-12 495.

CHAPTER 5

CONCLUSION

The main aim of this project is to produce valuable products form PJ biomass, through pyrolysis, which could be account for the energy spent on removing this biomass. This thesis mainly focuses on

1. Biomass characterization and pyrolysis of PJ wood, bark and mixture
2. Parametric study on pyrolysis of PJ mixture biomass
3. Catalytic pyrolysis of PJ biomass with HZSM5 and red mud

Biomass characterization showed that bark had high ash content and low bulk density, which had a negative effect while considering as a fuel source. The presence of bark in the mixture affected the ash, carbon, nitrogen, oxygen and energy content of PJ mixture when compared to PJ wood. Pyrolysis of PJ wood, bark and mixture showed that bark reduced the bio-oil yield, increased the char/coke yield and viscosity of the bio-oil produced. The effect of temperature on the pyrolysis of PJ mixture showed that less viscous bio-oil was produced at the temperature (475 ^{o}C) which produced maximum bio-oil yield. The results obtained show that PJ biomass can be effectively used in pyrolysis process for producing value added products.

Response surface methodology was conducted with the help of box behnken design in order to optimize the factors for desired yields. The total liquid, organic, char and gas yields are affected by the individual, quadratic and interaction terms of the factors. The results obtained showed that temperature had positive effect on water and gas yield and negative effect on total liquid, organic and char yield; gas flow rate had positive effect on total liquid and organic yield and negative yield on water and char yield; the feed rate had negative effect on total liquid, organic and water. Thus, the result from this study could be used for maximizing the yield of bio-oil, biochar or gas.

Catalytic pyrolysis of pinyon/juniper biomass was demonstrated using silica sand, HZSM5, and red mud as effective pyrolysis media. The HZSM5 and red mud had catalytic effect on the pyrolysis of the feedstock resulting in oils with much lower viscosity than the oils produced using silica sand as the pyrolysis medium. The pyrolysis oils generated using the red mud had viscosity that were seven times lower than the oils produced using silica sand. The reaction pathway of the red mud was quite different from that of the HZSM5 and silica sand. Red mud rejected oxygen from the biomass pyrolysis vapors probably through decarboxylation reaction instead of decarbonylation reaction observed for the HZSM5. The red mud appeared to be stable and regenerable for catalytic pyrolysis reaction.